General Disclaimer

One or more of the Following Statements may affect this Document

- This document has been reproduced from the best copy furnished by the organizational source. It is being released in the interest of making available as much information as possible.

- This document may contain data, which exceeds the sheet parameters. It was furnished in this condition by the organizational source and is the best copy available.

- This document may contain tone-on-tone or color graphs, charts and/or pictures, which have been reproduced in black and white.

- This document is paginated as submitted by the original source.

- Portions of this document are not fully legible due to the historical nature of some of the material. However, it is the best reproduction available from the original submission.

NASA TECHNICAL MEMORANDUM

NASA TM 73,271

NASA TM 73,271

AERODYNAMIC CHARACTERISTICS OF AN F-8 AIRCRAFT CONFIGURATION WITH A VARIABLE CAMBER WING AT MACH NUMBERS FROM 1.5 TO 2.0

Frederick W. Boltz

Ames Research Center
Moffett Field, California 94035

December 1977

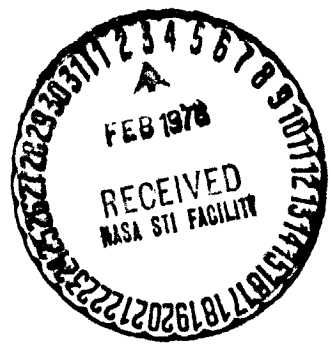

1. Report No.	2. Government Accession No.	3. Recipient's Catalog No.
TM 73,271		

4. Title and Subtitle	5. Report Date
AERODYNAMIC CHARACTERISTICS OF AN F-8 AIRCRAFT CONFIGURATION WITH A VARIABLE CAMBER WING AT MACH NUMBERS FROM 1.5 TO 2.0	December 1977
	6. Performing Organization Code
7. Author(s)	8. Performing Organization Report No.
Frederick W. Boltz	A-7141
	10. Work Unit No.
9. Performing Organization Name and Address	505-11-41
NASA Ames Research Center, Moffett Field, Calif. 94035	11. Contract or Grant No.
	13. Type of Report and Period Covered
12. Sponsoring Agency Name and Address	Technical Memorandum
National Aeronautics and Space Administration Washington, D. C. 20546	14. Sponsoring Agency Code

15. Supplementary Notes

16. Abstract

A 0.1-scale model of an F-8 aircraft was tested in the Ames 9- by 7-Foot Supersonic Wind Tunnel over a range of Mach numbers from 1.5 to 2.0. Reynolds number of 4.12 million was based on wing mean-aerodynamic chord for angles of attack varying from -2° to +12°. The model was equipped with an advanced-technology-conformal-variable-camber wing (ATCVCW) having simple hinge flaps. Data were also obtained for the model equipped with the basic F-8 wing and conventional (simple hinge) flaps. Model variables included aileron and wing trailing-edge deflections and horizontal tail incidence.

In general, the ATCVCW configuration produced slight improvements in lift-curve slope, drag, and static longitudinal stability over that of the basic F-8 wing configuration. Flap effectiveness was essentially the same for both wings.

17. Key Words (Suggested by Author(s))	18. Distribution Statement
F-8 aircraft model test Variable camber wing Simple hinge flaps	Unlimited STAR Category 08

19. Security Classif. (of this report)	20. Security Classif. (of this page)	21. No. of Pages	22. Price*
Unclassified	Unclassified	70	

*For sale by the National Technical Information Service, Springfield, Virginia 22161

CONTENTS

NOMENCLATURE

The axis system and sign convention are presented in figure 1. Data are presented in the body and stability axis coordinate systems. Because the data were computer plotted, the corresponding plot symbol, where used, is given together with the conventional symbol.

Symbol	Plot Symbol	Definition
a		speed of sound
A_b		base area
b		wing span
$\bar{c}$		wing mean aerodynamic chord
C_A		axial-force coefficient, axial force/$q_\infty S$
C_{A_b}		base-force coefficient, base force/$q_\infty S$
C_D	C_D	stability axis drag coefficient, drag/$q_\infty S$
C_{D_b}		stability axis base-drag coefficient, base drag/$q_\infty S$
C_L	C_L	lift coefficient, lift/$q_\infty S$
C_ℓ		body axis rolling-moment coefficient, rolling moment/$q_\infty Sb$
C_{ℓ_s}	C_ℓ(STAB)	stability axis rolling-moment coefficient, rolling-moment/$q_\infty Sb$
C_m	C_m	stability and body axis pitching-moment coefficient, pitching moment/$q_\infty S\bar{c}$
C_N		normal-force coefficient, normal force/$q_\infty S$
C_n	C_n(STAB)	stability and wind axis yawing-moment coefficient, yawing moment/$q_\infty Sb$

Symbol	Plot symbol	Definition
C_{n_b}		body axis yawing-moment coefficient, yawing moment/$q_\infty Sb$
C_y	Cy	stability and body axis side force coefficients, side force/$q_\infty S$
M_∞	MACH	free-stream Mach number
p_{t_∞}		free-stream total pressure
p_∞		free-stream static pressure
q_∞	Q	free-stream dynamic pressure
RN, RN/L	RN,RN/L	Reynolds number
S		wing area
T_{t_∞}		free-stream total temperature
V_∞		free-stream velocity
α	α	angle of attack, deg
β	BETA	angle of sideslip, deg
		Configuration notations:
B	B	basic F-8 body
H	H	basic F-8 horizontal tail
V	V	basic F-8 vertical tail
W_1	W1	basic F-8 wing
W_2	W2	variable camber wing with simple hinge flaps
W_3	W3	variable camber wing with conformal flaps

Symbol	Plot Symbol	Surface definition
δ_H	DH	horizontal tail incidence angle, positive trailing edge down, degrees
δ_{LTEO}	DETO-L	wing left outboard trailing edge deflection angle, positive trailing edge down, deg
δ_{RTEO}	DTEO-R	wing right outboard trailing edge deflection angle, positive trailing edge down, deg
δ_{TEI}	DTEI	wing inboard trailing edge deflection angle, positive trailing edge down, deg

AERODYNAMIC CHARACTERISTICS OF AN F-8 AIRCRAFT CONFIGURATION WITH A VARIABLE CAMBER WING AT MACH NUMBERS FROM 1.5 to 2.0

Frederick W. Boltz

Ames Research Center

SUMMARY

A 0.1-scale model of an F-8 aircraft was tested in the Ames 9- by 7-Foot Supersonic Wind Tunnel over a range of Mach numbers from 1.5 to 2.0. Reynolds number of 4.12 million was based on wing mean-aerodynamic chord for angles of attack varying from -2° to +12°. The model was equipped with an advanced-technology-conformal-variable-camber wing (ATCVCW) having simple hinge flaps. Data were also obtained for the model equipped with the basic F-8 wing and conventional (simple hinge) flaps. Model variables included aileron and wing trailing-edge deflections and horizontal tail incidence.

In general, the ATCVCW configuration produced slight improvements in lift-curve slope, drag, and static longitudinal stability over that of the basic F-8 wing configuration. Flap effectiveness was essentially the same for both wings.

INTRODUCTION

The camber of an airfoil has a fundamental effect on its aerodynamic performance and provides the maximum efficiency only at the design flight condition. To offset the reduction in efficiency at other flight conditions, various devices such as leading-edge slots and leading- and trailing-edge flaps have been employed. However, the resulting discontinuities in the airfoil contours produce disturbances in the flow which limit the aerodynamic gains from such devices. It would, therefore, be desirable to alter the camber in a manner so as to avoid such disturbances and maintain smooth flow across the airfoil. An example of such an approach is the variable-camber Krueger flap.

In order to investigate the effectiveness of the variable-camber concept for the improvement of performance and handling qualities of supersonic fighter/attack aircraft, a wind tunnel test was conducted in the Ames 9- by 7-Foot Supersonic Wind Tunnel. The results of that investigation, in which an F-8 aircraft configuration was used, are presented herein with a minimum of analysis.

TEST FACILITY

The investigation was performed in the Ames 9- by 7-Foot Supersonic Wind Tunnel. This tunnel is a variable-density, continuous-flow type with an adjustable nozzle to permit supersonic testing over a Mach number range continuously variable from 1.5 to 2.5. The nozzle is of the asymmetric, sliding-block type in which the variation of the test section Mach number is achieved by translating, in the streamwise direction, the fixed-contour block that forms the floor of the nozzle.

MODEL DESCRIPTION

The model tested was a 0.1-scale F-8 aircraft configuration. The geometry of the model is given in table 1. Drawings of the model are presented in figure 2, and photographs of the model installed in the Ames 12-Foot Pressure Wind Tunnel are presented in figure 3.

The model was tested with a wing designed to simulate the advanced-technology-conformal-variable-camber wing (ATCVCW) as well as with the basic F-8 wing. The variable-camber wing has a leading-edge sweep angle of 47.13°, a trailing-edge sweep angle of 20.28°, and a modified TR42A (Boeing Co.) airfoil section. The basic F-8 wing has a leading-edge sweep of 47.17°, a trailing-edge sweep of 20.35°, an NACA 65A006 airfoil section at the root, and an NACA 65A005 airfoil section at the tip. The horizontal and vertical tails have NACA 65A006 and modified NACA 65A005.3 airfoil sections, respectively.

The variable-camber wing was configured to allow simulation of leading- and trailing-edge deflections, and aileron deflections. In addition, the incidence angle of the horizontal tail could be varied.

The aft end of the model was modified to accept the sting support.

TESTING AND PROCEDURE

The investigation was performed at Mach numbers of 1.5, 1.6, 1.8, and 2.0 at a Reynolds number of 4.12 million based on the wing mean-aerodynamic chord. Data were obtained at model angles of attack from -2° to 12° at zero degrees sideslip angle.

Wing trailing-edge deflection angles of 0° and -2° were tested. Trailing-edge outboard deflection angles were set differentially (left/right) at 5°/-5° and 0°/-15°. The horizontal tail incidence was set at 0° and -5°.

Aerodynamic forces and moments on the model were measured using a six-component internal strain-gage balance. A pressure transducer, mounted in the model-support system, was used to measure model base pressure. The angle of attack was sensed by an angle transducer mounted on the model-support system.

The model was provided with boundary-layer-transition strips of glass beads having a nominal size of 0.0203 cm (0.0080 in.). A strip 0.3175 cm (0.125 in.) wide was placed on the wing upper surface and on the tail surfaces at 5 percent chord from the leading edge and on the wing lower surface at 30 percent chord. Transition strips were also located 1.27 cm (0.5 in.) aft on both the nose and the nose inlet. Trip effectiveness was not verified, but on the basis of experience, it was considered adequate.

DATA REDUCTION

The six-component force and moment data were reduced about the model moment-reference center in the body-axis system. The axis systems are defined in figure 1, and the moment center was assumed to be at fuselage station 114.79 cm, waterline 25.40 cm and buttock line 0. The angles of attack and angles of sideslip were corrected for deflection of the sting and balance under aerodynamic load. Angles of attack and appropriate aerodynamic coefficients were corrected for model weight tares. Body and stability-axis coefficients were corrected for base force, but no stream-angle corrections were applied to the data.

Data repeatability for the test was estimated by reviewing repeat points and is as follows:

C_L	$= \pm 0.0106$	C_ℓ	$= \pm 0.0016$	α	$= \pm 0.0500°$
C_D	$= \pm 0.0022$	C_m	$= \pm 0.0029$	β	$= \pm 0.0170°$
C_y	$= \pm 0.0054$	C_n	$= \pm 0.0008$	RN/L	$= \pm 0.1337 \times 10^6$/ft
				M_∞	$= \pm 0.0033$

RESULTS AND DISCUSSION

Lift, drag, and pitching-moment characteristics of the complete model (body-wing-tail) at Mach numbers of 1.5, 1.6, 1.8, and 2.0 are presented in figures 4 through 6 for various configurations and control surface deflections. In figure 6 the side-force, yawing moment, and rolling-moment

characteristics are also presented.

The effects of horizontal tail deflection for the model with the basic F-8 wing and with the variable-camber wing are shown in figure 4. Also included in this figure are tail-off data. It is seen that at the higher lift coefficients, there were small increases in lift-curve slope, small reductions in drag, and slight improvements in static longitudinal stability associated with the variable-camber wing. The horizontal tail effectiveness was about the same for the two different wing configurations.

The effects of trailing-edge flap deflection for the model with the variable-camber wing and simple hinge flaps are shown in figure 5. Both tail-on and tail-off data are presented. Indicated is that for both the horizontal tail on and off, there were small increases in lift-curve slope, small reductions in drag, and essentially no changes in static longitudinal stability associated with the use of conformal rather than simple hinge flaps. There was slightly greater flap effectiveness in the case of the conformal flaps.

The effects of aileron deflection for the model with the variable-camber wing and with the horizontal tail are shown in figure 6. It is seen that, in general, there was little difference in the effects produced on both the lateral-directional and longitudinal characteristics by differential aileron deflections of 5°/-5° as compared to those of 0°/-15°.

CONCLUDING REMARKS

The aerodynamic characteristics of a 0.1-scale model of an F-8 aircraft equipped with an advanced-technology-variable-camber wing at Mach numbers from 1.5 to 2.0 have been presented. Corresponding data are also presented for the model equipped with the basic F-8 wing. Conventional simple hinge flaps were tested on both wings.

In general, there were small improvements in lift-curve slope, drag, and static longitudinal stability associated with use of the variable-camber wing in place of the basic F-8 wing. Horizontal-tail and wing trailing-edge flap effectiveness was about the same for the two different wing configurations.

TABLE 1. - MODEL GEOMETRY

Wing assembly (Advanced Technology Wing)

Total area (reference)	0.3484 m^2 (3.750 ft^2)
Total exposed area	0.6580 m^2 (7.083 ft^2)
Span (reference)	1.0872 m (3.567 ft)
Mean aerodynamic chord (reference)	0.3591 m (1.178 ft)
Aspect ratio	3.4
Taper ratio	0.25
Dihedral	-5.00°
Incidence	5.00°
Twist	-7.22°
Sweepback angle	
Leading edge	47.13°
0.25 element line	42.00°
Trailing edge	20.28°
Root chord	0.5130 m (1.683 ft)
Tip chord	0.1283 m (0.4209 ft)
Airfoil section	
Root	Modified TR 42A
Tip	Modified TR 42A

Wing assembly (Basic F-8 wing)

Total area (reference)	0.3484 m^2 (3.750 ft^2)
Total exposed area	0.5907 m^2 (6.358 ft^2)
Span (reference)	1.0872 m (3.567 ft)
Mean aerodynamic chord (reference)	0.3591 m (1.178 ft)
Aspect ratio	3.4
Taper ratio	0.247
Dihedral	-5.00°
Incidence	-1.00°
Twist	0.0
Sweepback angle	
Leading edge	47.17°
0.25 element line	42.00°
Trailing edge	20.35°
Root chord	0.4663 m (1.530 ft)
Tip chord	0.1268 m (0.416 ft)
Airfoil section	
Root	NACA 65A006
Tip	NACA 65A005

TABLE 1. - Concluded.

Fuselage	
Length	1.6093 m (5.280 ft)
Maximum width	14.99 cm (5.90 in)
Maximum depth	19.28 cm (7.59 in)
Fineness ratio	10.88
Maximum cross-sectional area[a]	0.0242 ? (0.260 ft^2)
Planform area	0.2103 m^2 (2.264 ft^2)
Wetted area	0.7442 m^2 (8.010 ft^2)
Horizontal tail	
Planform area	0.0868 m^2 (0.9343 ft^2)
Exposed wetted area	0.1054 m^2 (1.135 ft^2)
Span	0.5538 m (1.817 ft)
Dihedral	5.42°
Mean aerodynamic chord	0.1864 m (0.612 ft)
Root chord length	0.2744 m (0.900 ft)
Tip chord length	0.0405 m (0.133 ft)
Sweepback angle	
Leading edge	50.46°
Hinge line	0.0
Trailing edge	20.12°
Vertical tail	
Planform area	0.0922 m^2 (0.9924 ft^2)
Exposed wetted area	0.1319 m^2 (1.420 ft^2)
Span	0.3683 m (1.208 ft)
Mean aerodynamic chord	0.2789 m (0.915 ft)
Root chord length	0.3967 m (1.302 ft)
Tip chord length	0.1041 m (0.342 ft)
Sweepback angle	
Leading edge	50.15°
Hinge line	22.00°
Trailing edge	22.00°

[a]Includes flow through duct area

INDEX OF DATA FIGURES

FIGURE		CONDITIONS VARYING	PLOTTED COEFFICIENTS SCHEDULE	PAGES
4	EFFECT OF HORIZ. TAIL FOR BASIC F-8 AND AT WINGS. NO WING CONTROL DEFL.	CONFIGURATION MACH, DH	A	1-12
5	EFFECT OF SYMMETRICAL T.E. SIMPLE HINGE FLAP DEFLECTIONS, TAIL OFF, ON.	CONFIGURATION DTEI, DTEO-L, DTEO-R,DH, MACH	A	13-24
6	EFFECT OF DIFFERENTIAL OUTBOARD CONFORMAL FLAP DEFLECTIONS	MACH, DTEO-L, DTEO-R	B	25-48

COEFFICIENTS SCHEDULE:

A) C_L versus α, C_D versus C_L, C_L versus C_m

B) C_Y, C_n(STAB), C_ℓ(STAB), C_L versus α; C_D versus C_L; C_L versus C_m

Notes:

1. Positive directions of force coefficients, moment coefficients, and angles are indicated by arrows
2. For clarity, origins of wind and stability axes have been displaced from the center of gravity

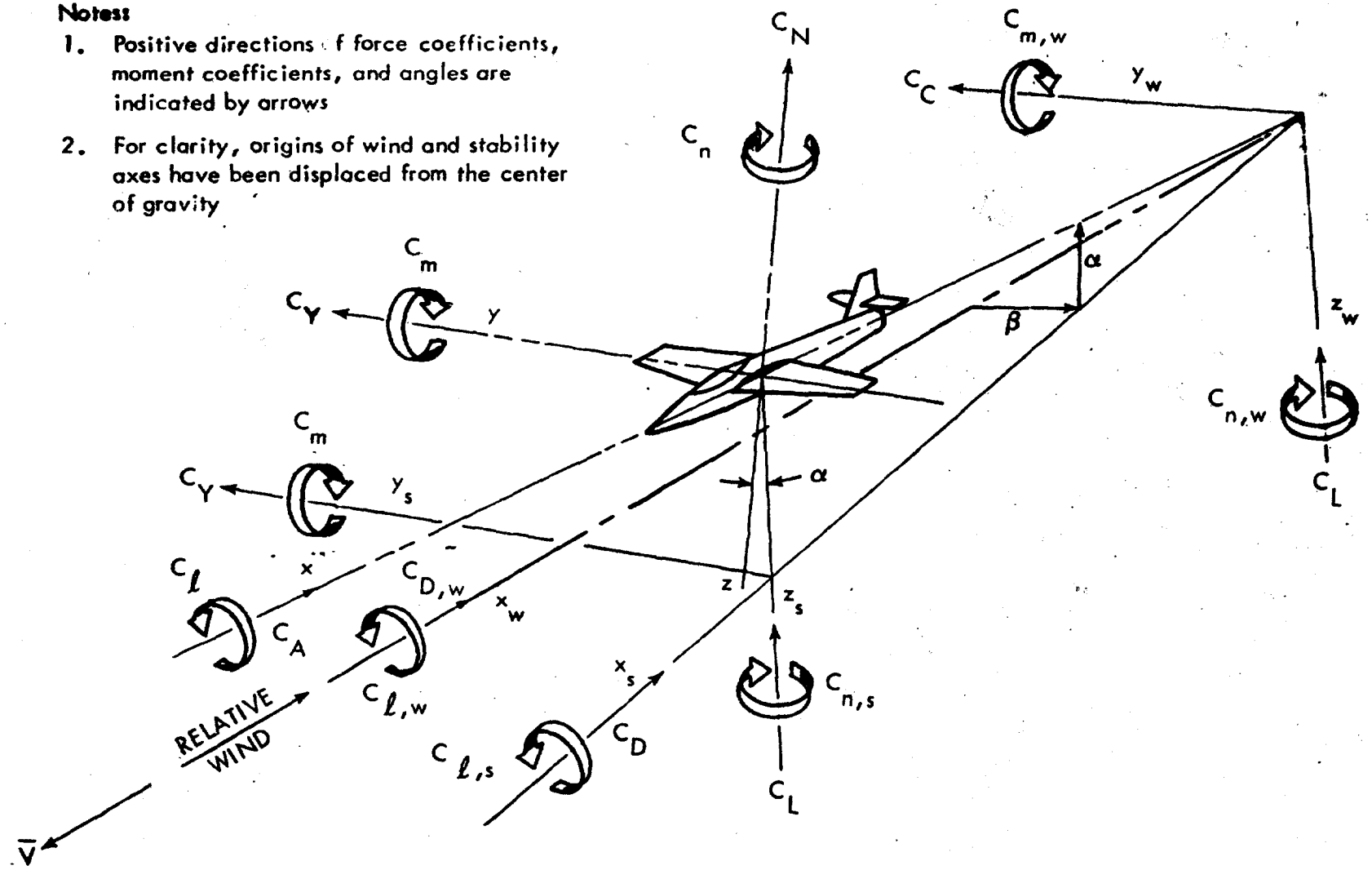

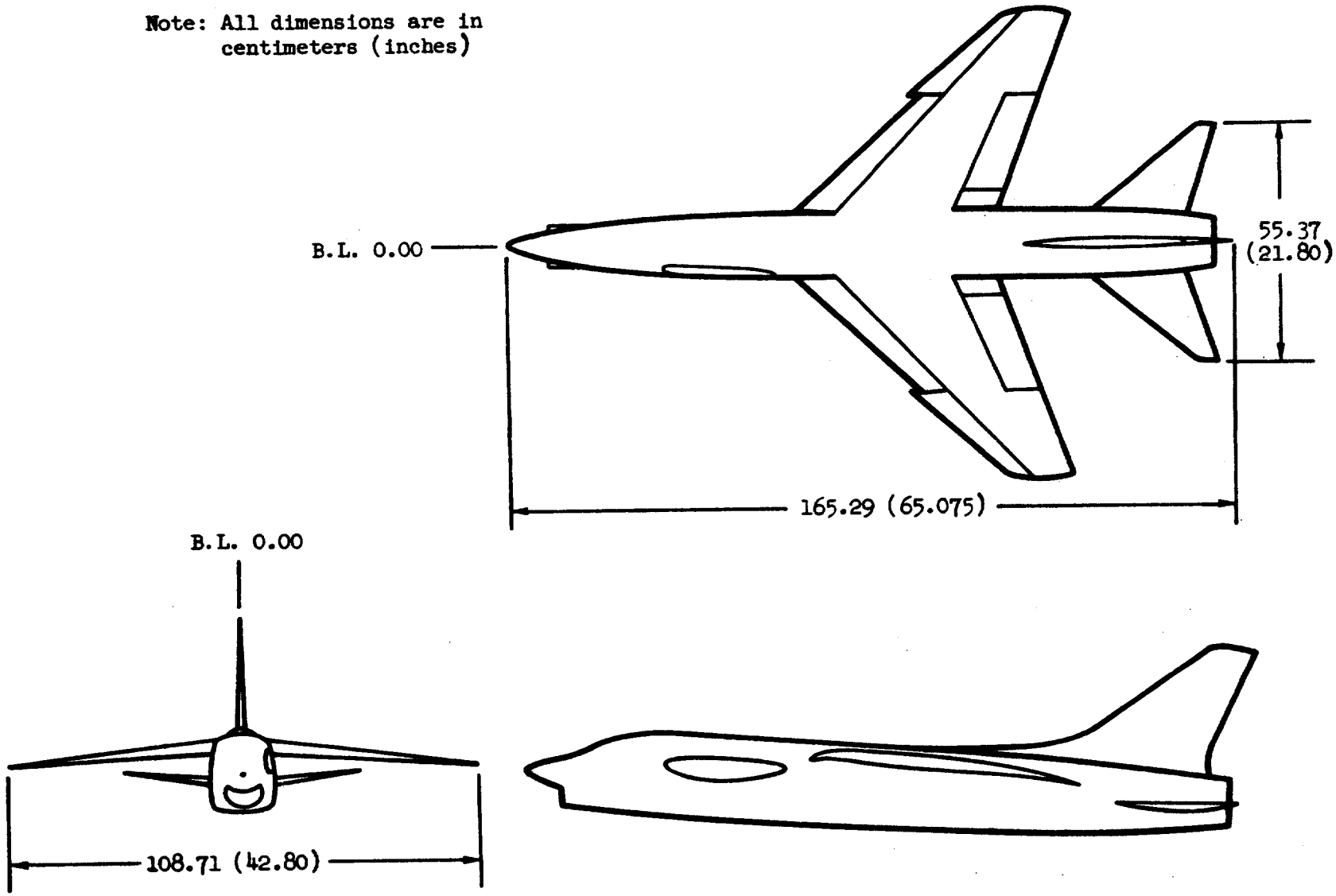

(a) Three view

Figure 2. - Model drawings.

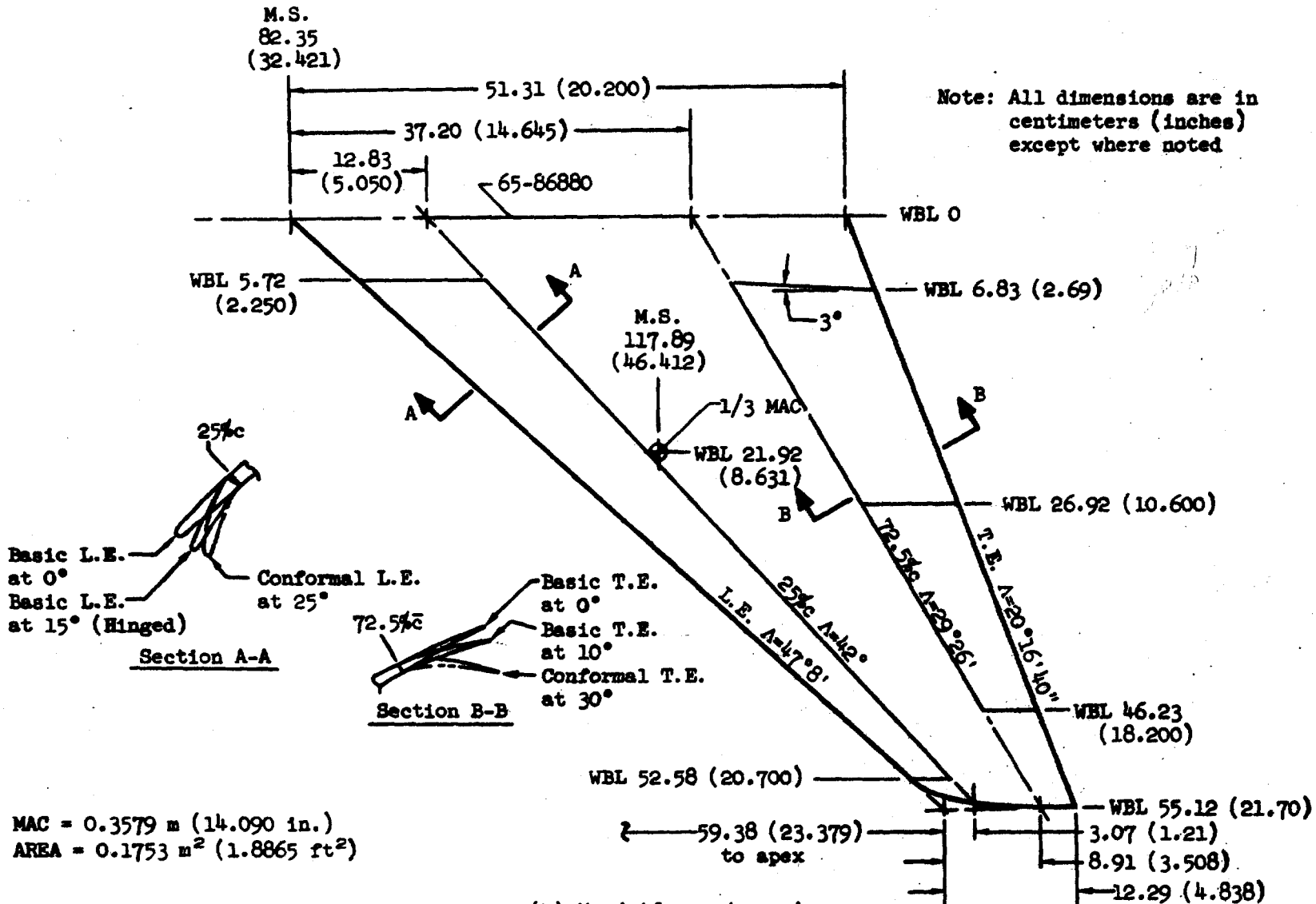

(b) Variable-camber wing

Figure 2. - Continued.

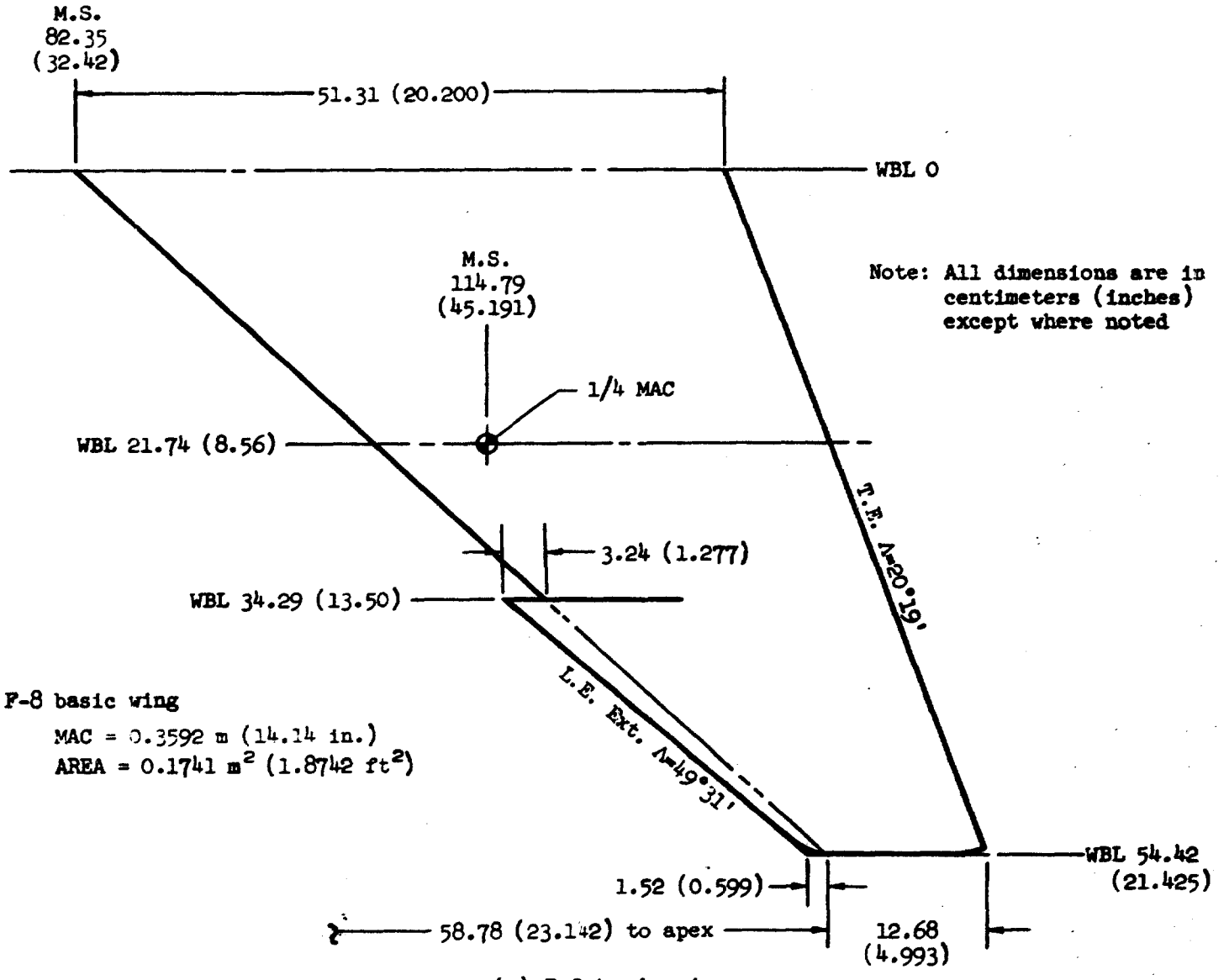

(c) F-8 basic wing

Figure 2. - Continued.

Note: All dimensions are in centimeters (inches) except where noted

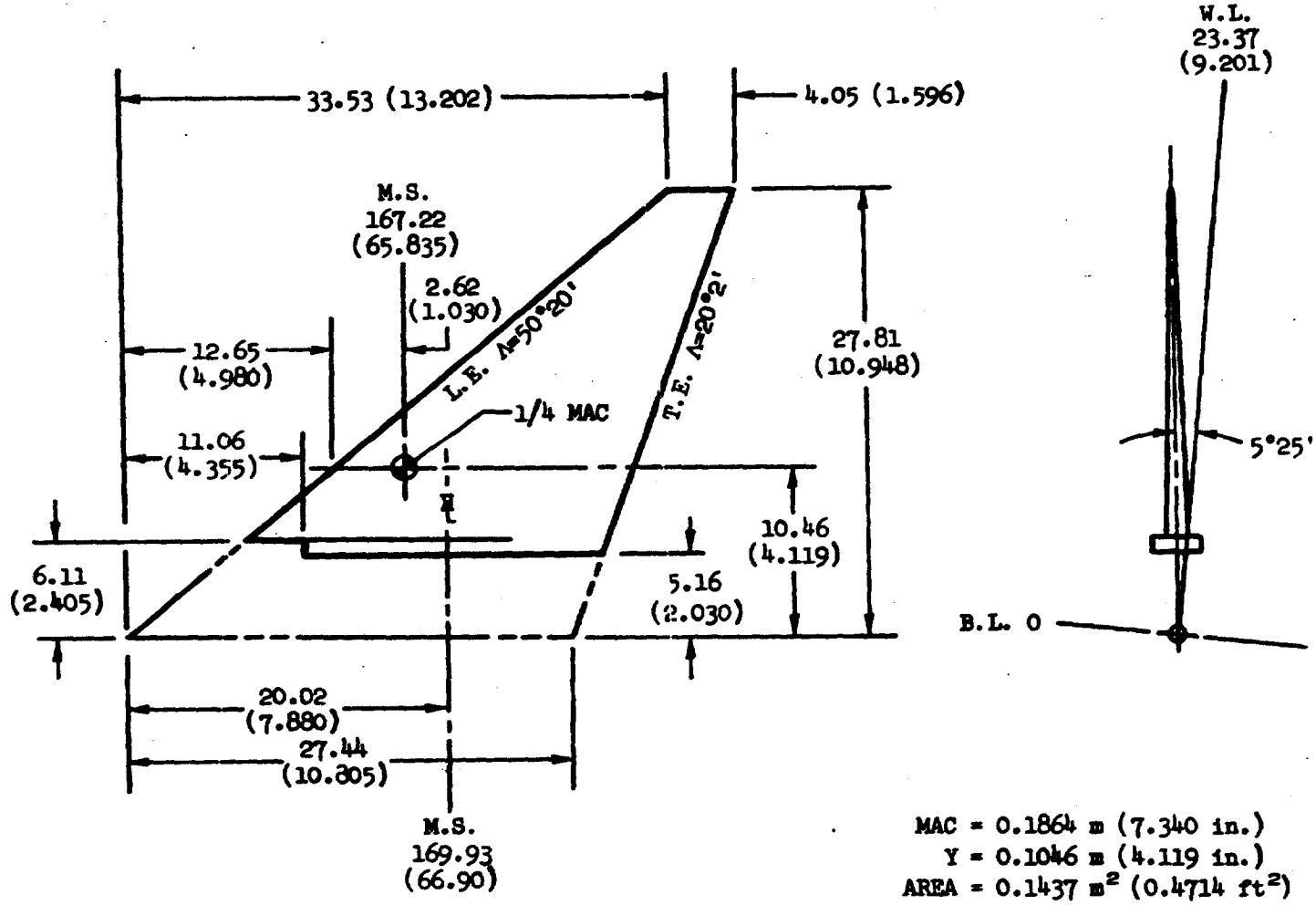

MAC = 0.1864 m (7.340 in.)
Y = 0.1046 m (4.119 in.)
AREA = 0.1437 m^2 (0.4714 ft^2)

(d) Horizontal tail

Figure 2. - Continued.

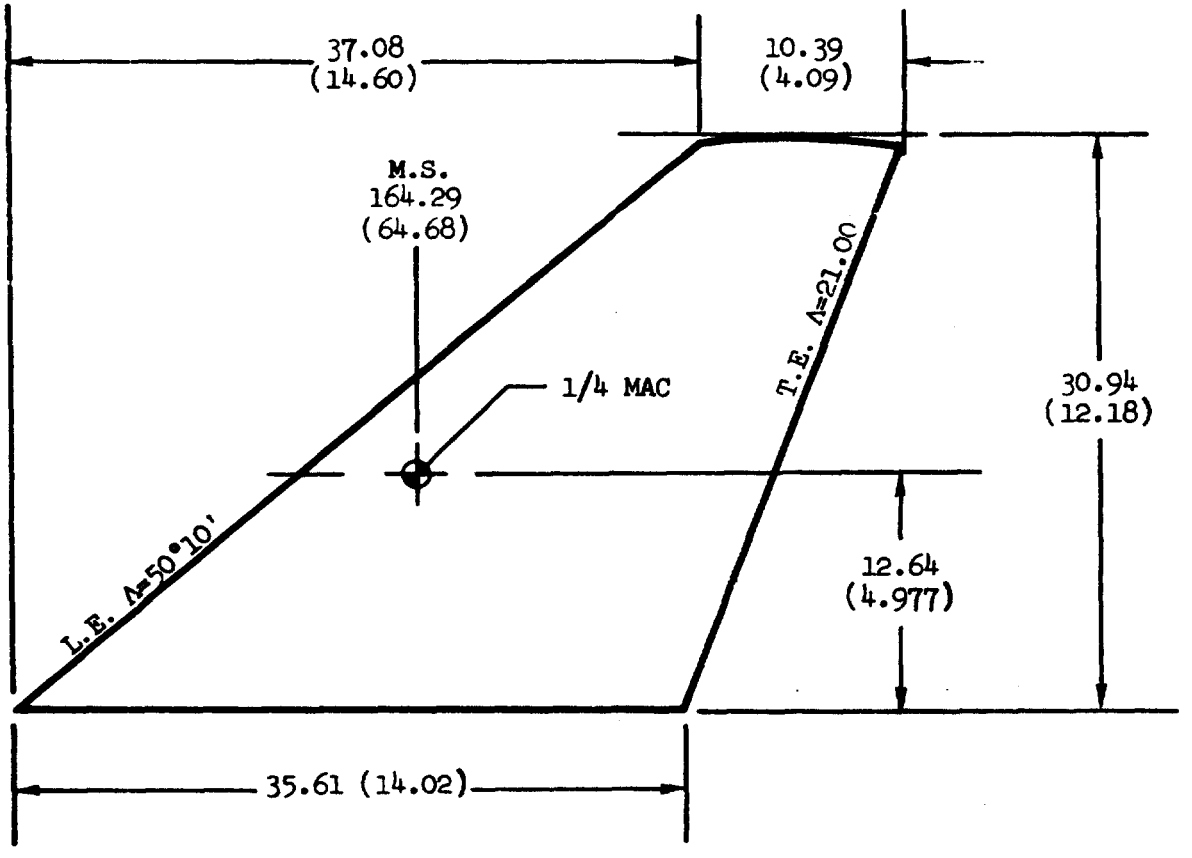

MAC = 0.2530 ft (9.962 in.)
AREA = 0.07115 m^2 (0.7659 ft^2)

Note: All dimensions are in centimeters (inches) except where noted

(e) Vertical tail

Figure 2. - Continued.

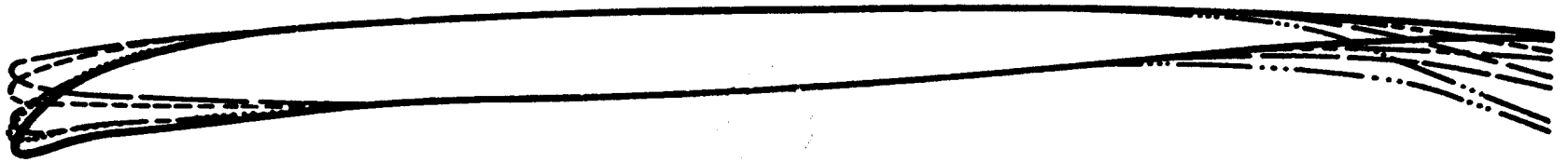

——————— 30° L.E.

..... 22.5° L.E.

——— - ——— - ——— 15° L.E.

— — — — — — — — — — 7.5° L.E.

——— ——— ——— 10° T.E.

——— - - ——— - - ——— 5° T.E.

———···———···———··· 18° T.E.

(f) Some typical leading- and trailing-edge angles for variable camber wing

Figure 2. - Concluded.

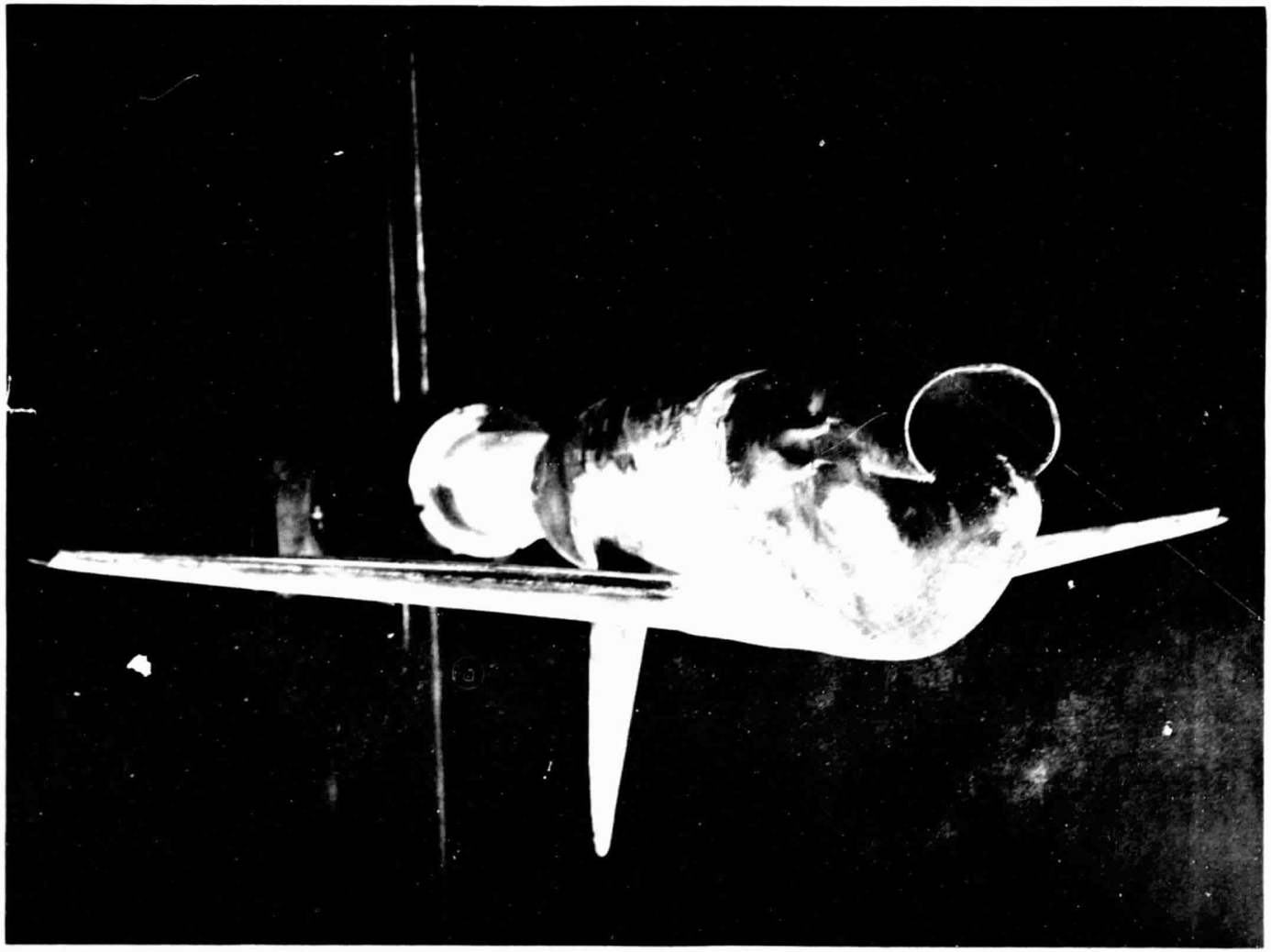

(a) Three-quarter front view

Figure 3. - Model installation photographs.

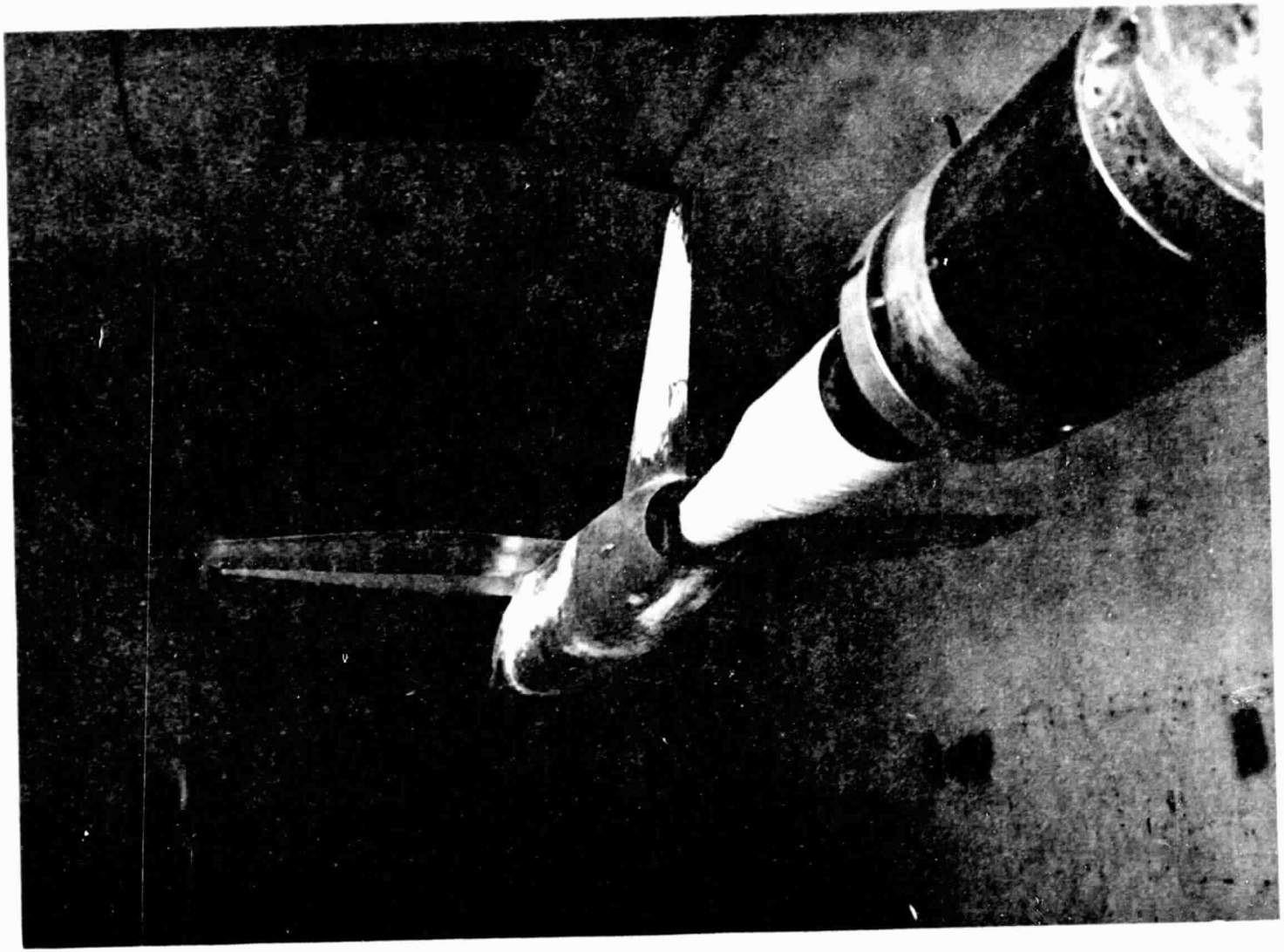

(b) Three-quarter rear view

Figure 3. - Concluded.

DATA

DATA SET	SYMBOL	CONFIGURATION DESCRIPTION	DH	BETA
(ABD002)	○	BVH1		.000
(ABD003)	□	BVH1H	.000	.000
(ABD004)	◇	BVH1H	-5.000	.000
(ABD005)	△	BVH3		.000
(ABD008)	◁	BVH3H	.000	.000
(ABD009)	▷	BVH3H	-5.000	.000

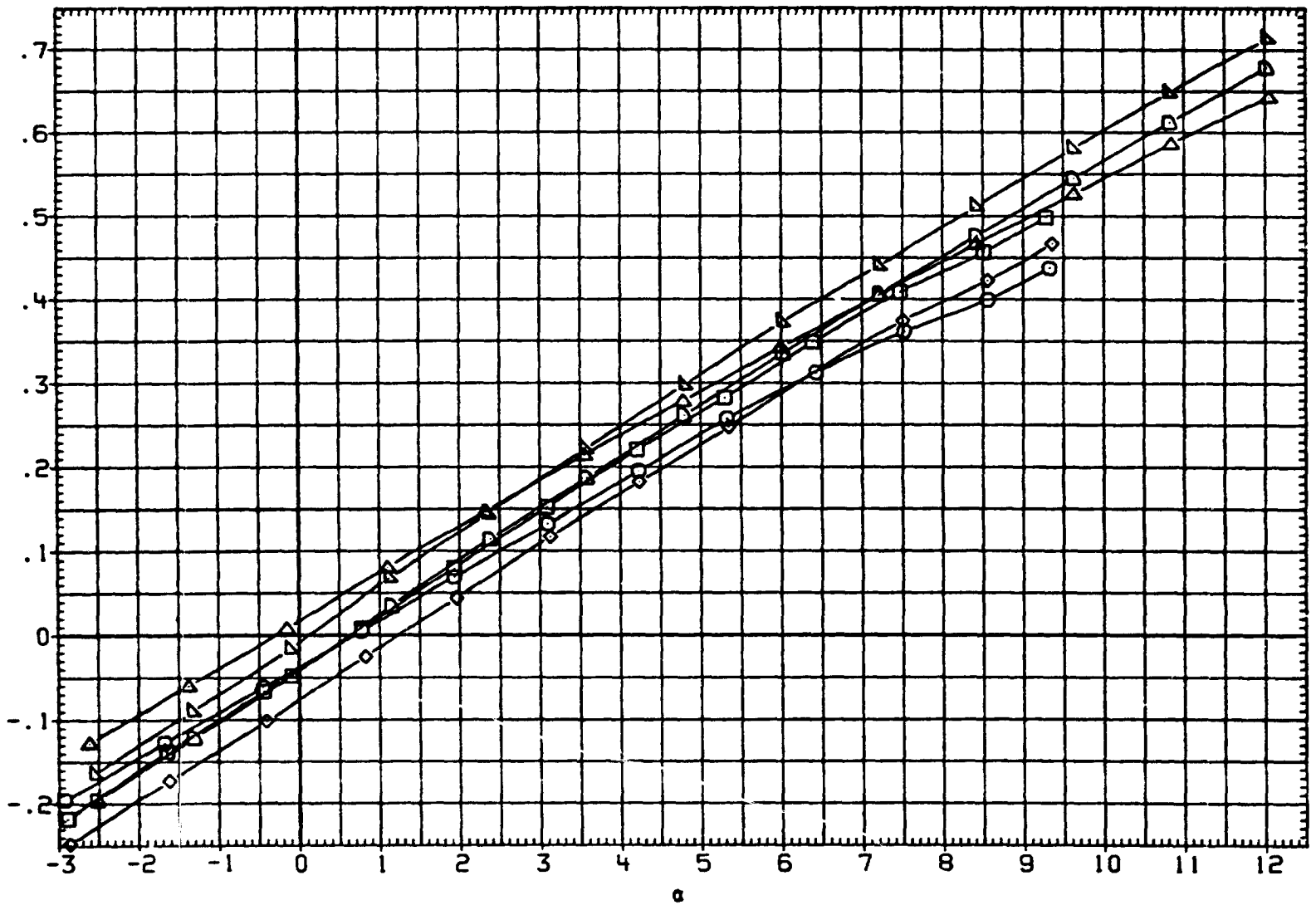

FIG 4. EFFECT OF HORIZ. TAIL FOR BASIC F-8 AND AT WINGS. NO WING CONTROL DEFL.

(A)MACH = 1.50

DATA SET	SYMBOL	CONFIGURATION DESCRIPTION	DH	BETA
(ABD002)	○	BVWI		.000
(ABD003)	□	BVWIH	.000	.000
(ABD004)	◇	BVWIH	-5.000	.000
(ABD005)	△	BVW3		.000
(ABD008)	◁	BVW3H	.000	.000
(ABD009)	D	BVW3H	-5.000	.000

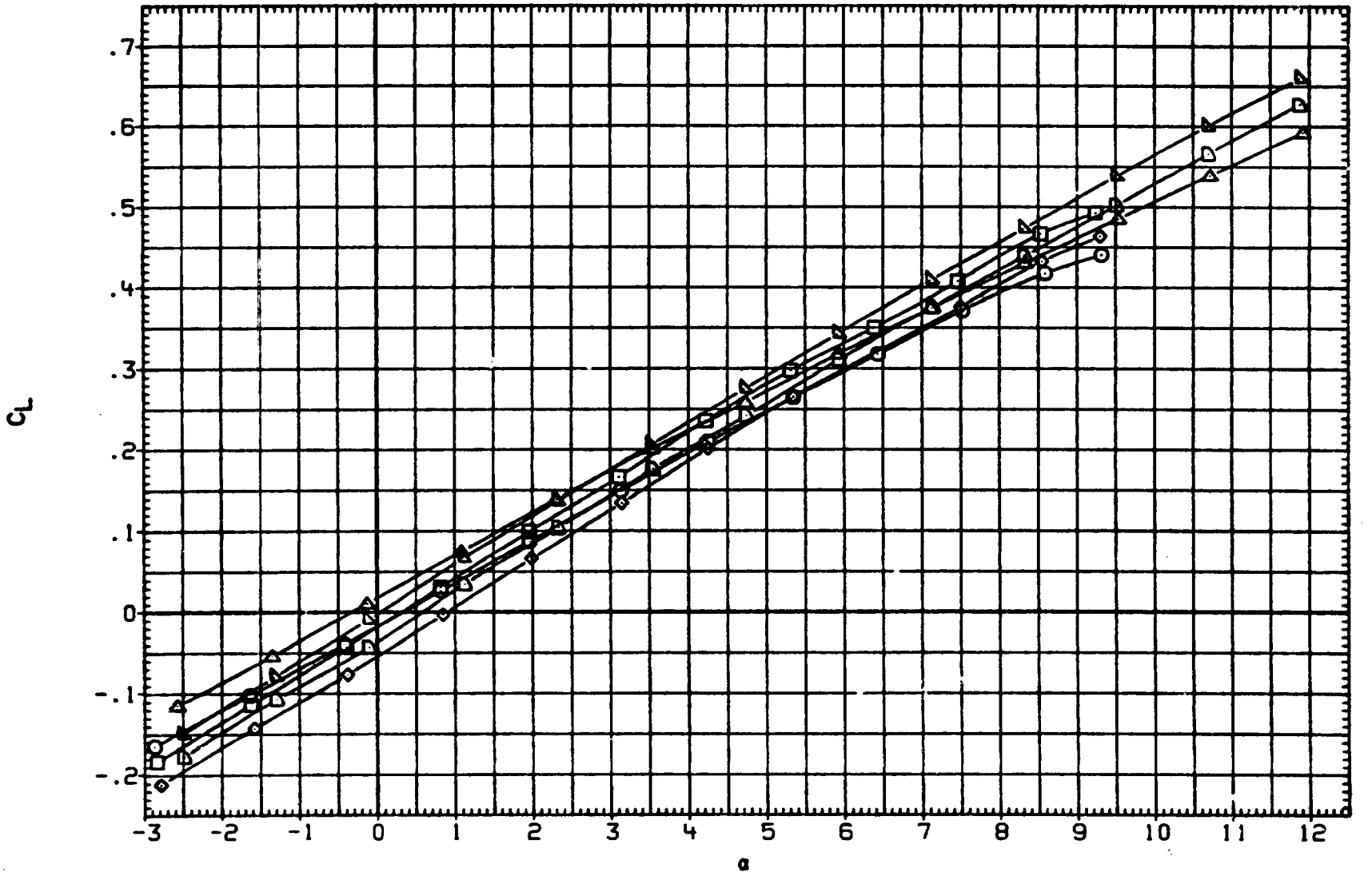

FIG 4. EFFECT OF HORIZ. TAIL FOR BASIC F-8 AND AT WINGS. NO WING CONTROL DEFL.

(B)MACH = 1.60

DATA SET	SYMBOL	CONFIGURATION DESCRIPTION	DH	BETA
(AB0002)	○	BVWI		.000
(AB0003)	□	BVWIH	.000	.000
(AB0004)	◇	BVWIH	-5.000	.000
(AB0005)	△	BVW3		.000
(AB0008)	⊲	BVW3H	.000	.000
(AB0009)	D	BVW3H	-5.000	.000

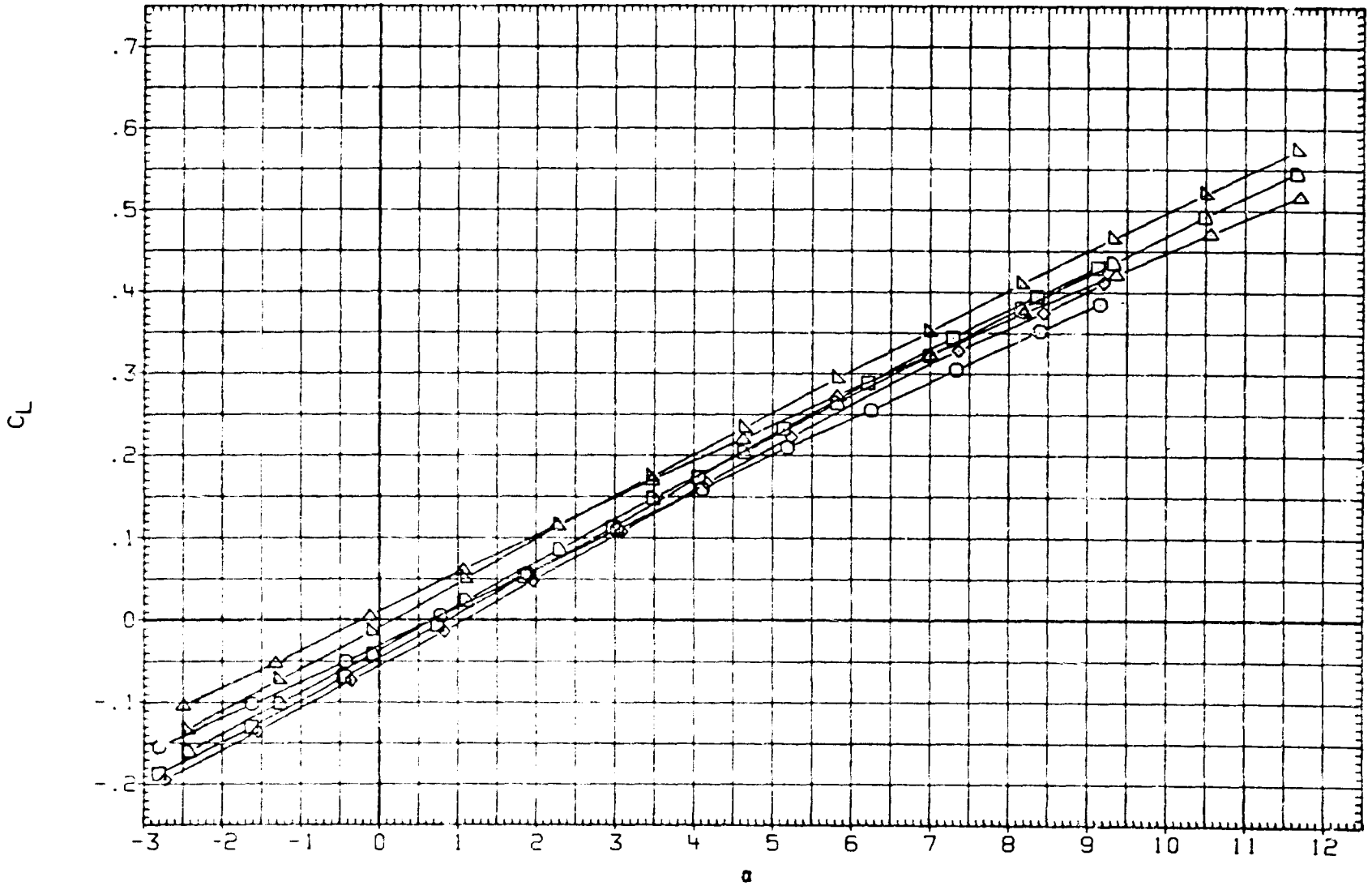

FIG 4. EFFECT OF HORIZ. TAIL FOR BASIC F-8 AND AT WINGS, NO WING CONTROL DEFL.

DATA SET	SYMBOL	CONFIGURATION DESCRIPTION	DH	BETA
(AFD002)	○	BVWI		.000
(ABD003)	□	BVWIH	.000	.000
(ABD004)	◇	BVWIH	-5.000	.000
(ABD005)	△	BVW3		.000
(ABD008)	◁	BVW3H	.000	.000
(ABD009)	D	BVW3H	-5.000	.000

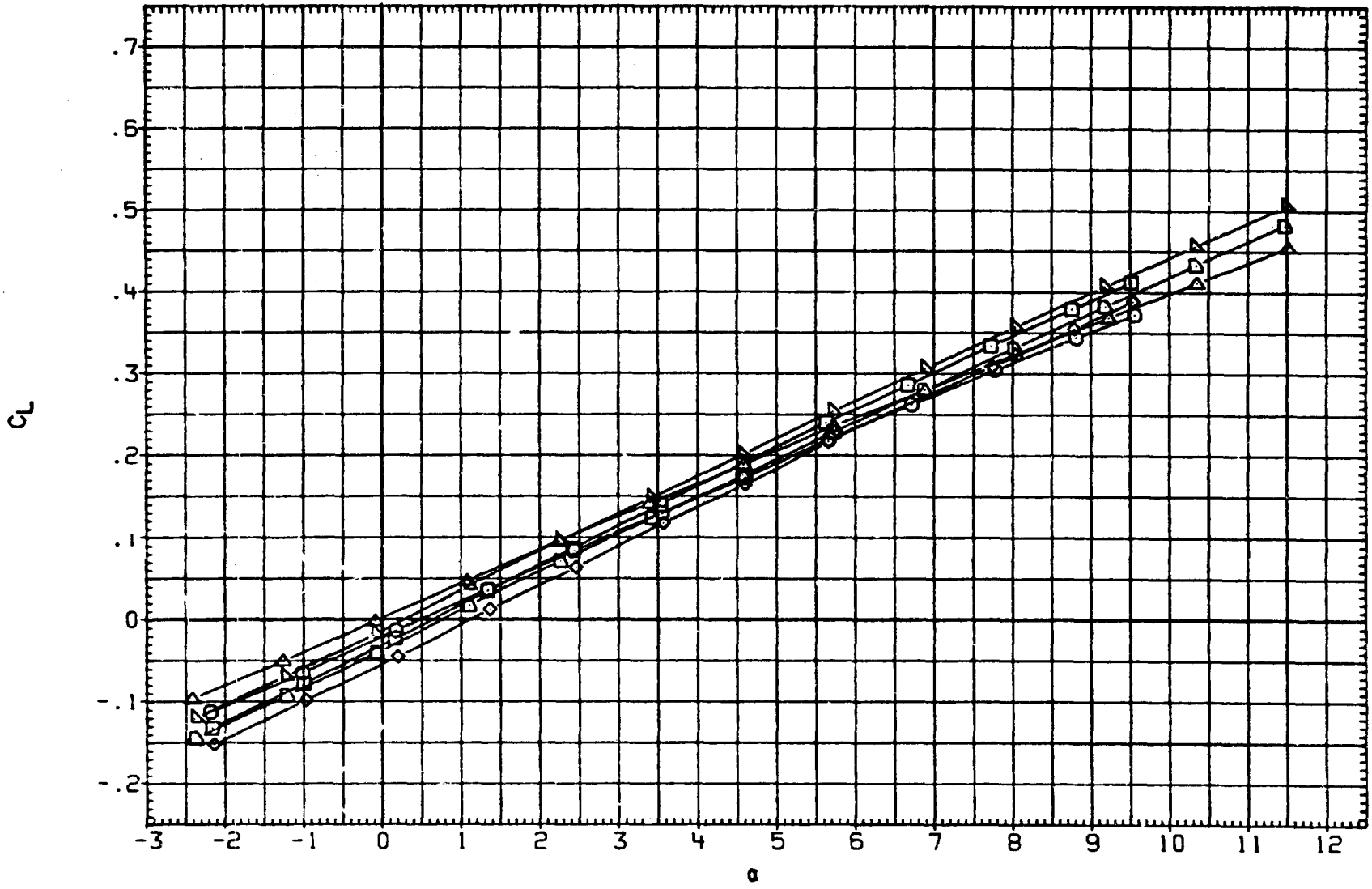

FIG 4. EFFECT OF HORIZ. TAIL FOR BASIC F-8 AND AT WINGS. NO WING CONTROL DEFL.

(D)MACH = 2.00

DATA SET	SYMBOL	CONFIGURATION DESCRIPTION	DH	BETA
(ABD002)	○	BVW1		.000
(ABD003)	□	BVW1H	.000	.000
(ABD004)	◇	BVW1H	-5.000	.000
(ABD005)	△	BVW3		.000
(ABD008)	◁	BVW3H	.000	.000
(ABD009)	D	BVW3H	-5.000	.000

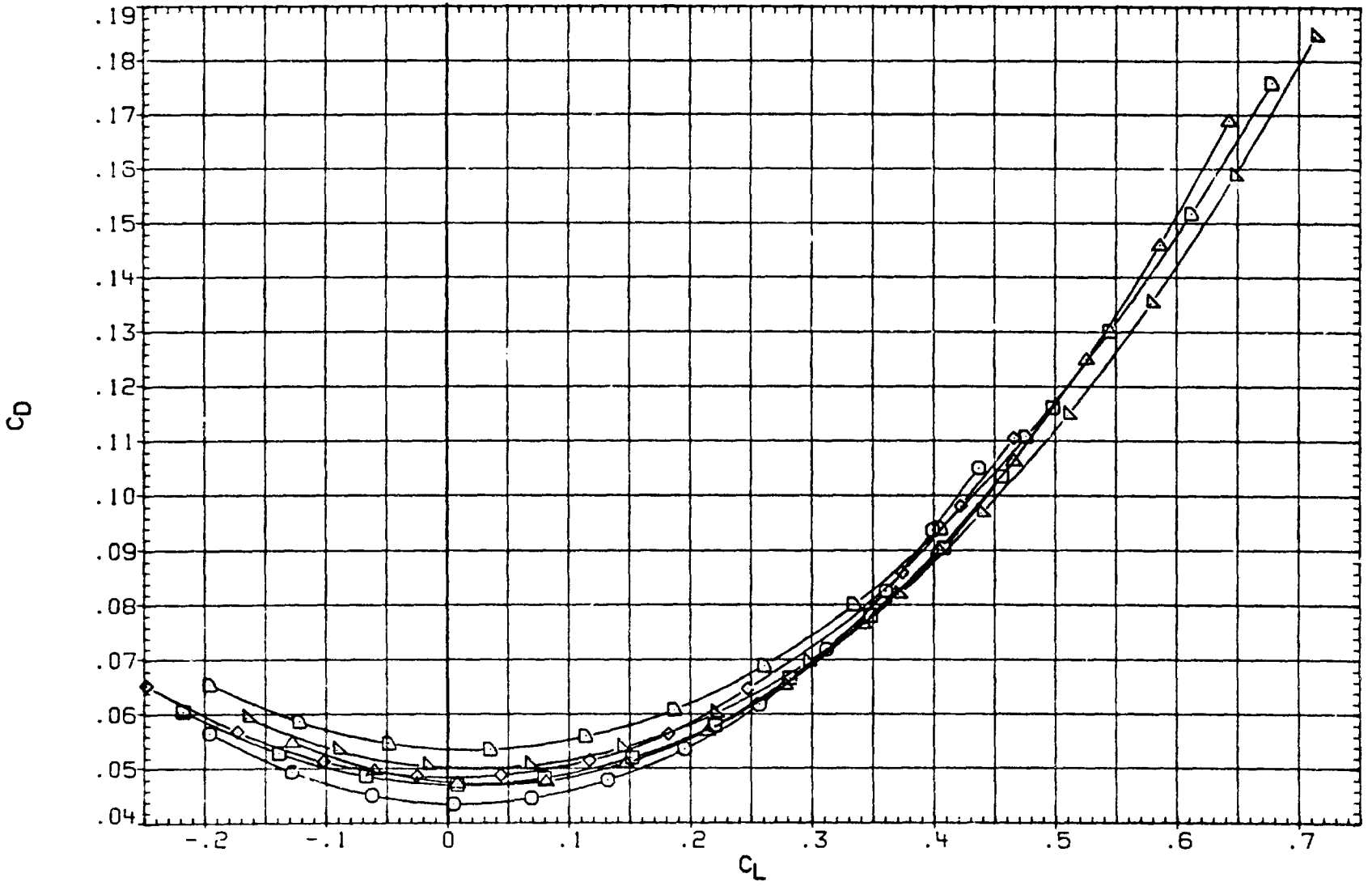

FIG 4. EFFECT OF HORIZ. TAIL FOR BASIC F-8 AND AT WINGS. NO WING CONTROL DEFL.

DATA SET	SYMBOL	CONFIGURATION DESCRIPTION	DH	BETA
(ABD002)	○	BVH1		.000
(ABD003)	□	BVH1H	.000	.000
(ABD004)	◇	BVH1H	-5.000	.000
(ABD005)	△	BVH3		.000
(ABD008)	◁	BVH3H	.000	.000
(ABD009)	D	BVH3H	-5.000	.000

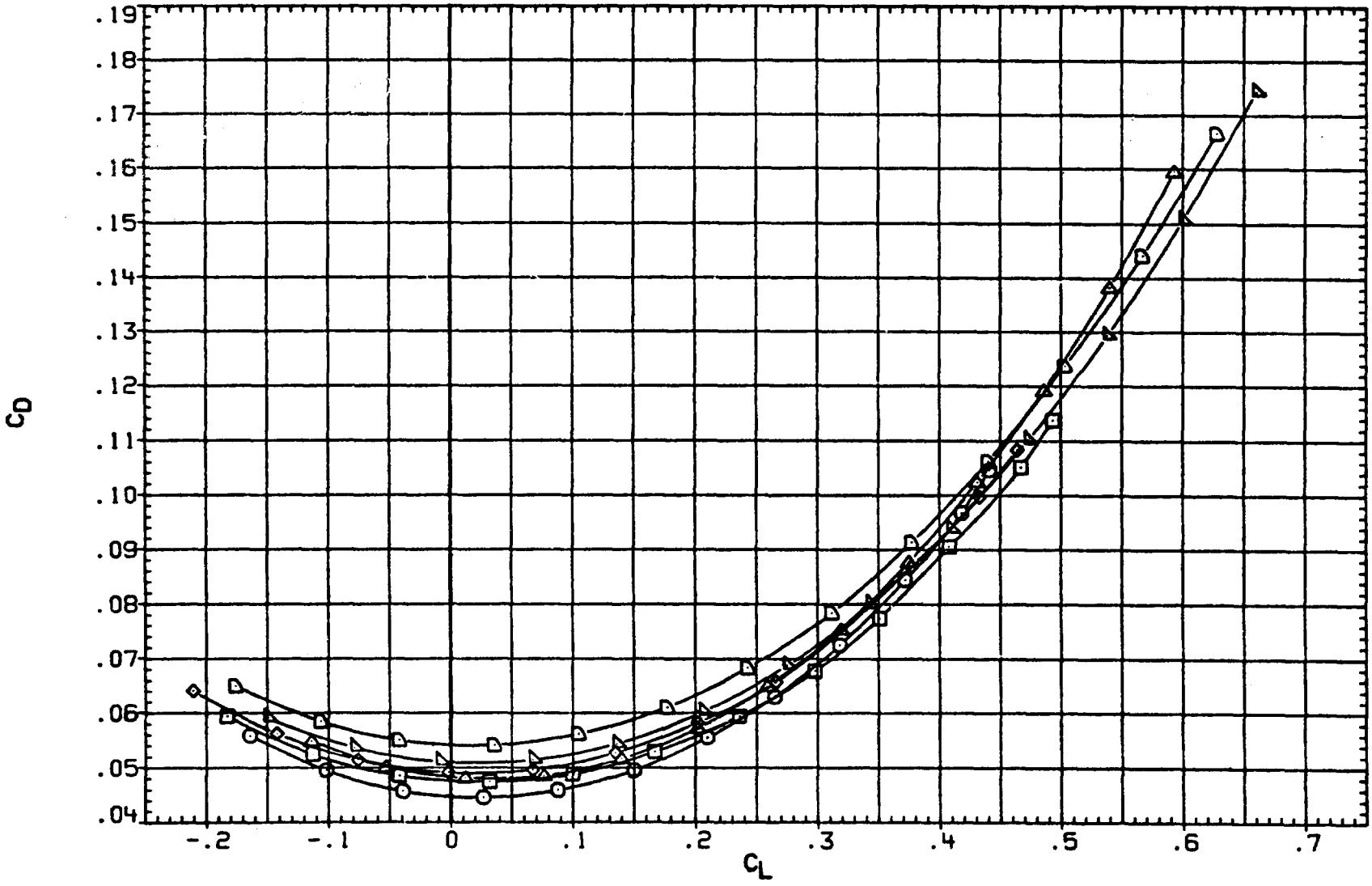

FIG 4. EFFECT OF HORIZ. TAIL FOR BASIC F-8 AND AT WINGS. NO WING CONTROL DEFL.

(B)MACH = 1.60

DATA SET	SYMBOL	CONFIGURATION DESCRIPTION	DH	BETA
(ABD002)	○	BVH1		.000
(ABD003)	□	BVH1H	.000	.000
(ABD004)	◇	BVH1H	-5.000	.000
(ABD005)	△	BVH3		.000
(ABD008)	◁	BVH3H	.000	.000
(ABD009)	▷	BVH3H	-5.000	.000

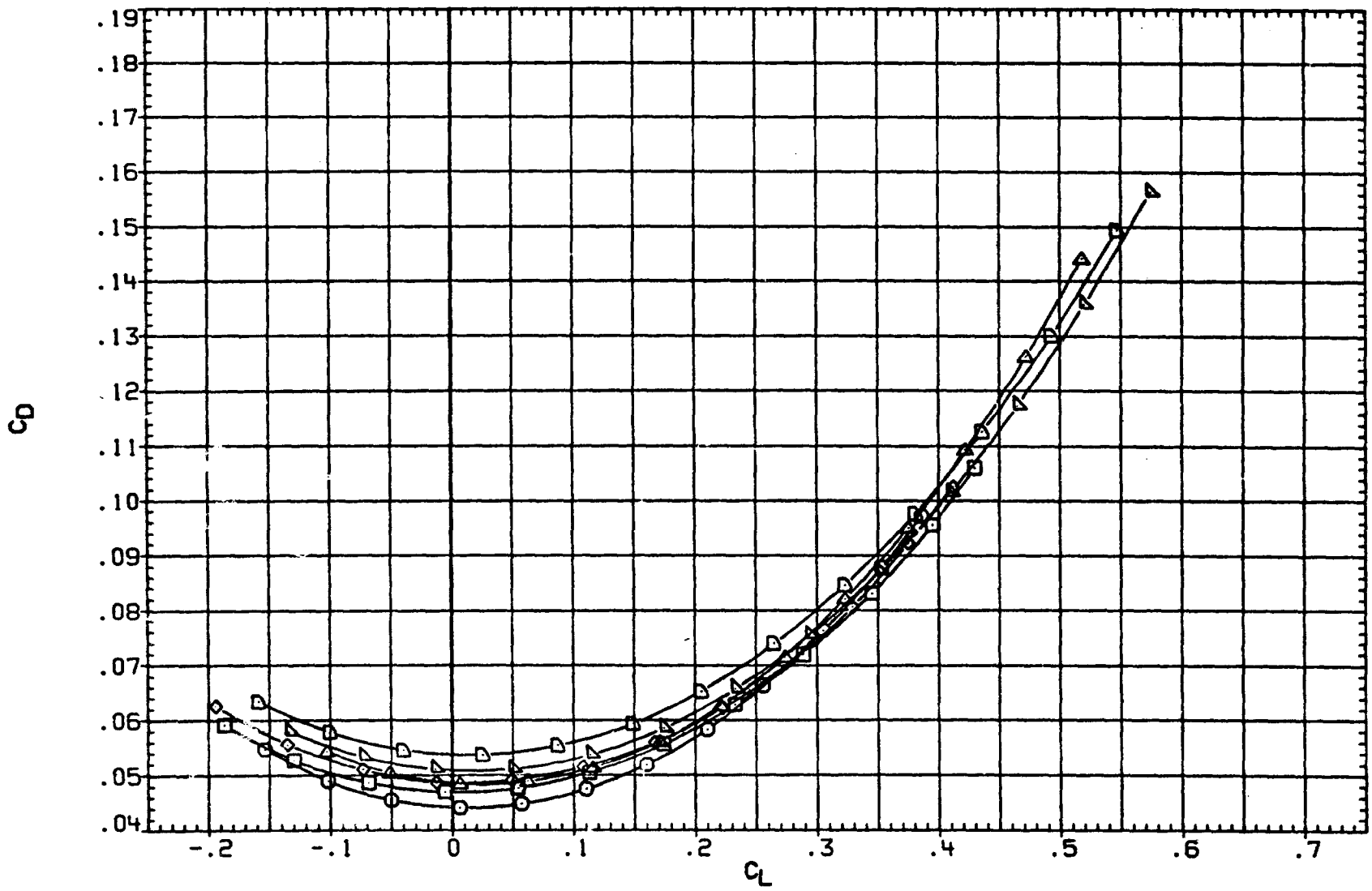

FIG 4. EFFECT OF HORIZ. TAIL FOR BASIC F-8 AND AT WINGS. NO WING CONTROL DEFL.

DATA SET	SYMBOL	CONFIGURATION DESCRIPTION	DH	BETA
(ABD002)	○	BVW1		.000
(ABD003)	□	BVW1H	.000	.000
(ABD004)	◇	BVW1H	-5.000	.000
(ABD005)	△	BVW3		.000
(ABD008)	◁	BVW3H	.000	.000
(ABD009)	D	BVW3H	-5.000	.000

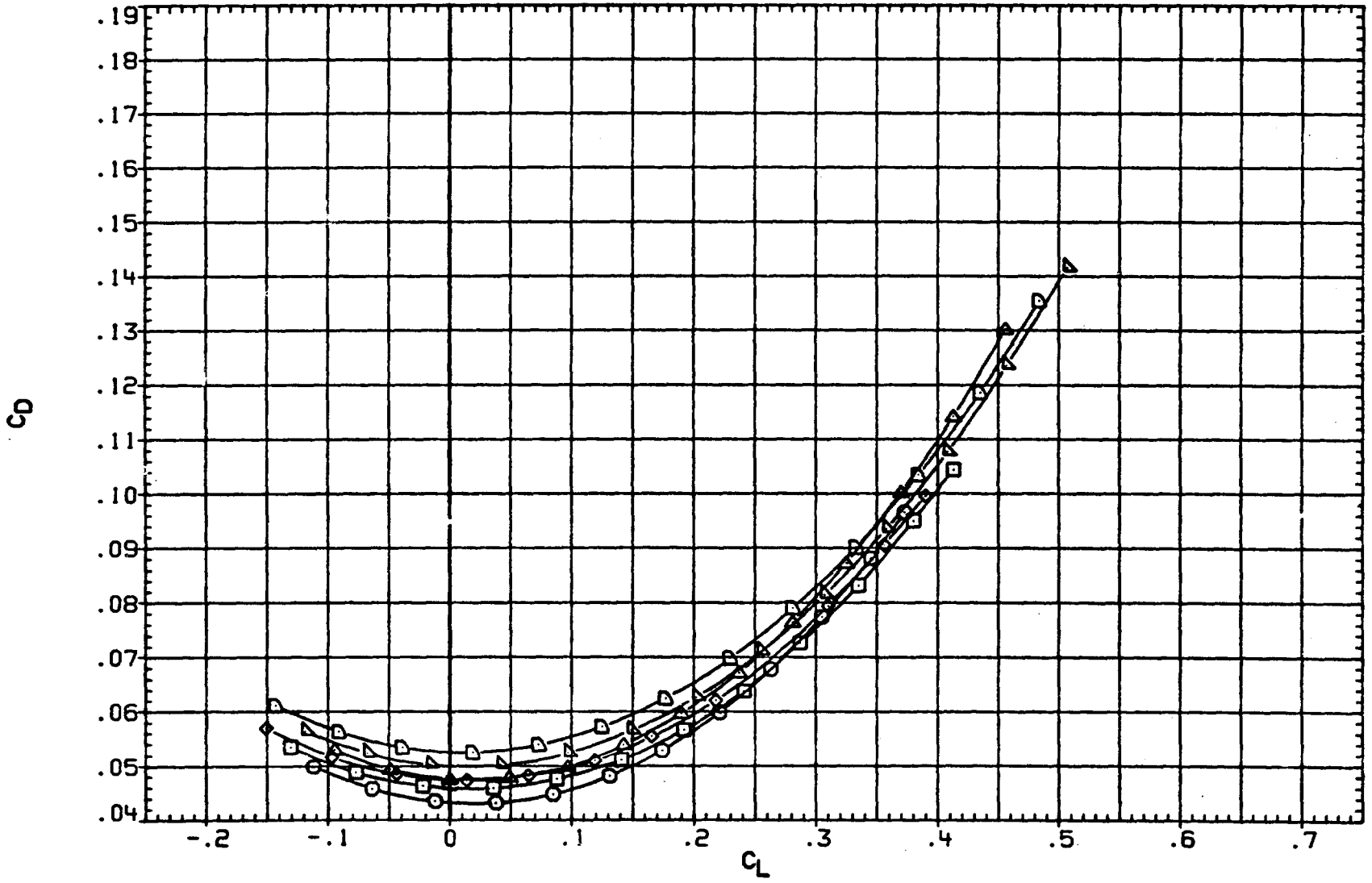

FIG 4. EFFECT OF HORIZ. TAIL FOR BASIC F-8 AND AT WINGS. NO WING CONTROL DEFL.

(D)MACH = 2.00

DATA SET	SYMBOL	CONFIGURATION DESCRIPTION	DH	BETA
(ABD002)	○	BVH1		.000
(ABD003)	□	BVH1H	.000	.000
(ABD004)	◇	BVH1H	-5.000	.000
(ABD005)	△	BVH3		.000
(ABD008)	◁	BVH3H	.000	.000
(ABD009)	▷	BVH3H	-5.000	.000

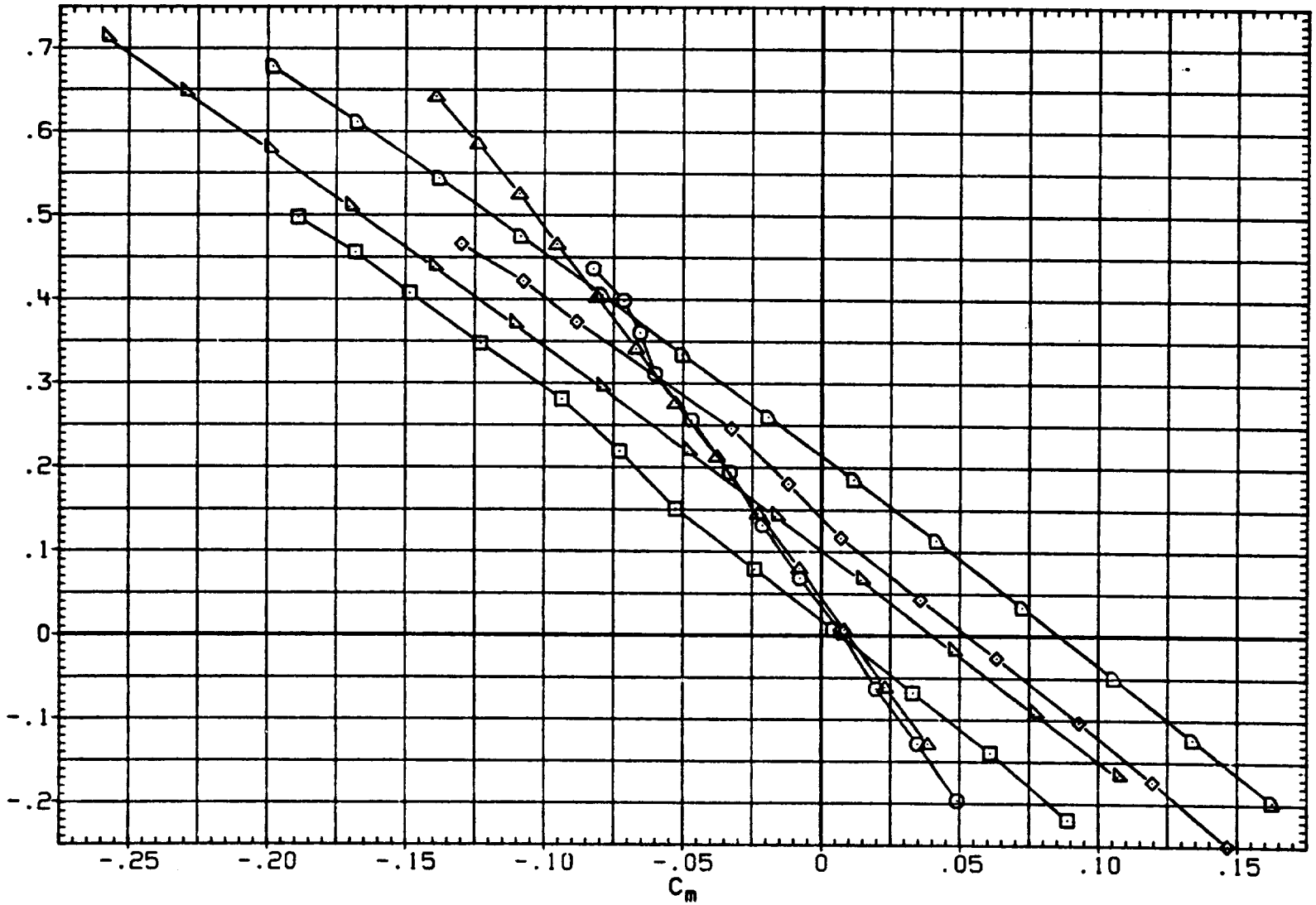

FIG 4. EFFECT OF HORIZ. TAIL FOR BASIC F-8 AND AT WINGS. NO WING CONTROL DEFL.

(A)MACH = 1.50

DATA SET	SYMBOL	CONFIGURATION DESCRIPTION	DH	BETA
(ABD002)	○	BVH1		.000
(ABD003)	□	BVH1H	.000	.000
(ABD004)	◇	BVH1H	-5.000	.000
(ABD005)	△	BVH3		.000
(ABD008)	◁	BVH3H	.000	.000
(ABD009)	▷	BVH3H	-5.000	.000

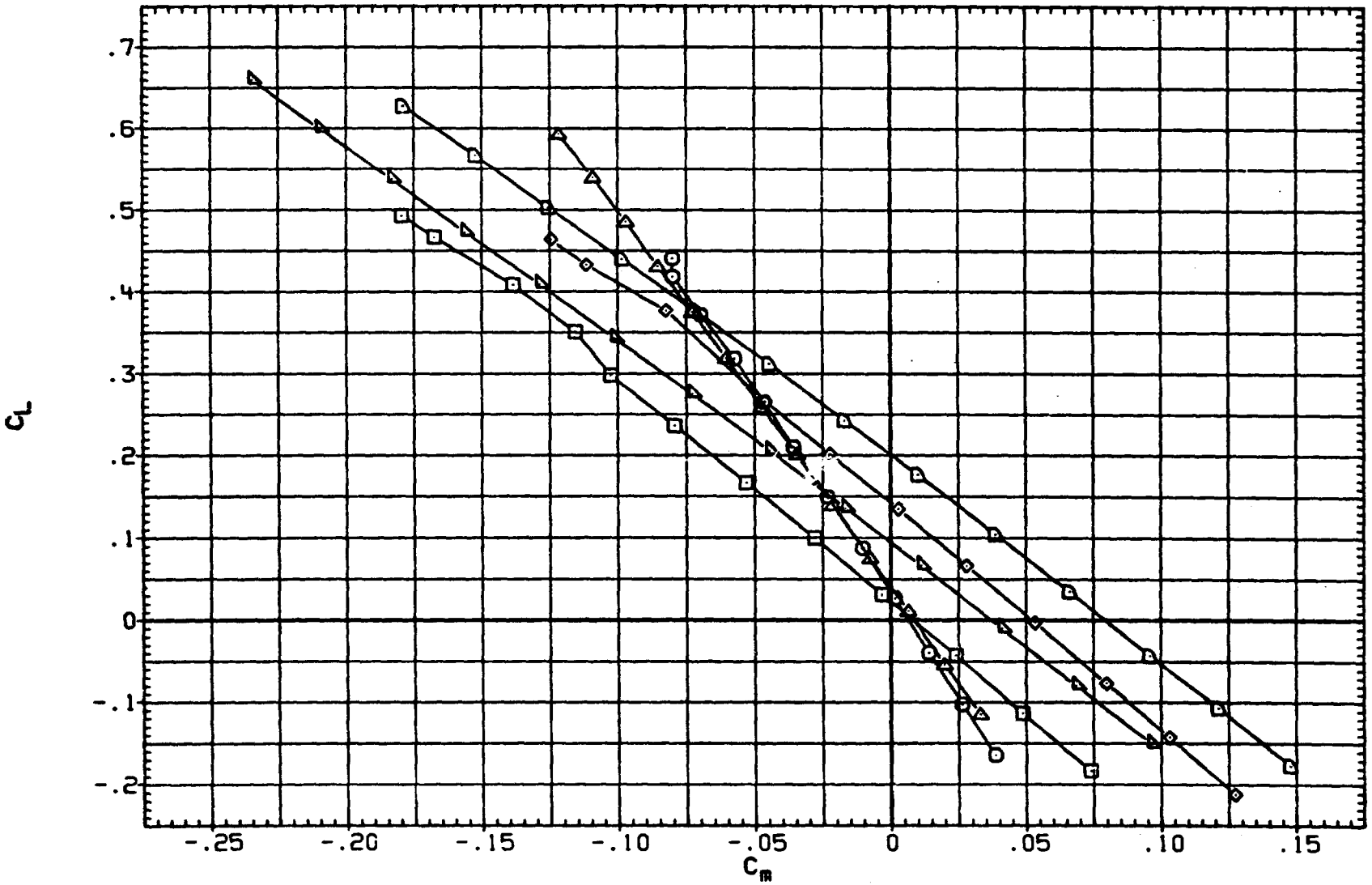

FIG 4. EFFECT OF HORIZ. TAIL FOR BASIC F-8 AND AT WINGS. NO WING CONTROL DEFL.

(B)MACH = 1.60

DATA SET	SYMBOL	CONFIGURATION DESCRIPTION	DH	BETA
(AB0002)	○	BVWI		.000
(AB0003)	□	BVWIH	.000	.000
(AB0004)	◇	BVWIH	-5.000	.000
(AB0005)	△	BVW3		.000
(AB0008)	◁	BVW3H	.000	.000
(AB0009)	▷	BVW3H	-5.000	.000

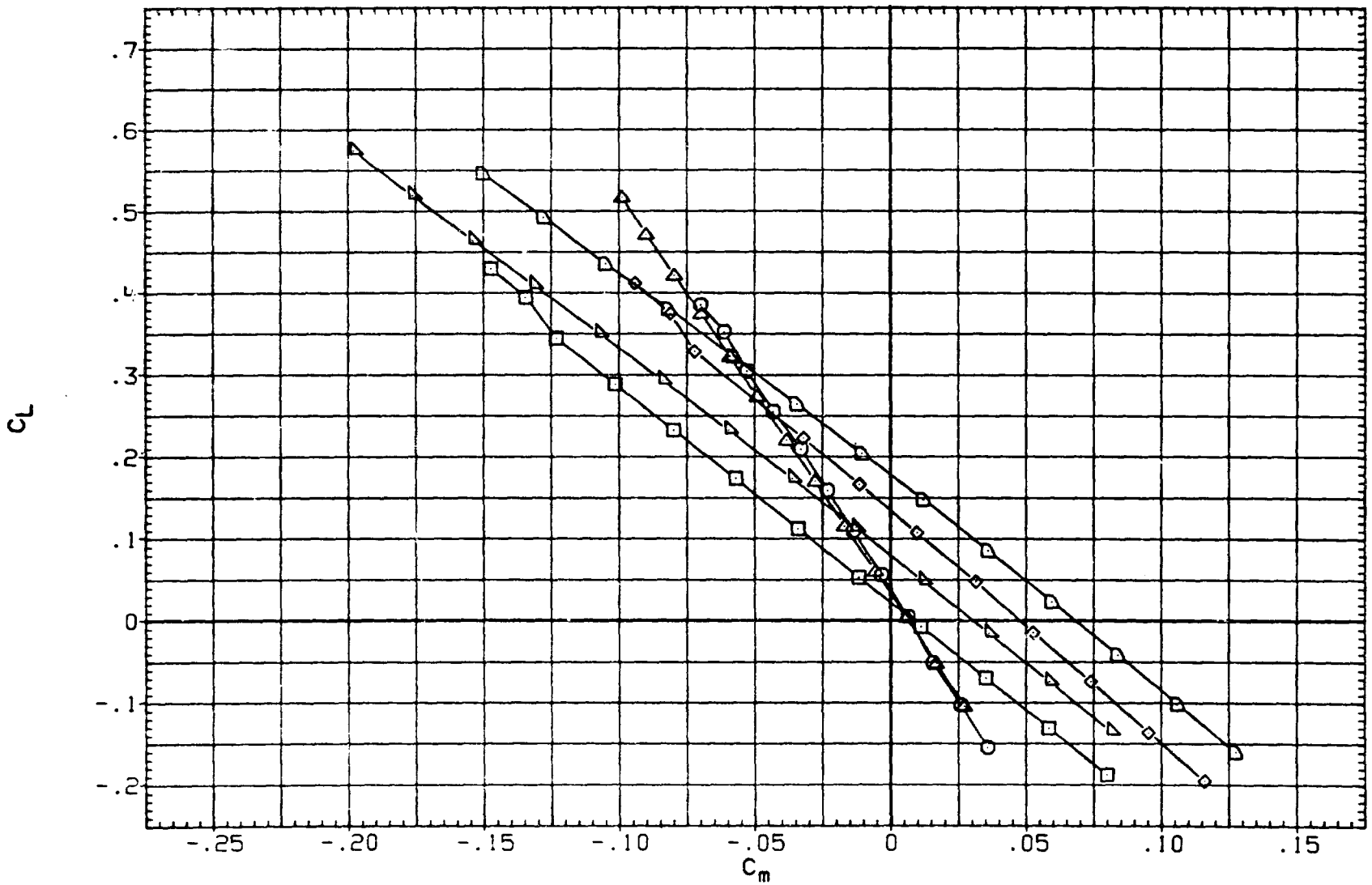

FIG 4. EFFECT OF HORIZ. TAIL FOR BASIC F-8 AND AT WINGS. NO WING CONTROL DEFL.

DATA SET	SYMBOL	CONFIGURATION DESCRIPTION	DH	BETA
(ABD002)	○	BVW1		.000
(ABD003)	□	BVW1H	.000	.000
(ABD004)	◇	BVW1H	-5.000	.000
(ABD005)	△	BVW3		.000
(ABD008)	◁	BVW3H	.000	.000
(ABD009)	⬠	BVW3H	-5.000	.000

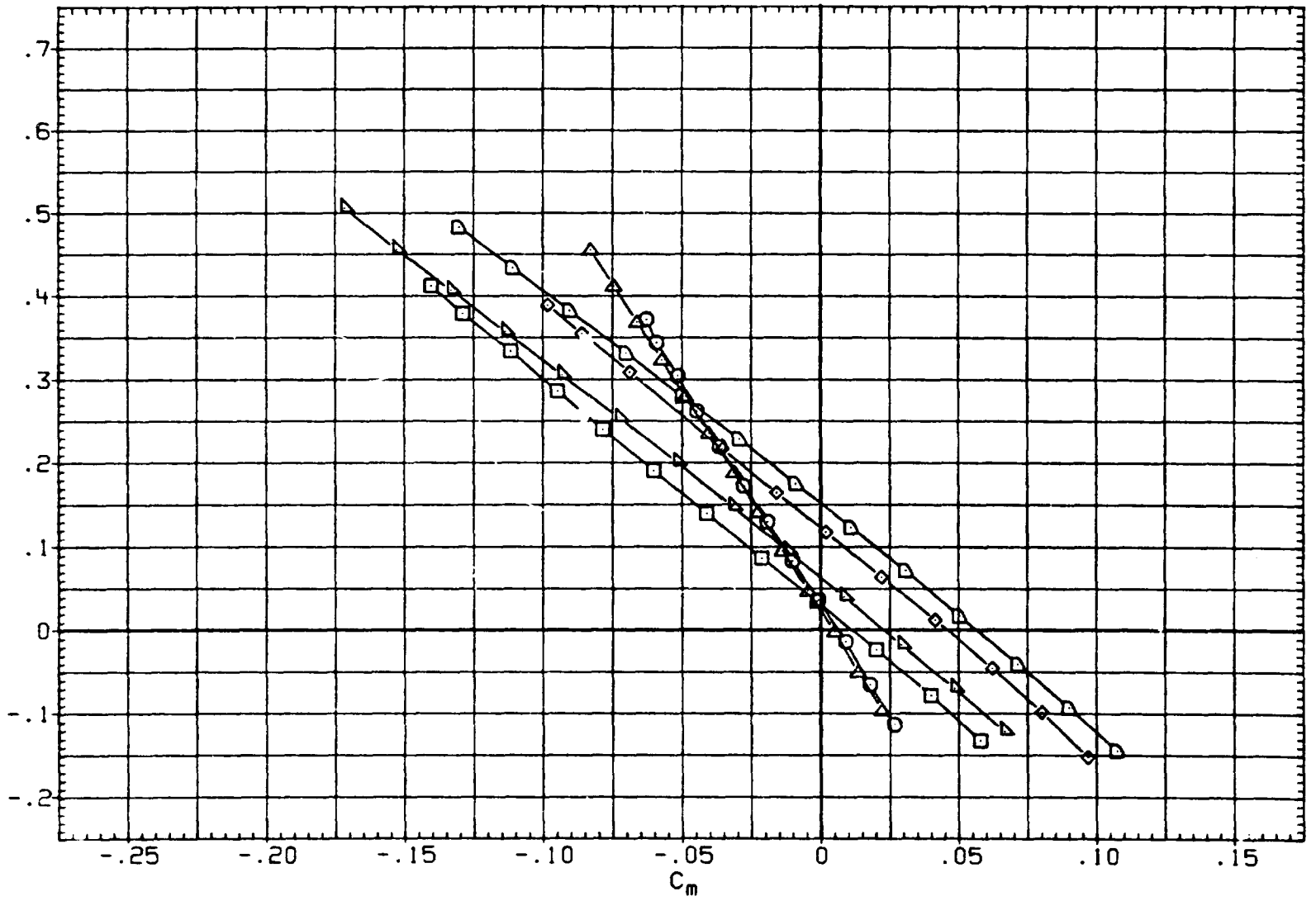

FIG 4. EFFECT OF HORIZ. TAIL FOR BASIC F-8 AND AT WINGS. NO WING CONTROL DEFL.

(D)MACH = 2.00

DATA SET	SYMBOL	CONFIGURATION DESCRIPTION	DTEI	DTEO-L	DTEO-R	DH
(ABD005)	○	BVH3	.000	.000	.000	
(ABD006)	□	DATA NOT AVAILABLE	-2.000	-2.000	-2.000	
(ABD008)	◇	BVH3H	.000	.000	.000	.000
(ABD007)	△	BVH2H	-2.000	-2.000	-2.000	.000

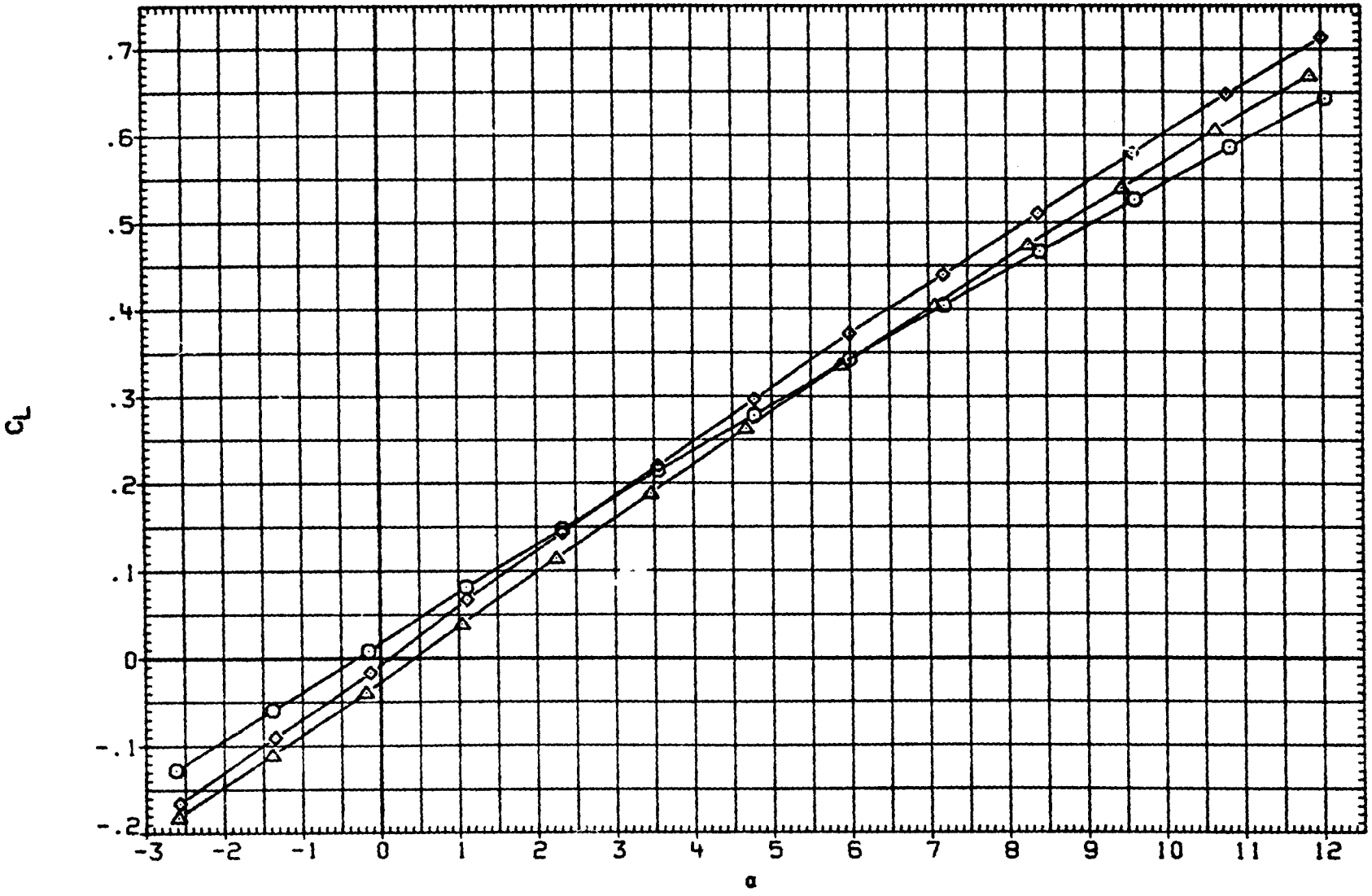

FIG. 5 EFFECT OF SYMMETRICAL T.E. SIMPLE HINGE FLAP DEFLECTIONS, TAIL OFF, ON.

(A)MACH = 1.50

DATA SET	SYMBOL	CONFIGURATION DESCRIPTION	DTE1	DTEO-L	DTEO-R	DH
(ABD005)	○	BVW3	.000	.000	.000	
(ABD006)	□	BVW2	-2.000	-2.000	-2.000	
(ABD008)	◇	BVW3H	.000	.000	.000	.000
(ABD007)	△	BVW2H	-2.000	-2.000	-2.000	.000

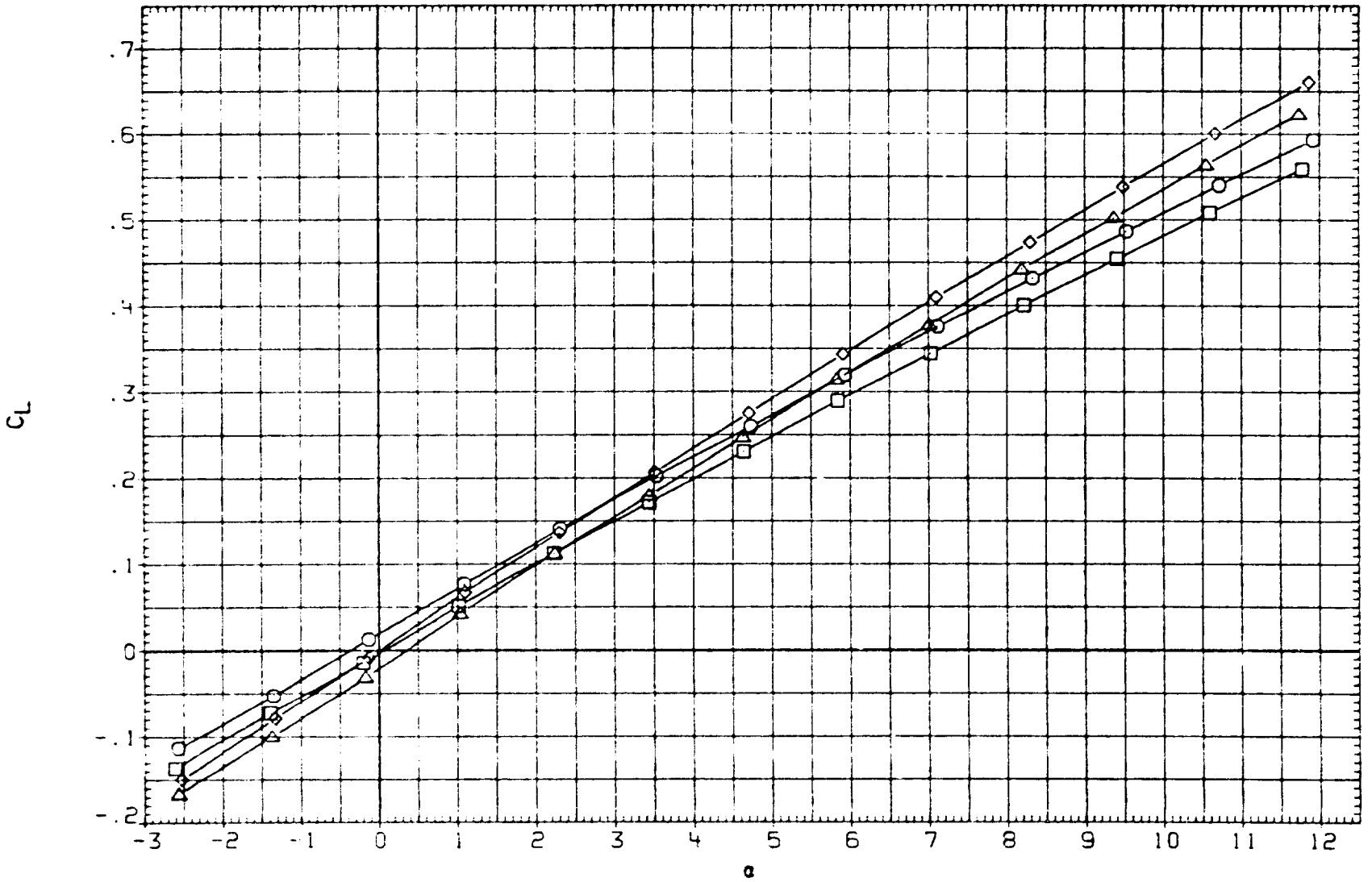

FIG. 5 EFFECT OF SYMMETRICAL T.E. SIMPLE HINGE FLAP DEFLECTIONS, TAIL OFF, ON.

(B) MACH = 1.59

DATA SET	SYMBOL	CONFIGURATION DESCRIPTION	DTEI	DTEO-L	DTEO-R	DH
(ABD005)	○	BVW3	.000	.000	.000	
(ABD006)	□	BVW2	-2.000	-2.000	-2.000	
(ABD008)	◇	BVW3H	.000	.000	.000	.000
(ABD007)	△	BVW2H	-2.000	-2.000	-2.000	.000

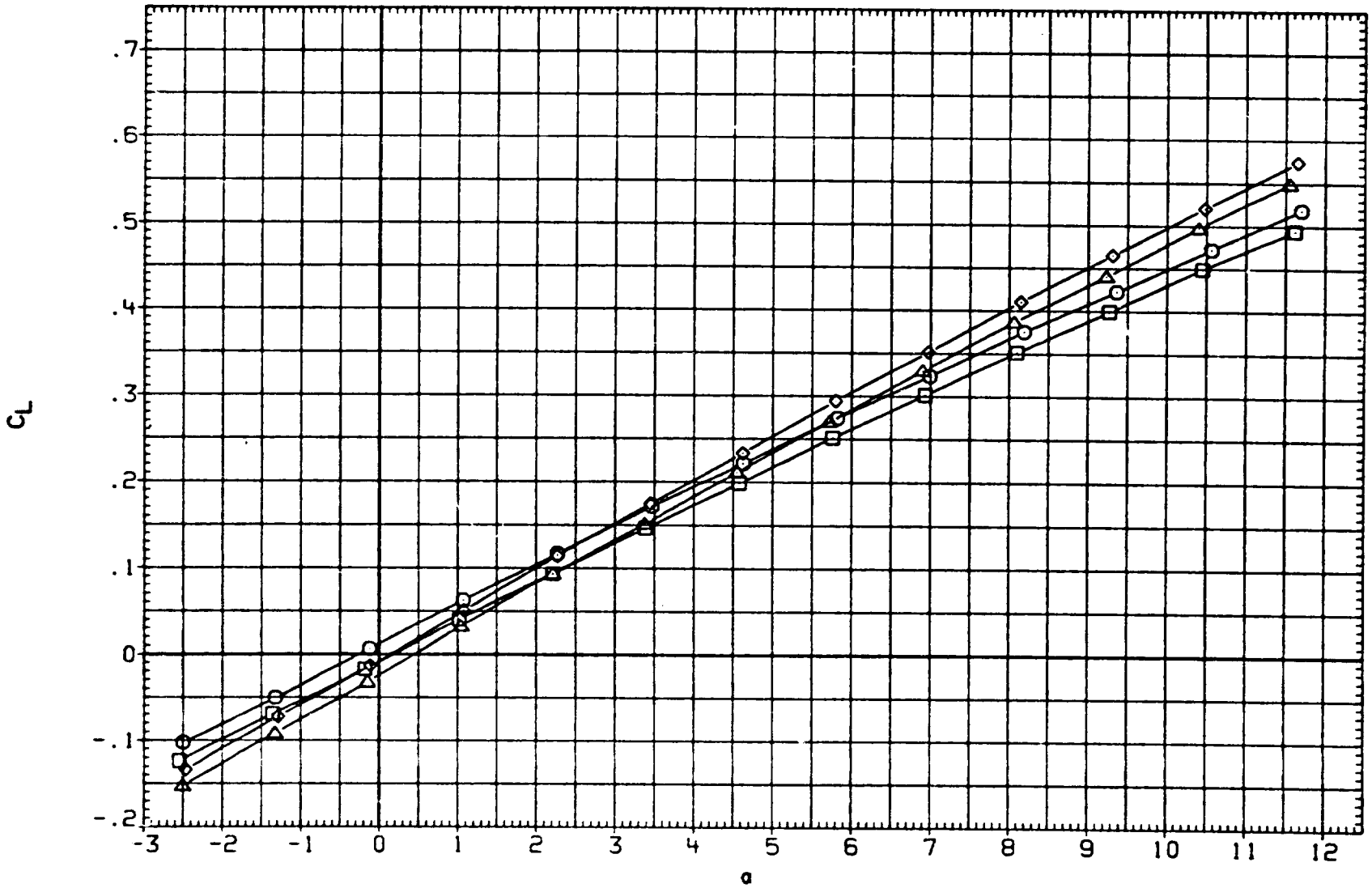

FIG. 5 EFFECT OF SYMMETRICAL T.E. SIMPLE HINGE FLAP DEFLECTIONS, TAIL OFF, ON.

(C)MACH = 1.80

DATA SET	SYMBOL	CONFIGURATION DESCRIPTION	DTEI	DTEO-L	DTEO-R	DH
(ABD005)	○	BVH3	.000	.000	.000	
(ABD006)	□	BVH2	-2.000	-2.000	-2.000	
(ABD008)	◇	BVH3H	.000	.000	.000	.000
(ABD007)	△	BVH2H	-2.000	-2.000	-2.000	.000

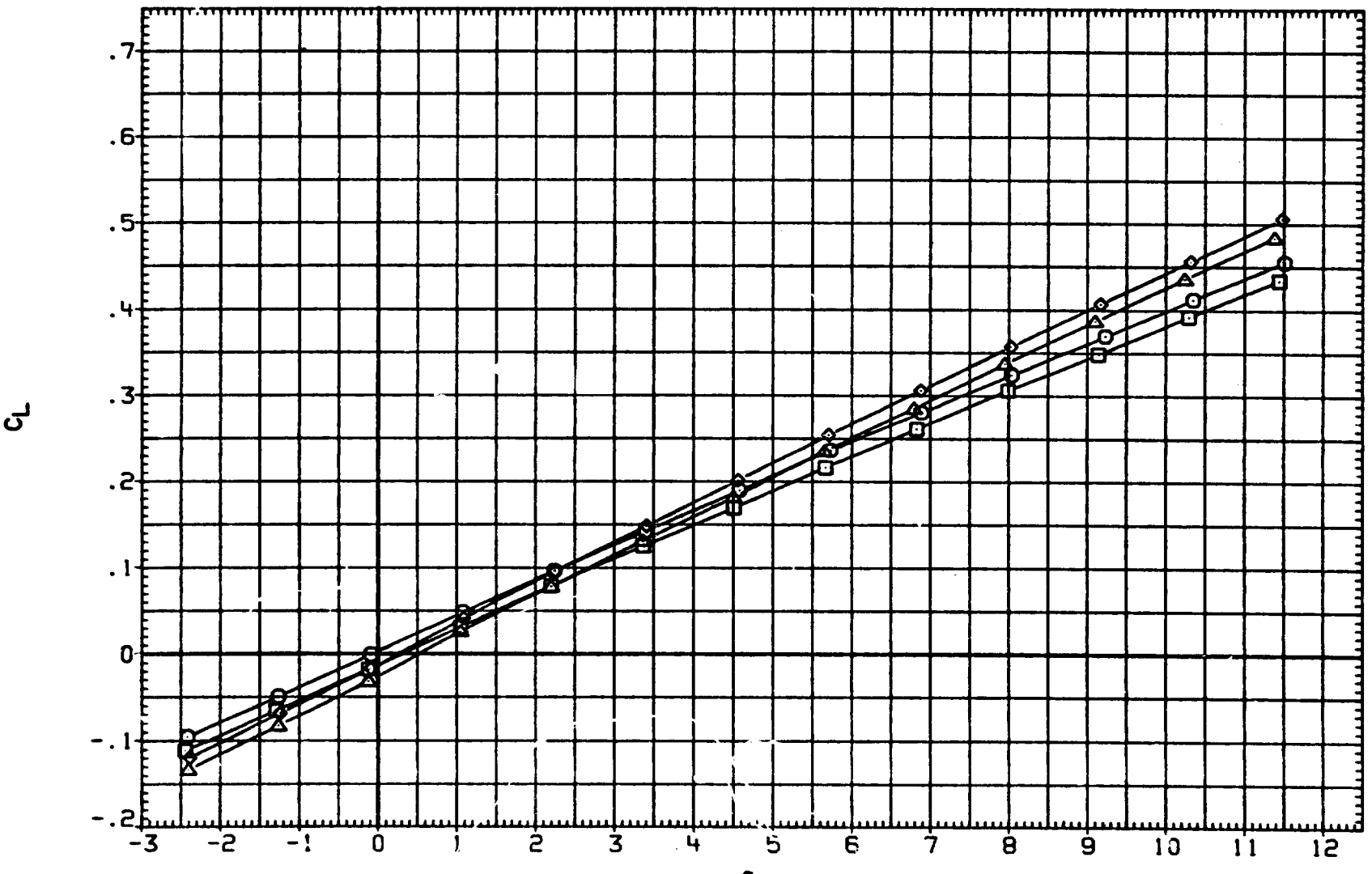

FIG. 5 EFFECT OF SYMMETRICAL T.E. SIMPLE HINGE FLAP DEFLECTIONS, TAIL OFF, ON.

(D)MACH = 2.00

DATA SET	SYMBOL	CONFIGURATION DESCRIPTION	DTEI	DTEO-L	DTEO-R	DH
(ABD005)	○	BVW3	.000	.000	.000	
(ABD006)	□	DATA NOT AVAILABLE	-2.000	-2.000	-2.000	
(ABD008)	◇	BVW3H	.000	.000	.000	.000
(ABD007)	△	BVW2H	-2.000	-2.000	-2.000	.000

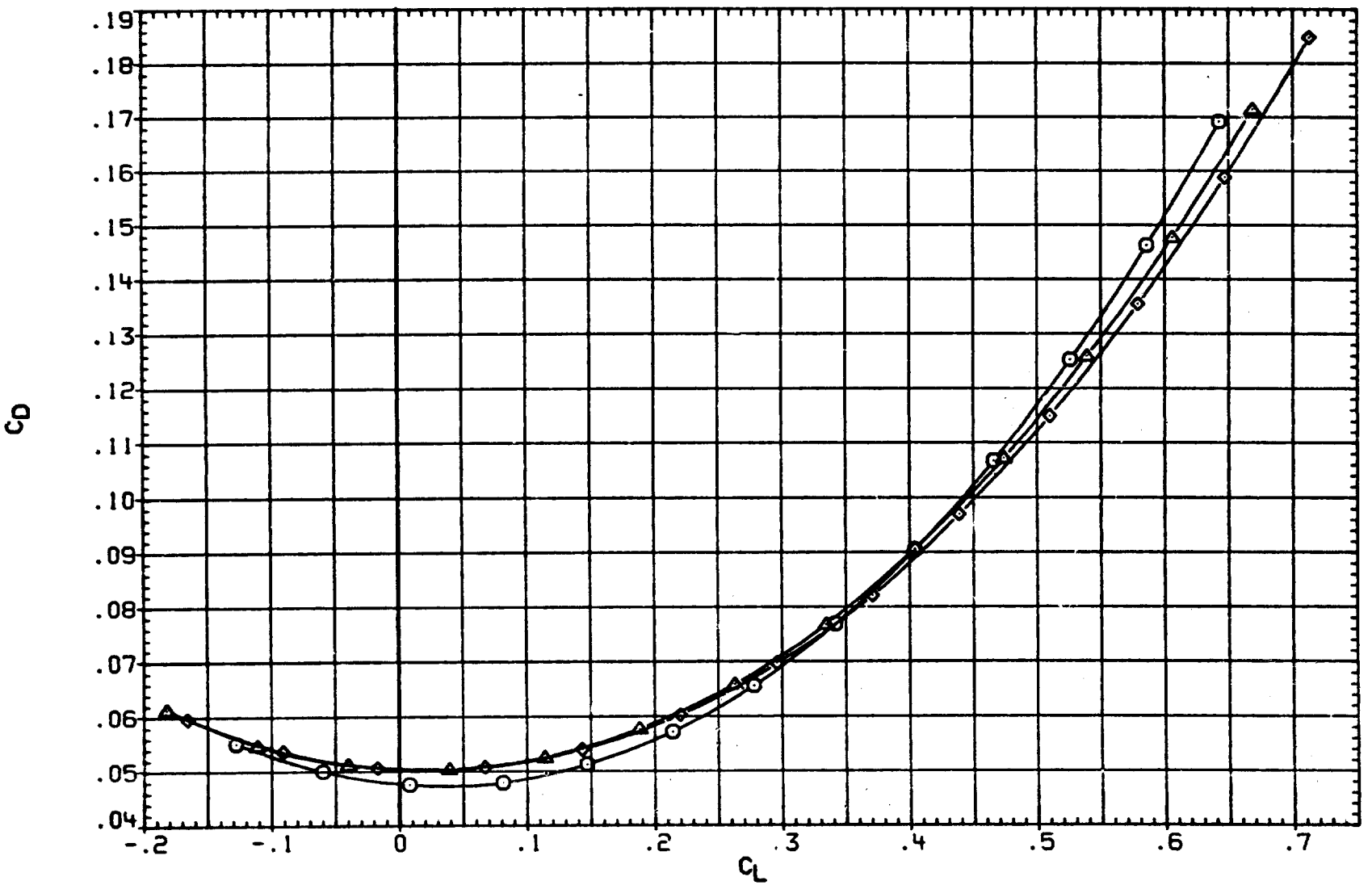

FIG. 5 EFFECT OF SYMMETRICAL T.E. SIMPLE HINGE FLAP DEFLECTIONS, TAIL OFF, ON.

(A)MACH = 1.50

DATA SET	SYMBOL	CONFIGURATION DESCRIPTION	DTEI	DTEO-L	DTEO-R	DH
(ABD005)	○	BVW3	.000	.000	.000	
(ABD006)	□	BVW2	-2.000	-2.000	-2.000	
(ABD008)	◇	BVW3H	.000	.000	.000	.000
(ABD007)	△	BVW2H	-2.000	-2.000	-2.000	.000

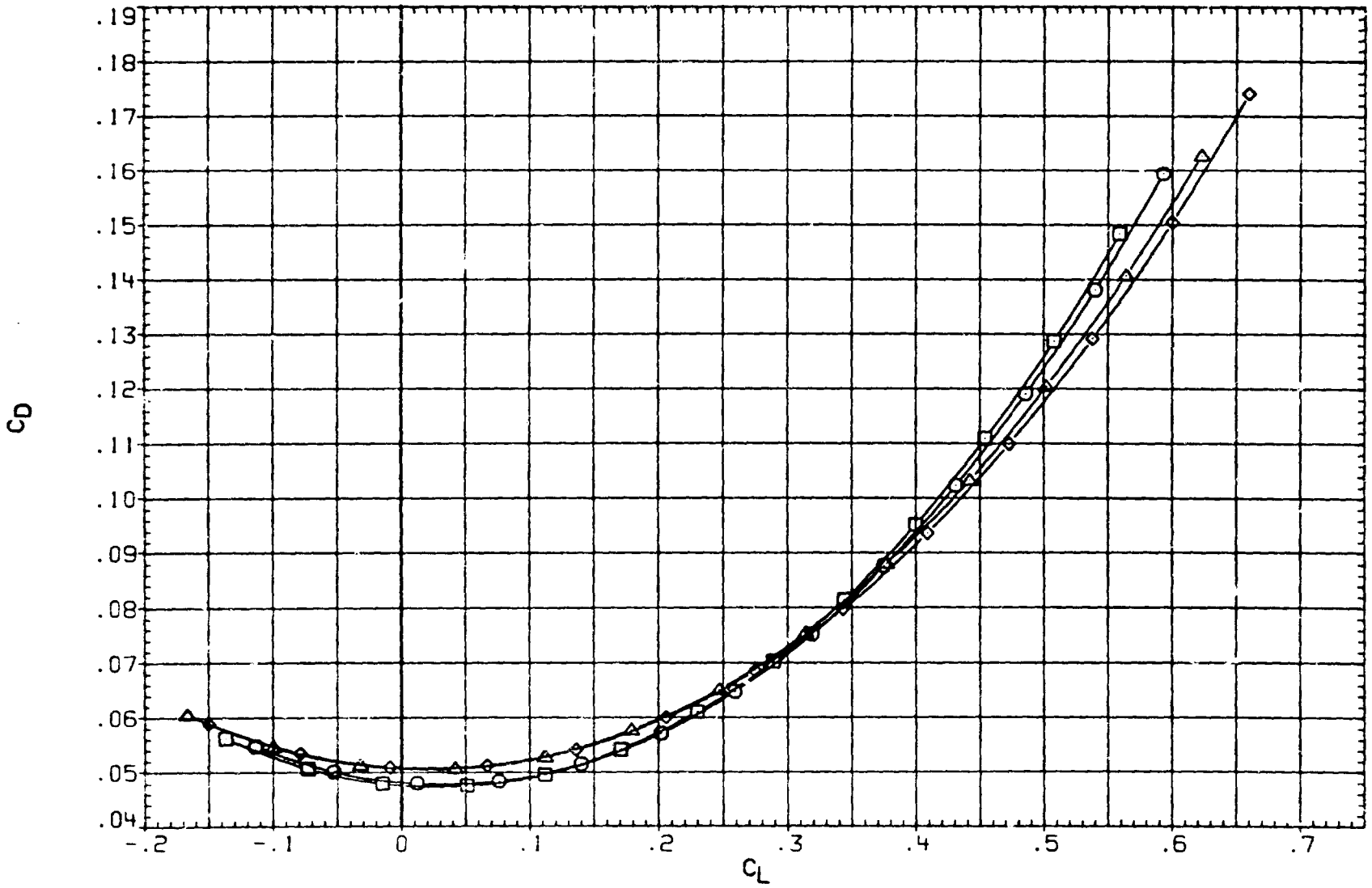

FIG. 5 EFFECT OF SYMMETRICAL T.E. SIMPLE HINGE FLAP DEFLECTIONS, TAIL OFF, ON.

(B)MACH = 1.59

DATA SET	SYMBOL	CONFIGURATION DESCRIPTION	DTEI	DTEO-L	DTEO-R	DH
(ABD005)	○	BVH3	.000	.000	.000	
(ABD006)	□	BVH2	-2.000	-2.000	-2.000	
(ABD008)	◇	BVH3H	.000	.000	.000	.000
(ABD007)	△	BVH2H	-2.000	-2.000	-2.000	.000

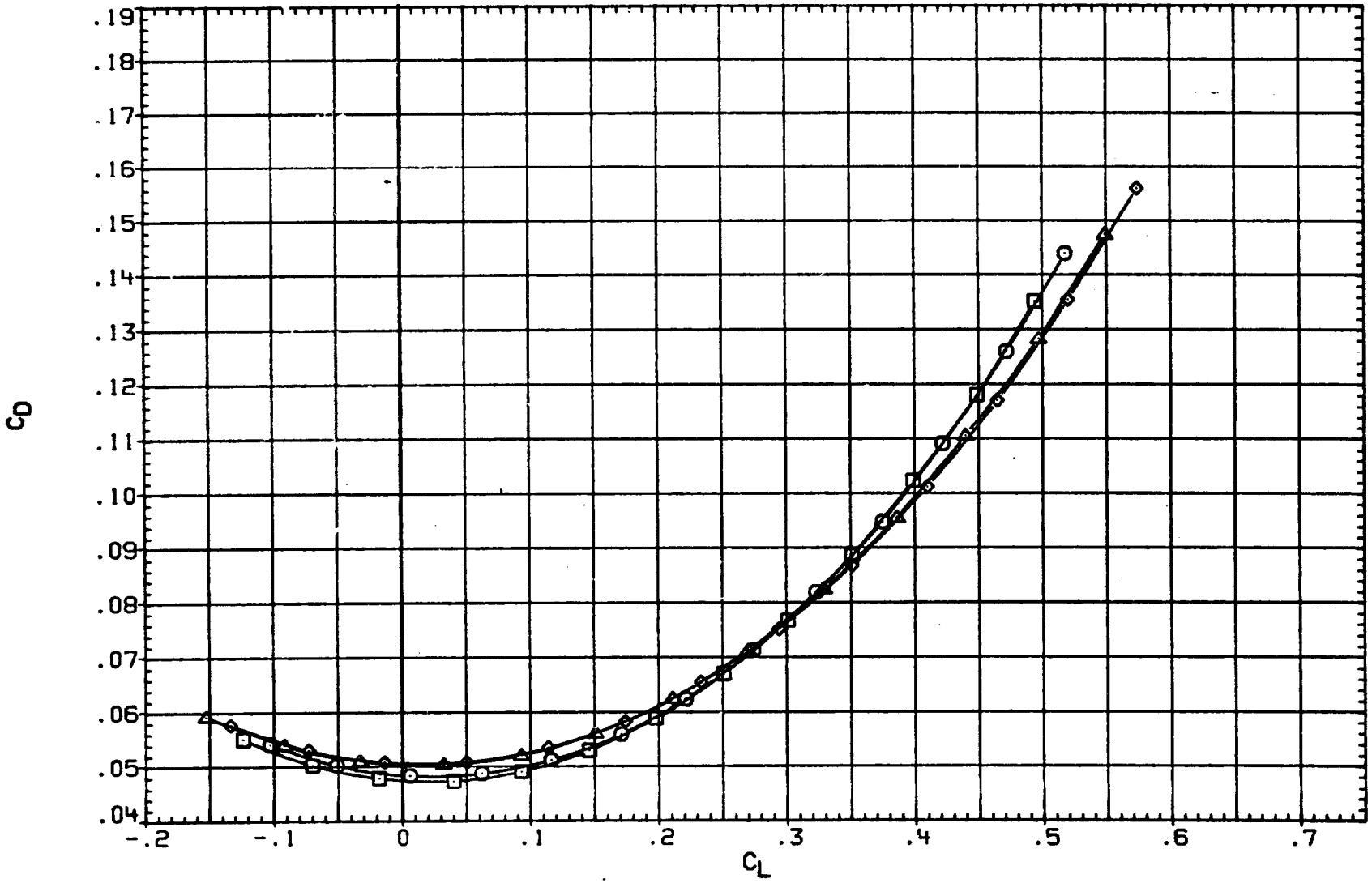

FIG. 5 EFFECT OF SYMMETRICAL T.E. SIMPLE HINGE FLAP DEFLECTIONS, TAIL OFF, ON.

(C)MACH = 1.80

DATA SET	SYMBOL	CONFIGURATION DESCRIPTION	DTEI	DTEO-L	DTEO-R	DH
(ABD005)	○	BVH3	.000	.000	.000	
(ABD006)	□	BVH2	-2.000	-2.000	-2.000	
(ABD008)	◇	BVH3H	.000	.000	.000	.000
(ABD007)	△	BVH2H	-2.000	-2.000	-2.000	.000

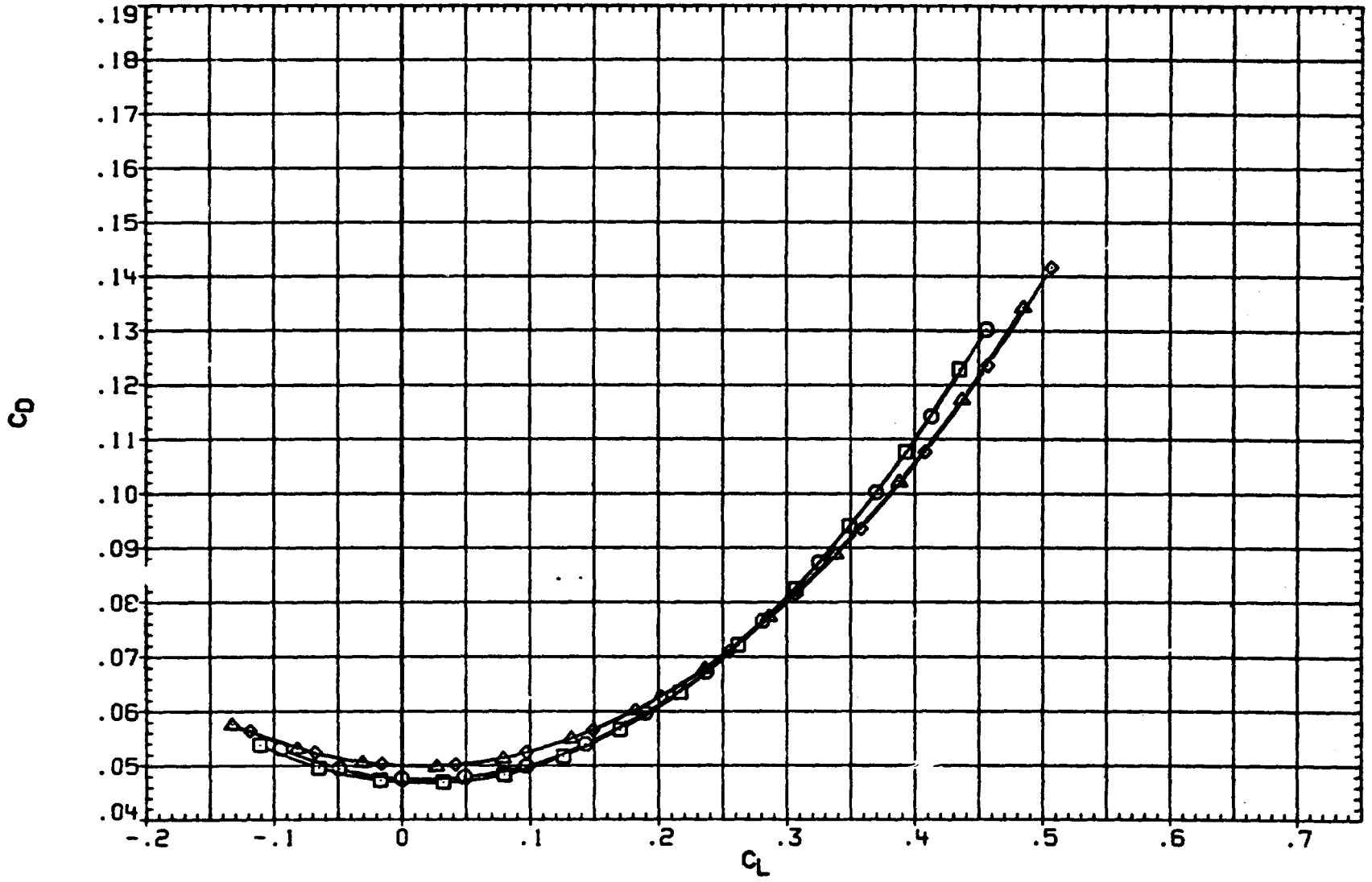

FIG. 5 EFFECT OF SYMMETRICAL T.E. SIMPLE HINGE FLAP DEFLECTIONS, TAIL OFF, ON.

(D)MACH = 2.00

DATA SET	SYMBOL	CONFIGURATION DESCRIPTION	DTEI	DTEO-L	DTEO-R	DH
(ABD005)	○	BVW3	.000	.000	.000	
(ABD006)	□	DATA NOT AVAILABLE	-2.000	-2.000	-2.000	
(ABD008)	◇	BVW3H	.000	.000	.000	.000
(ABD007)	△	BVW2H	-2.000	-2.000	-2.000	.000

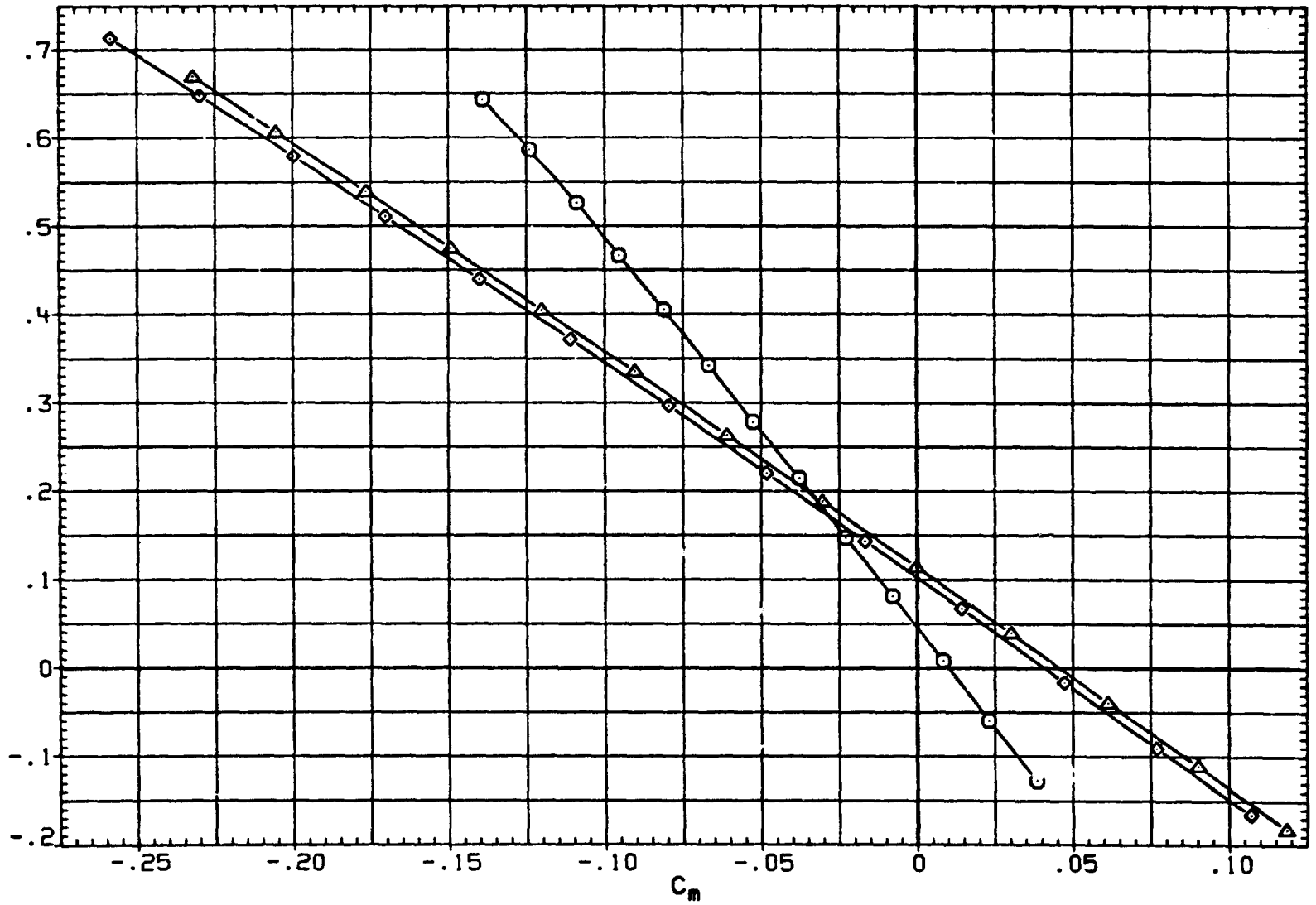

FIG. 5 EFFECT OF SYMMETRICAL T.E. SIMPLE HINGE FLAP DEFLECTIONS, TAIL OFF, ON.

DATA SET	SYMBOL	CONFIGURATION DESCRIPTION	DTEI	DTEO-L	DTEO-R	OH
(ABD005)	○	BVH3	.000	.000	.000	
(ABD006)	□	BVH2	-2.000	-2.000	-2.000	
(ABD008)	◇	BVH3H	.000	.000	.000	.000
(ABD007)	△	BVH2H	-2.000	-2.000	-2.000	.000

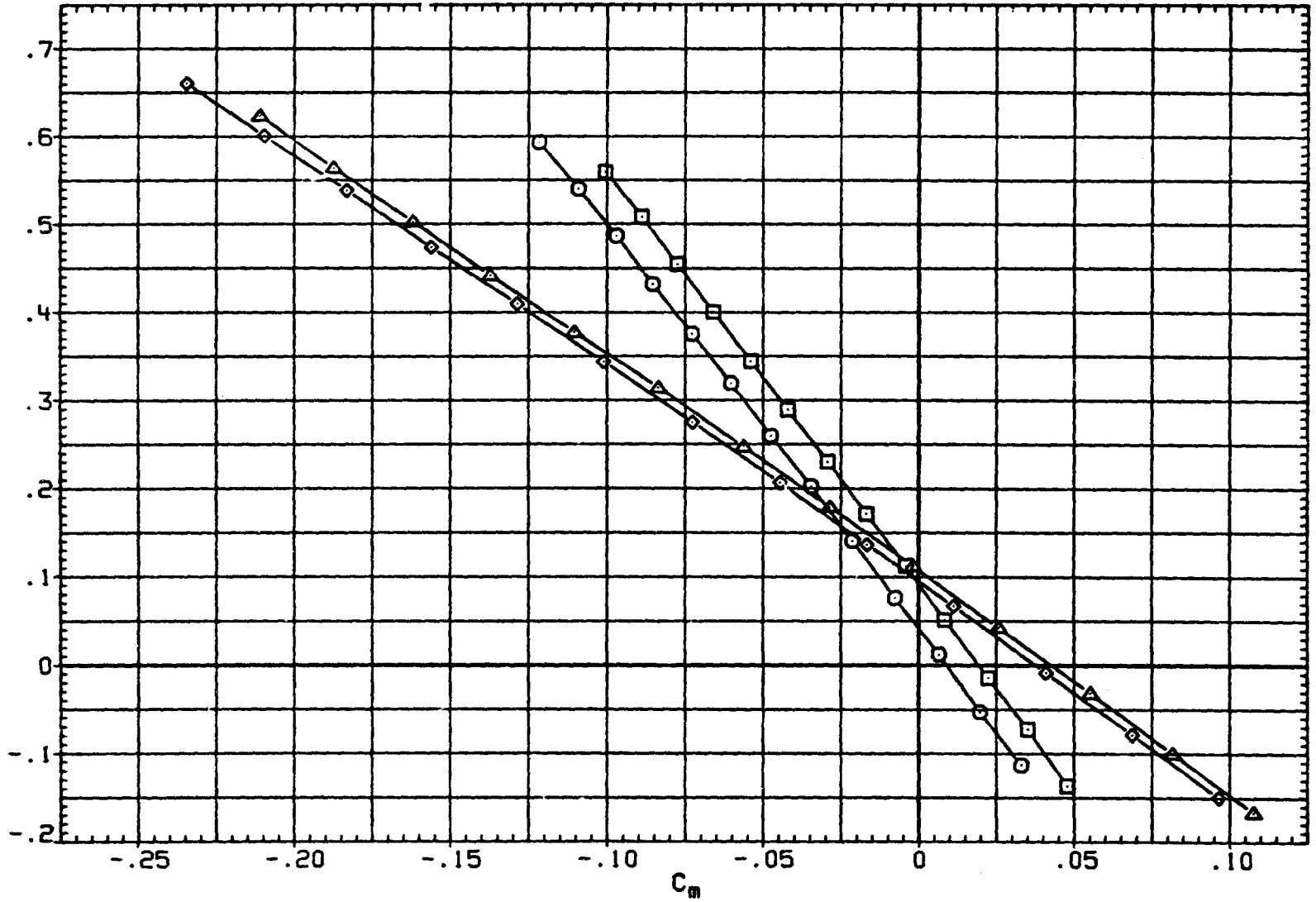

FIG. 5 EFFECT OF SYMMETRICAL T.E. SIMPLE HINGE FLAP DEFLECTIONS, TAIL OFF, ON.

(B) MACH = 1.59

DATA SET	SYMBOL	CONFIGURATION DESCRIPTION	DTEI	DTEO-L	DTEO-R	DH
(ABD005)	○	BVH3	.000	.000	.000	
(ABD006)	□	BVH2	-2.000	-2.000	-2.000	
(ABD008)	◇	BVH3H	.000	.000	.000	.000
(ABD007)	△	BVH2H	-2.000	-2.000	-2.000	.000

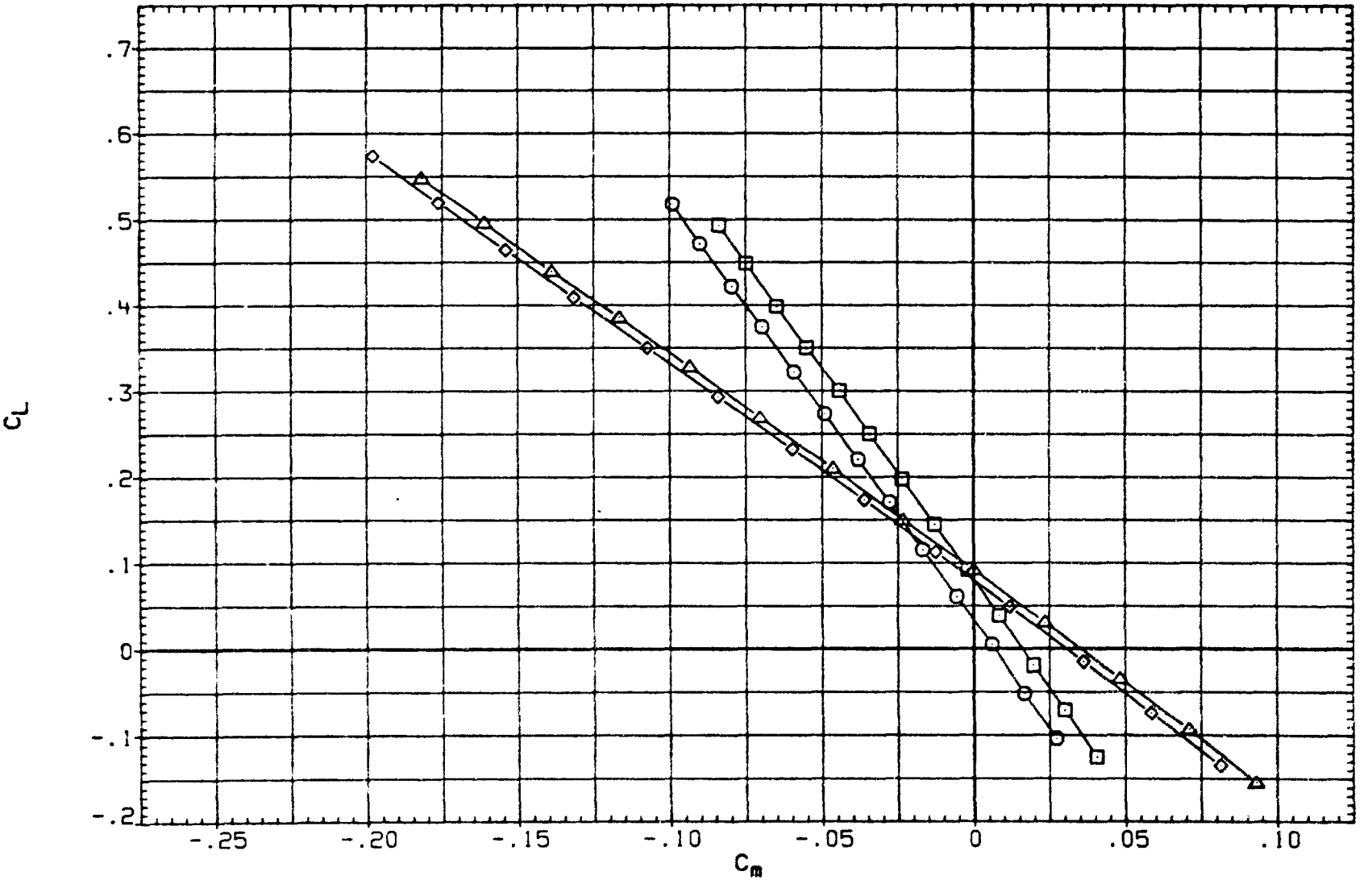

FIG. 5 EFFECT OF SYMMETRICAL I.F. SIMPLE HINGE FLAP DEFLECTIONS, TAIL OFF, ON

DATA SET	SYMBOL	CONFIGURATION DESCRIPTION	DTEI	DTEO-L	DTEO-R	DH
(ABD005)	○	BVW3	.000	.000	.000	
(ABD006)	□	BVW2	-2.000	-2.000	-2.000	
(ABD008)	◇	BVW3H	.000	.000	.000	.000
(ABD007)	△	BVW2H	-2.000	-2.000	-2.000	.000

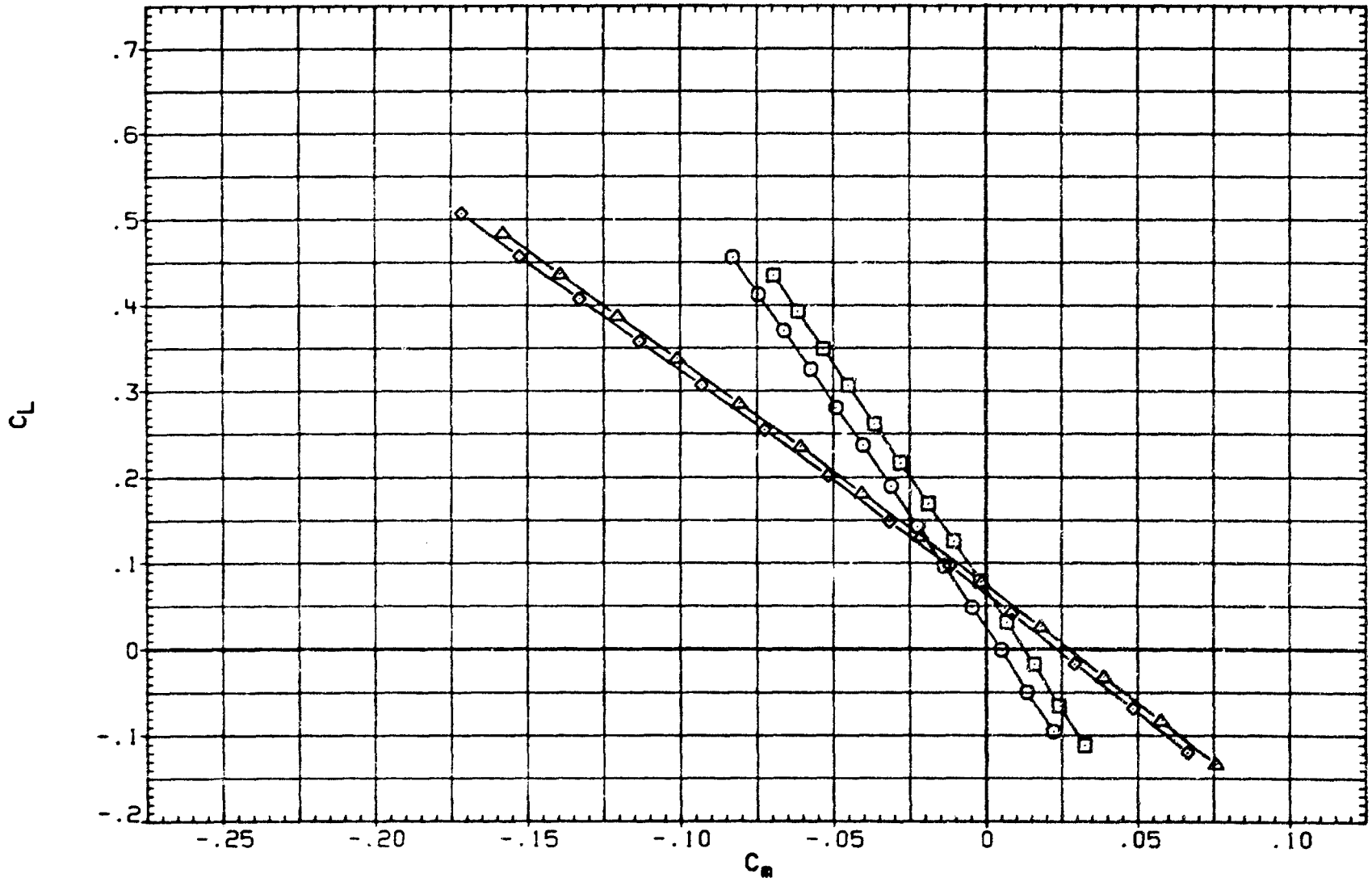

FIG. 5 EFFECT OF SYMMETRICAL T.E. SIMPLE HINGE FLAP DEFLECTIONS, TAIL OFF, ON.

(D)MACH = 2.00

DATA SET	SYMBOL	CONFIGURATION DESCRIPTION	DTEO-L	DTEO-R	DH	DTEI
(AB0008)	○	BVH3H	.000	.000	.000	.000
(AB0010)	□	BVH3H	5.000	-5.000	.000	.000
(AB0011)	◇	BVH3H	.000	-15.000	.000	.000

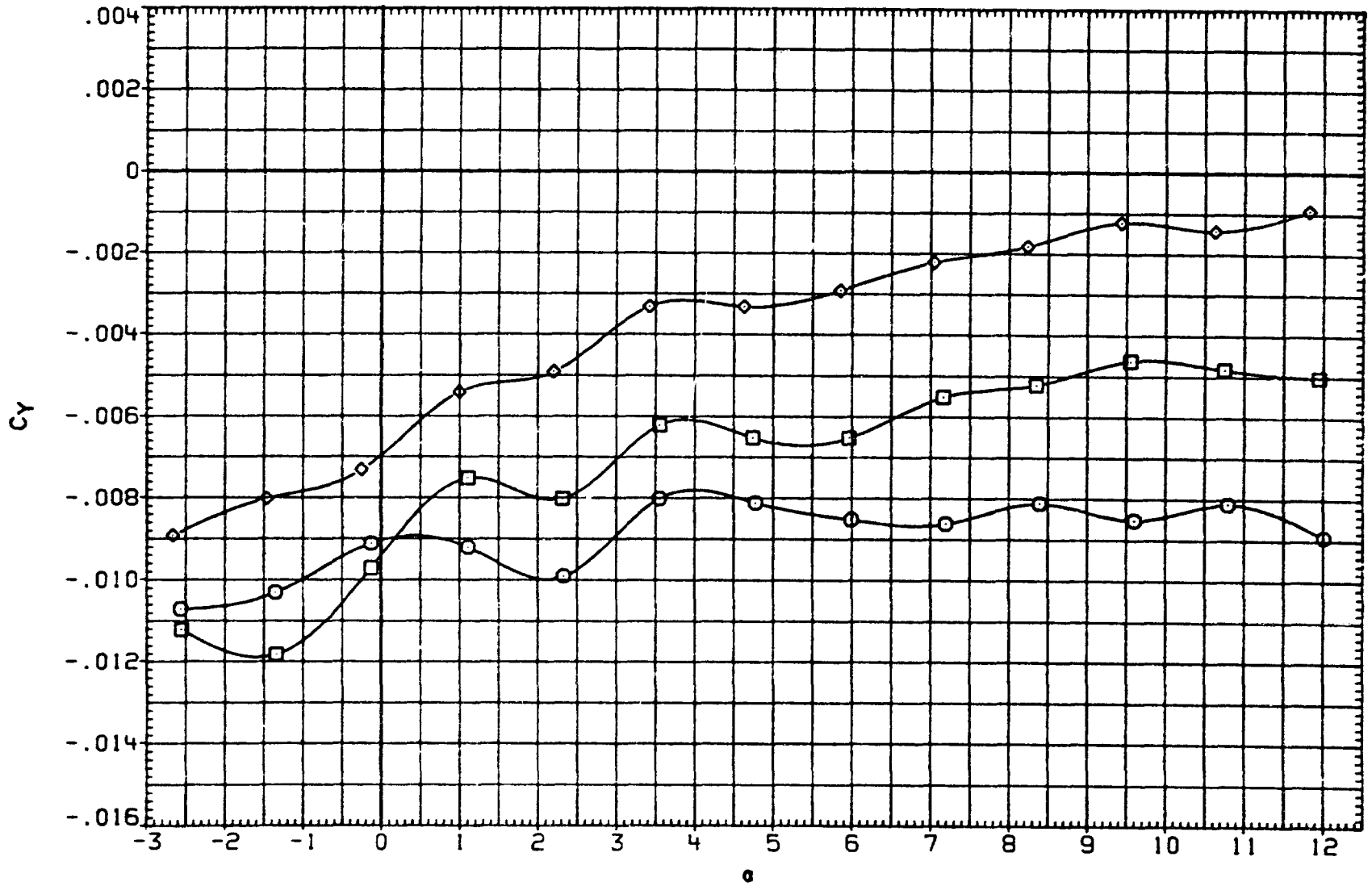

FIG 6. EFFECT OF DIFFERENTIAL OUTBOARD CONFORMAL FLAP DEFLECTIONS.

(A)MACH = 1.50

DATA SET	SYMBOL	CONFIGURATION DESCRIPTION	DTEO-L	DTEO-R	DH	DTEI
(ABD008)	○	BVW3H	.000	.000	.000	.000
(ABD010)	□	BVW3H	5.000	-5.000	.000	.000
(ABD011)	◇	BVW3H	.000	-15.000	.000	.000

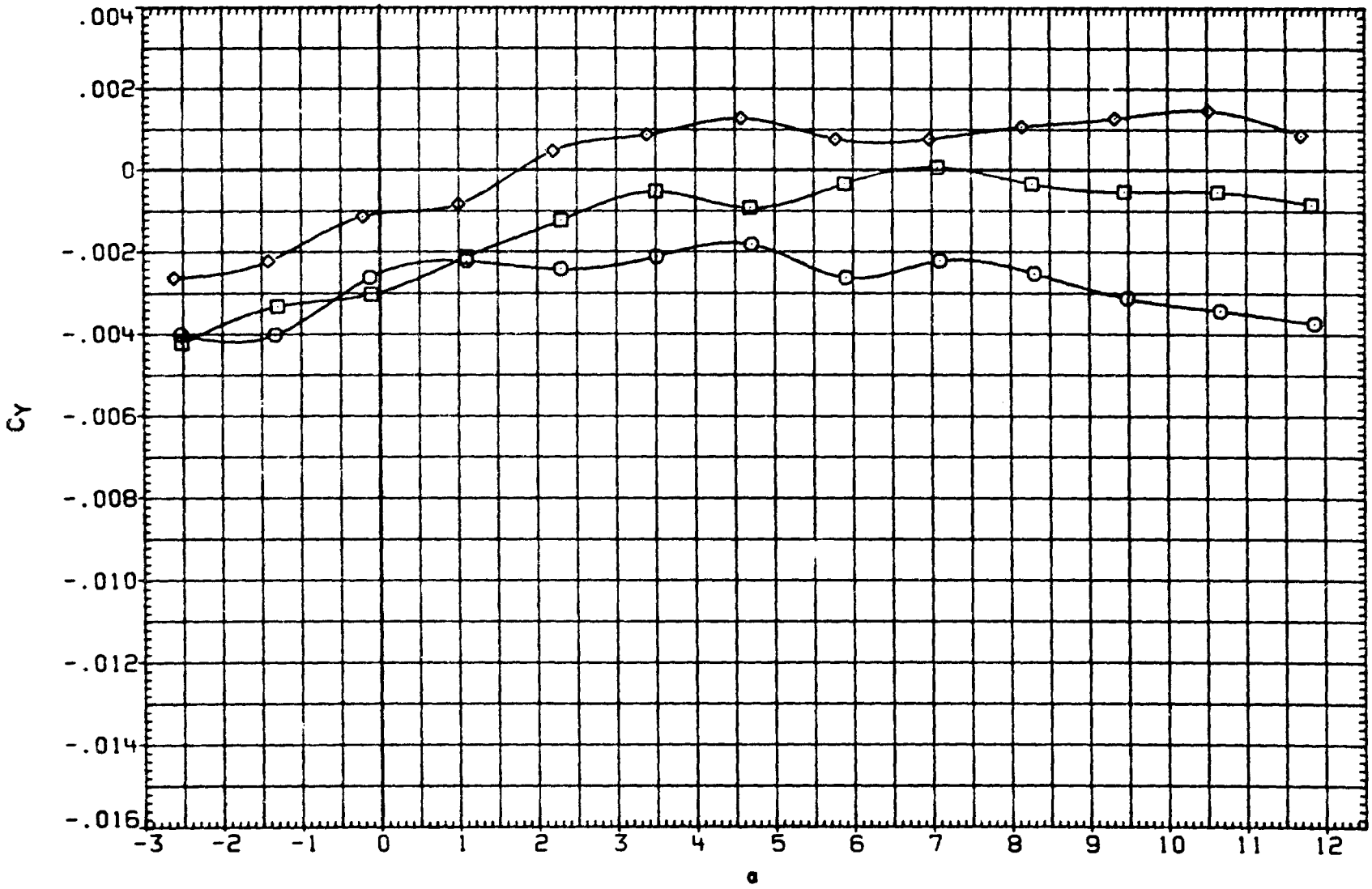

FIG 6. EFFECT OF DIFFERENTIAL OUTBOARD CONFORMAL FLAP DEFLECTIONS.

(B)MACH = 1.60

DATA SET	SYMBOL	CONFIGURATION DESCRIPTION	DTEO-L	DTEO-R	DH	DTEI
(ABD008)	○	BVW3H	.000	.000	.000	.000
(ABD010)	□	BVW3H	5.000	-5.000	.000	.000
(ABD011)	◇	BVW3H	.000	-15.000	.000	.000

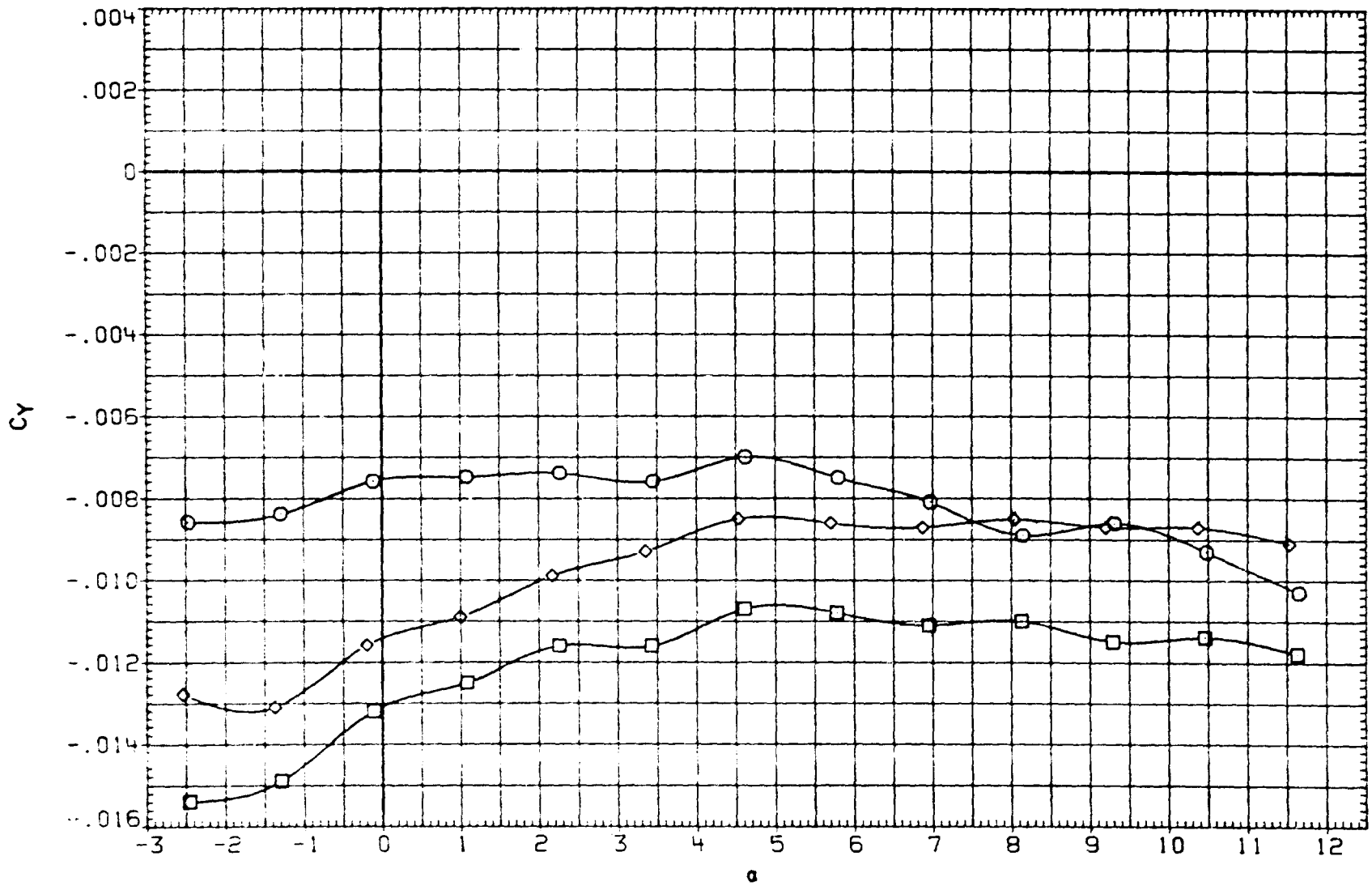

FIG 6. EFFECT OF DIFFERENTIAL OUTBOARD CONFORMAL FLAP DEFLECTIONS.

DATA SET	SYMBOL	CONFIGURATION DESCRIPTION	DTEO-L	DTEO-R	DH	DTEI
(ABD008)	○	BVH3H	.000	.000	.000	.000
(ABD010)	□	BVH3H	5.000	-5.000	.000	.000
(ABD011)	◇	BVH3H	.000	-15.000	.000	.000

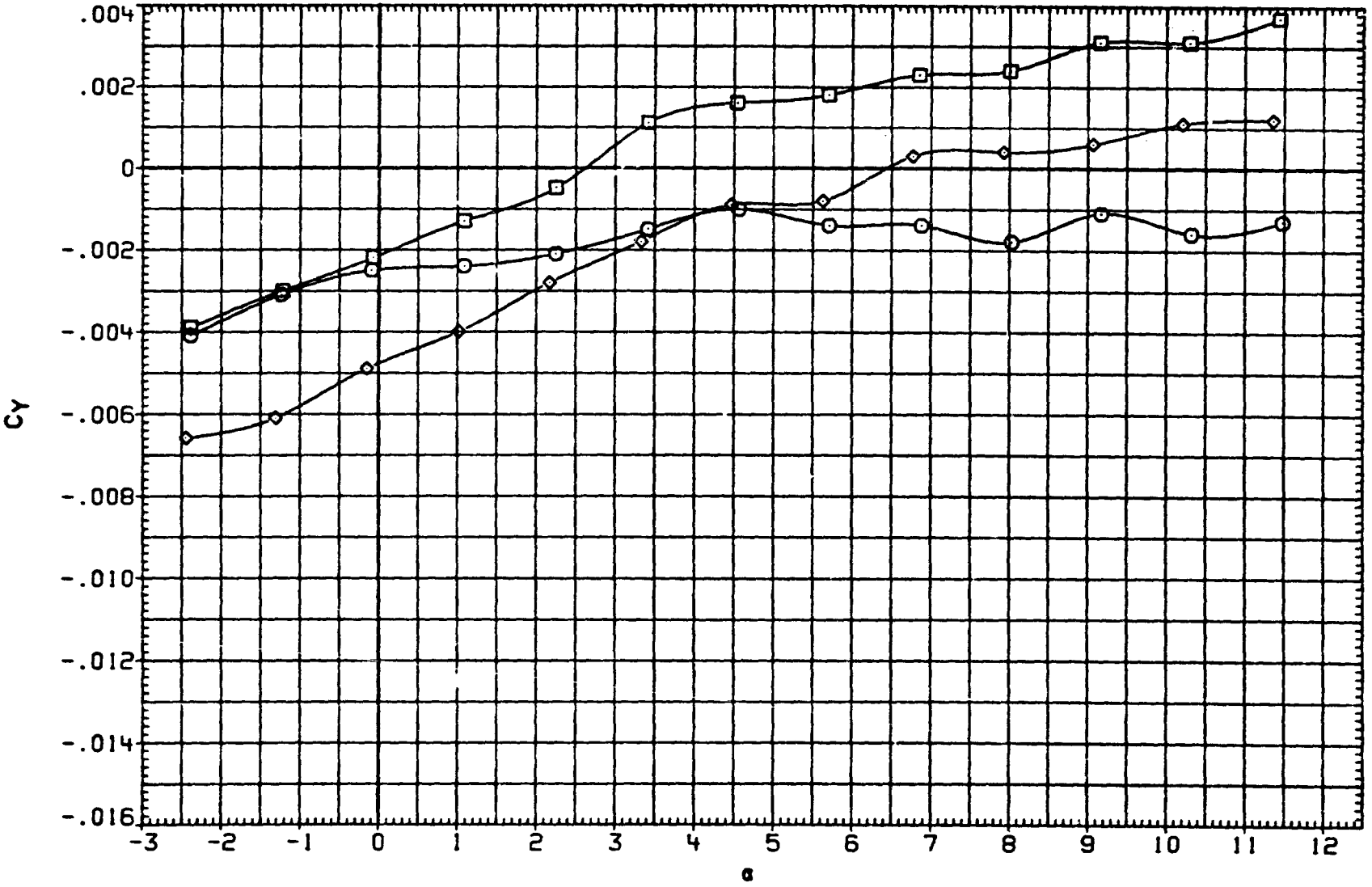

FIG 6. EFFECT OF DIFFERENTIAL OUTBOARD CONFORMAL FLAP DEFLECTIONS.

(D)MACH = 2.00

DATA SET	SYMBOL	CONFIGURATION DESCRIPTION	DTEO-L	DTEO-R	DH	DTEI
(ABD008)	○	BVH3H	.000	.000	.000	.000
(ABD010)	□	BVH3H	5.000	-5.000	.000	.000
(ABD011)	◇	BVH3H	.000	-15.000	.000	.000

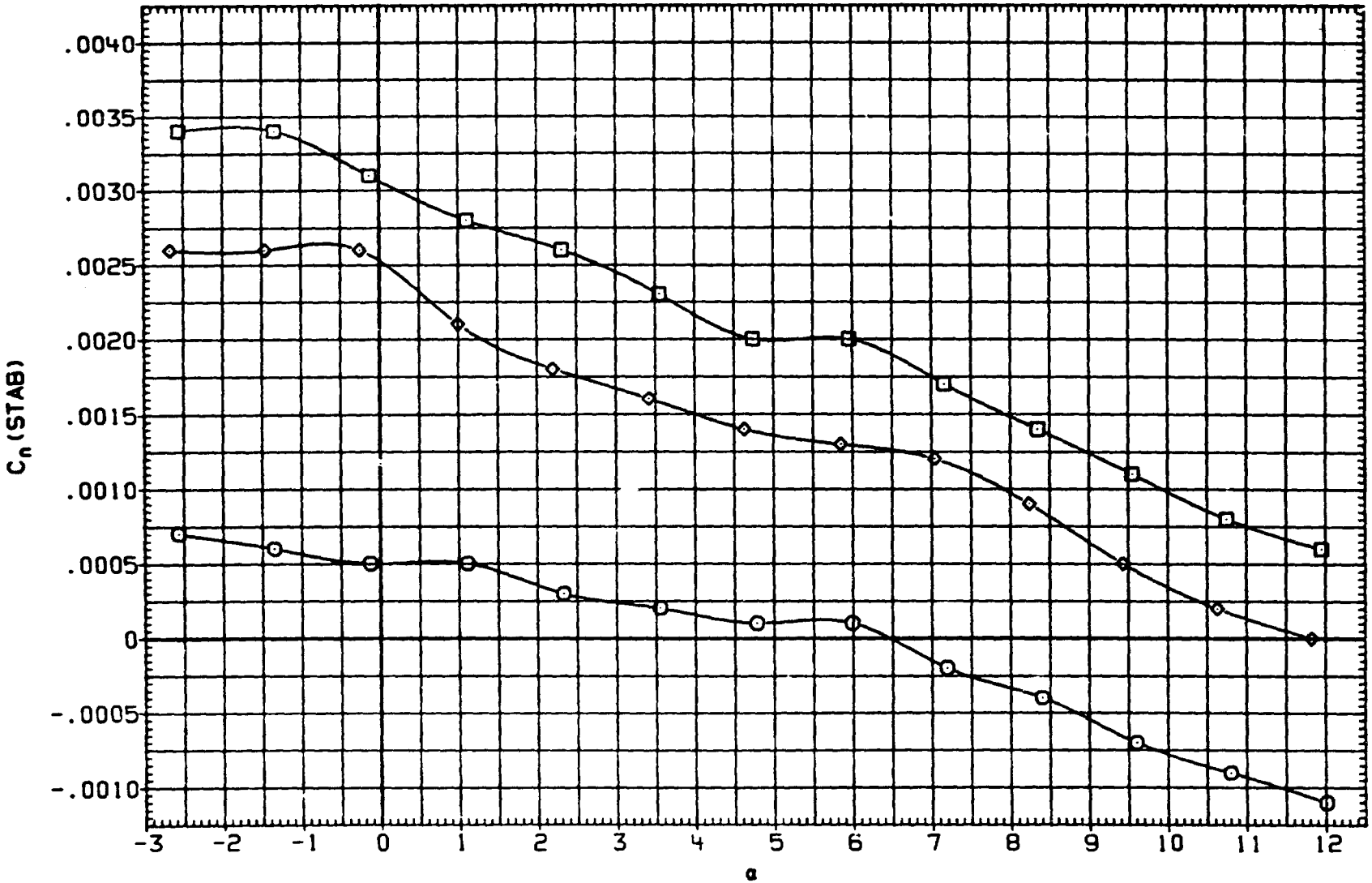

FIG 6. EFFECT OF DIFFERENTIAL OUTBOARD CONFORMAL FLAP DEFLECTIONS.

(A)MACH = 1.50

DATA SET	SYMBOL	CONFIGURATION DESCRIPTION	DTEO-L	DTEO-R	DH	DTEI
(AB0008)	○	BVW3H	.000	.000	.000	.000
(AB0010)	□	BVW3H	5.000	-5.000	.000	.000
(AB0011)	◇	BVW3H	.000	-15.000	.000	.000

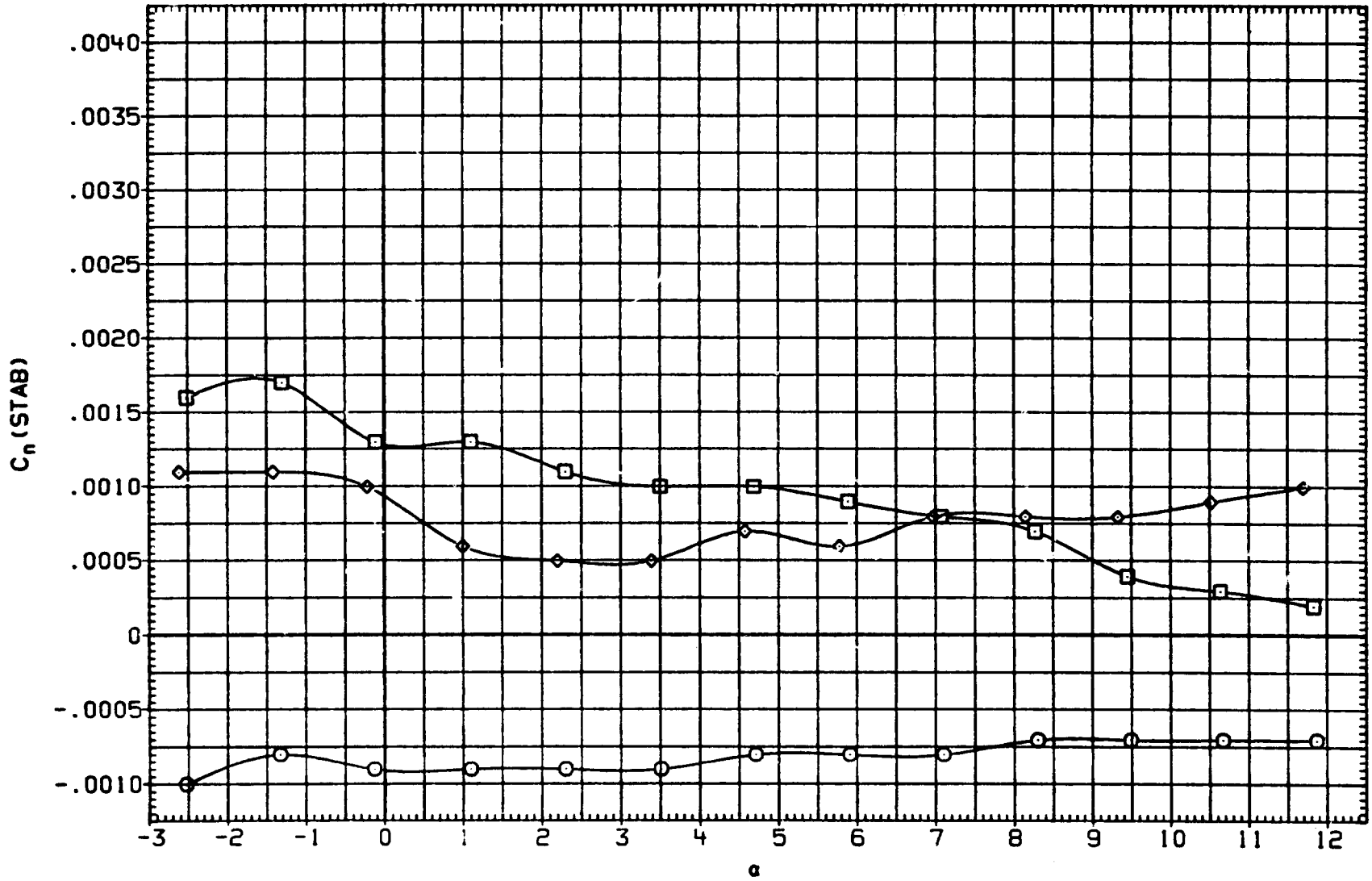

FIG 6. EFFECT OF DIFFERENTIAL OUTBOARD CONFORMAL FLAP DEFLECTIONS.

(B)MACH = 1.60

DATA SET	SYMBOL	CONFIGURATION DESCRIPTION	DTEO-L	DTEO-R	DH	DTEI
(AB0008)	○	BVW3H	.000	.000	.000	.000
(AB0010)	□	BVW3H	5.000	-5.000	.000	.000
(AB0011)	◇	BVW3H	.000	-15.000	.000	.000

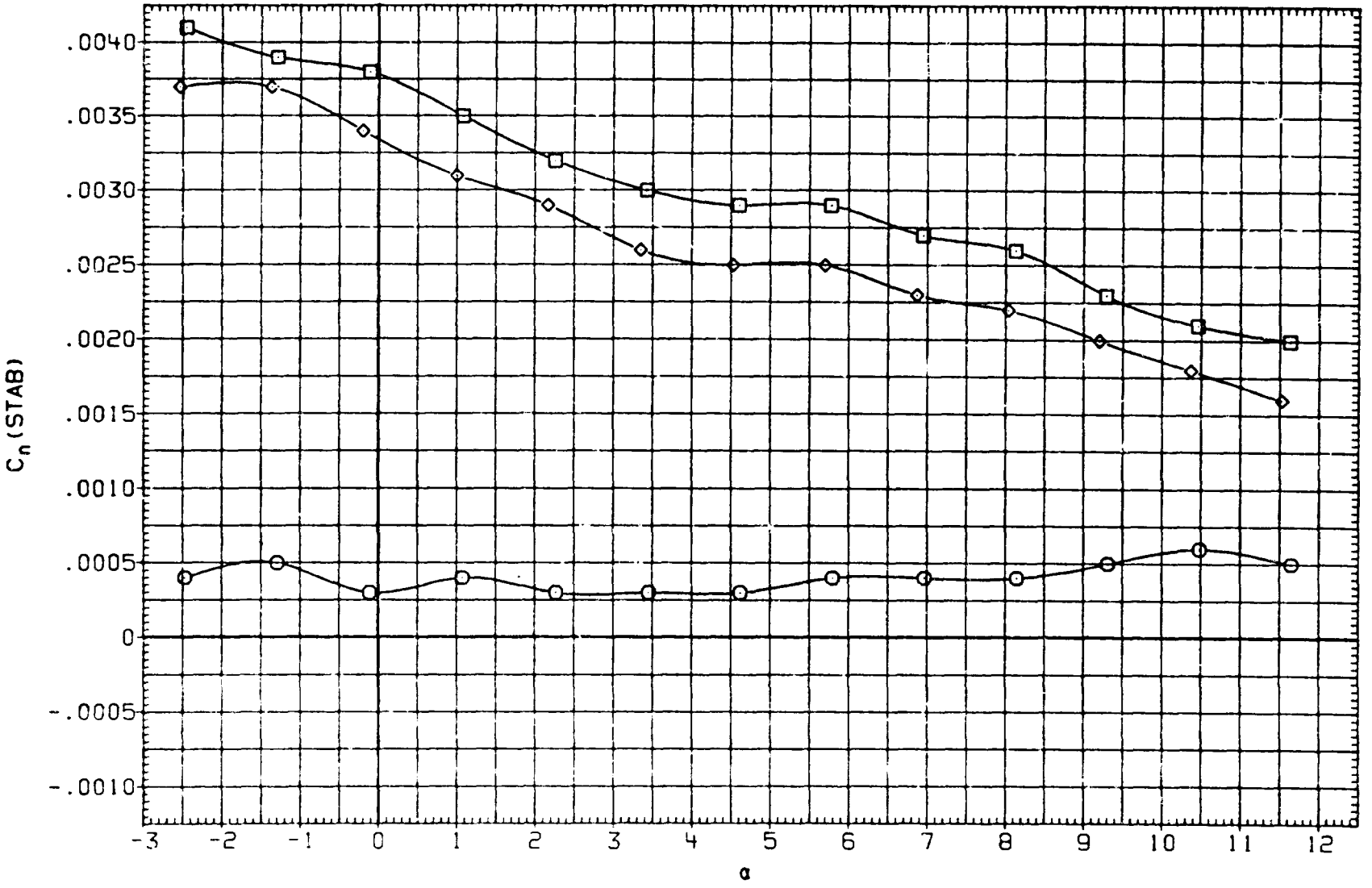

FIG 6. EFFECT OF DIFFERENTIAL OUTBOARD CONFORMAL FLAP DEFLECTIONS.

DATA SET	SYMBOL	CONFIGURATION DESCRIPTION	DTEO-L	DTEO-R	DH	DTEI
(ABD008)	○	BVW3H	.000	.000	.000	.000
(ABD010)	□	BVW3H	5.000	-5.000	.000	.000
(ABD011)	◇	BVW3H	.000	-15.000	.000	.000

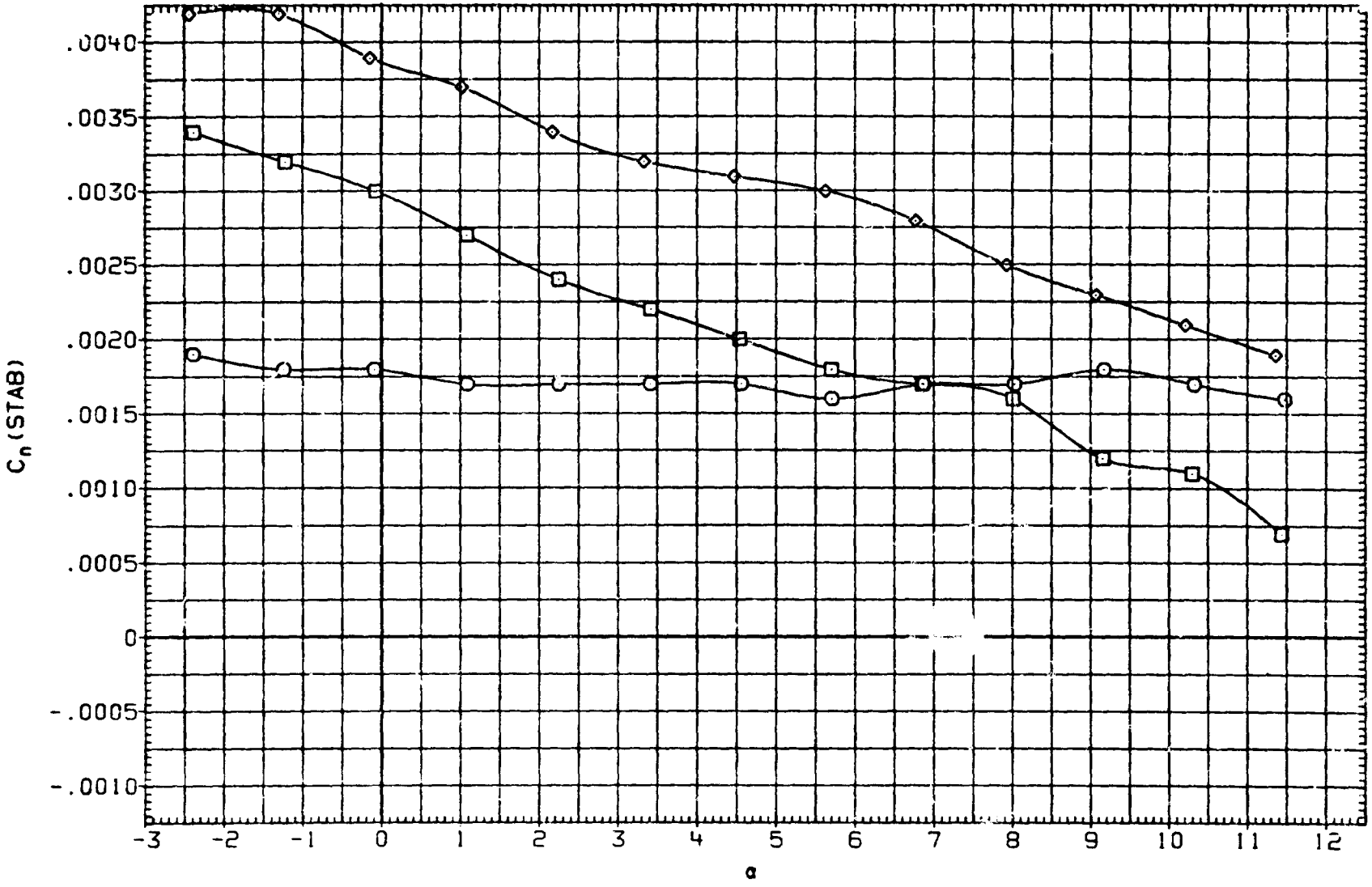

FIG 6. EFFECT OF DIFFERENTIAL OUTBOARD CONFORMAL FLAP DEFLECTIONS.

(D)MACH = 2.00

DATA SET	SYMBOL	CONFIGURATION DESCRIPTION	DTEO-L	DTEO-R	DH	DTEI
(ABD008)	○	BVH3H	.000	.000	.000	.000
(ABD010)	□	BVH3H	5.000	-5.000	.000	.000
(ABD011)	◇	BVH3H	.000	-15.000	.000	.000

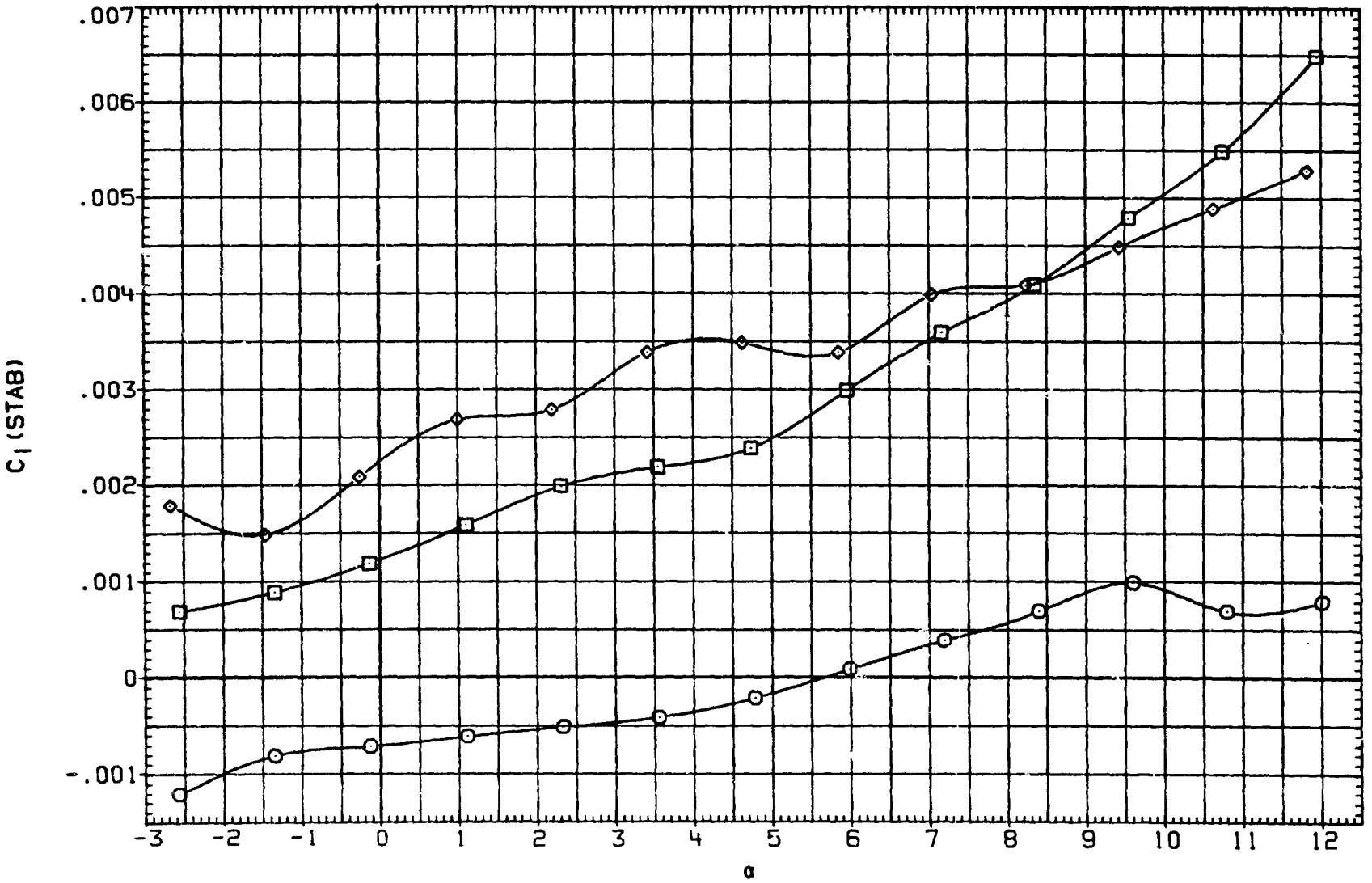

FIG 6. EFFECT OF DIFFERENTIAL OUTBOARD CONFORMAL FLAP DEFLECTIONS.

DATA SET	SYMBOL	CONFIGURATION DESCRIPTION	DTEO-L	DTEO-R	DH	DTEI
(ABD008)	○	BVW3H	.000	.000	.000	.000
(ABD010)	□	BVW3H	5.000	-5.000	.000	.000
(ABD011)	◇	BVW3H	.000	-15.000	.000	.000

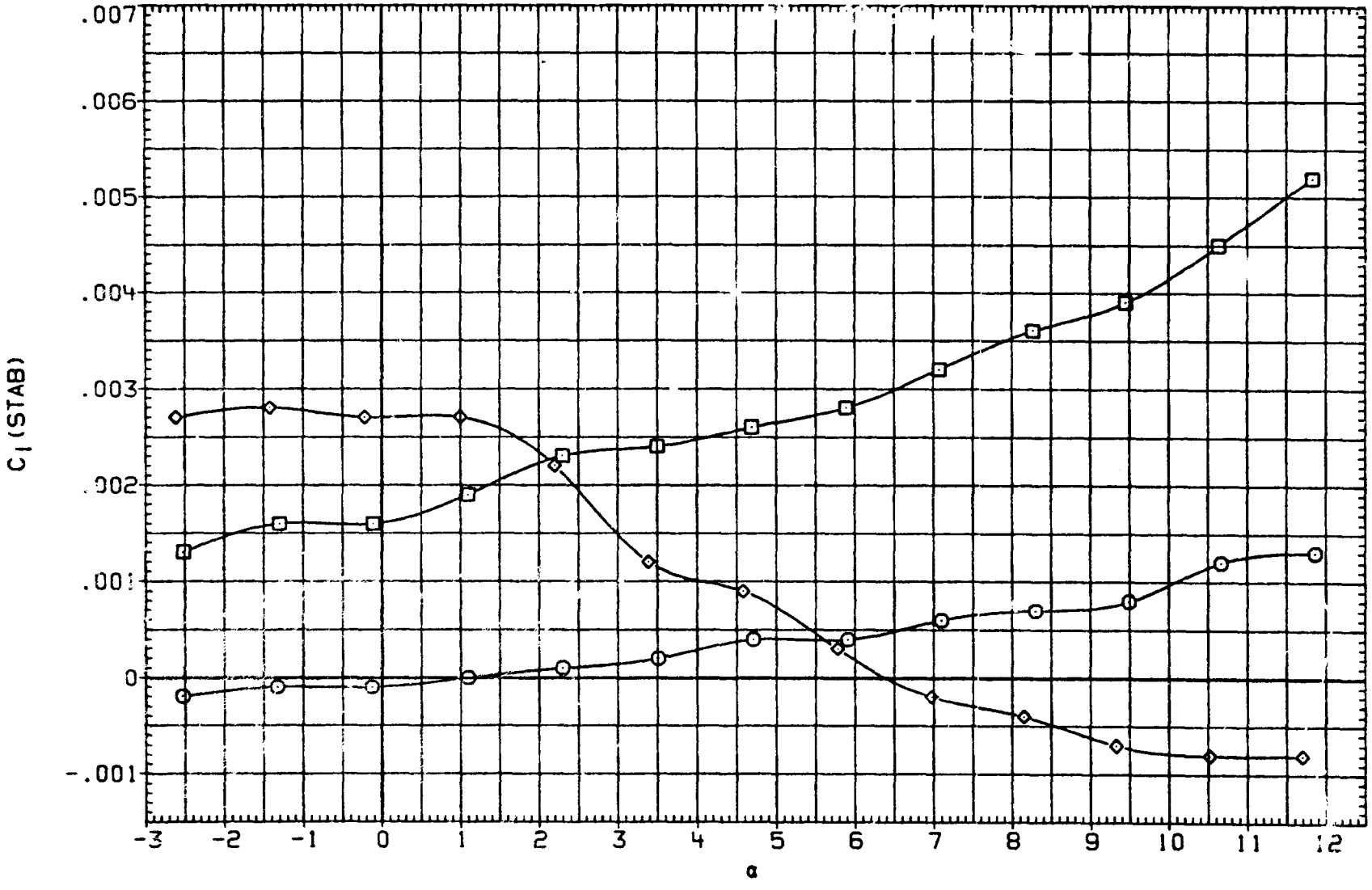

FIG 6. EFFECT OF DIFFERENTIAL OUTBOARD CONFORMAL FLAP DEFLECTIONS.

(B)MACH = 1.60

DATA SET	SYMBOL	CONFIGURATION DESCRIPTION	DTEO-L	DTEO-R	DH	DTEI
(ABD008)	○	BVW3H	.000	.000	.000	.000
(ABD010)	□	BVW3H	5.000	-5.000	.000	.000
(ABD011)	◇	BVW3H	.000	-15.000	.000	.000

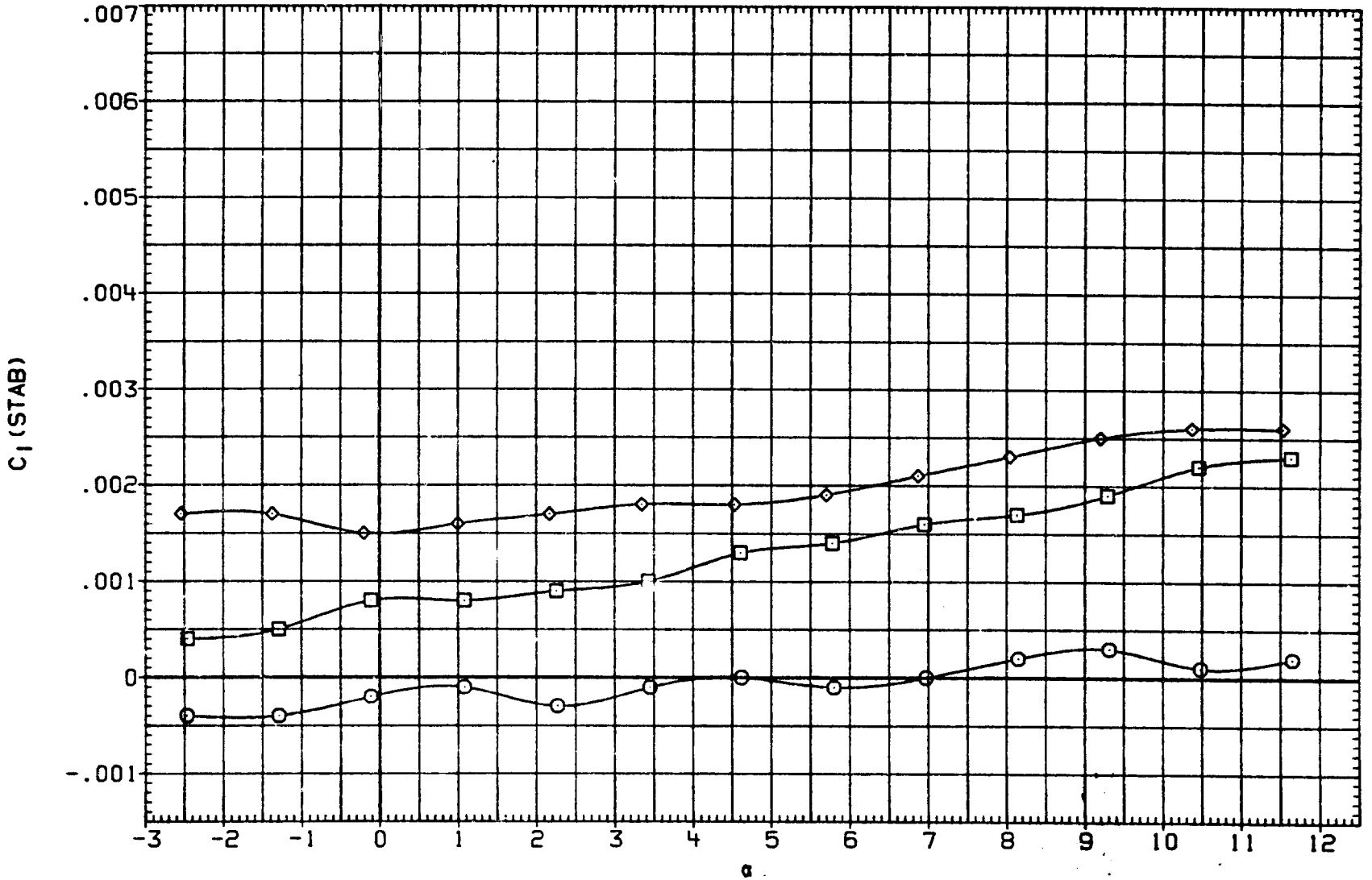

FIG 6. EFFECT OF DIFFERENTIAL OUTBOARD CONFORMAL FLAP DEFLECTIONS.

(C)MACH = 1.80

DATA SET	SYMBOL	CONFIGURATION DESCRIPTION	DTEO-L	DTEO-R	DH	DTEI
(ABD008)	○	BVW3H	.000	.000	.000	.000
(ABD010)	□	BVW3H	5.000	-5.000	.000	.000
(ABD011)	◇	BVW3H	.000	-15.000	.000	.000

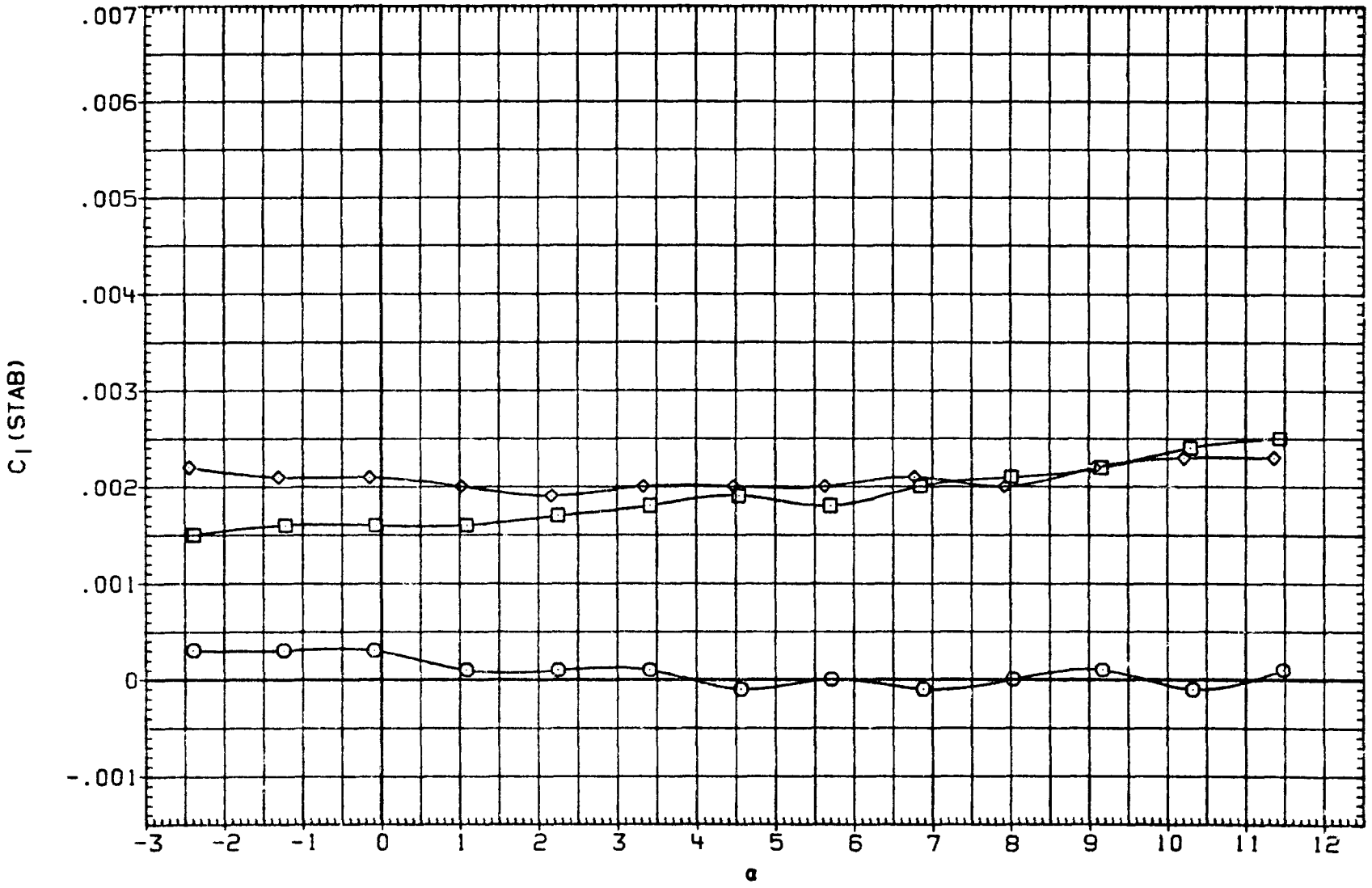

FIG 6. EFFECT OF DIFFERENTIAL OUTBOARD CONFORMAL FLAP DEFLECTIONS.

(D)MACH = 2.00

DATA SET	SYMBOL	CONFIGURATION DESCRIPTION	DTEO-L	DTEO-R	DH	DTEI
(ABD008)	○	BVH3H	.000	.000	.000	.000
(ABD010)	□	BVH3H	5.000	-5.000	.000	.000
(ABD011)	◇	BVH3H	.000	-15.000	.000	.000

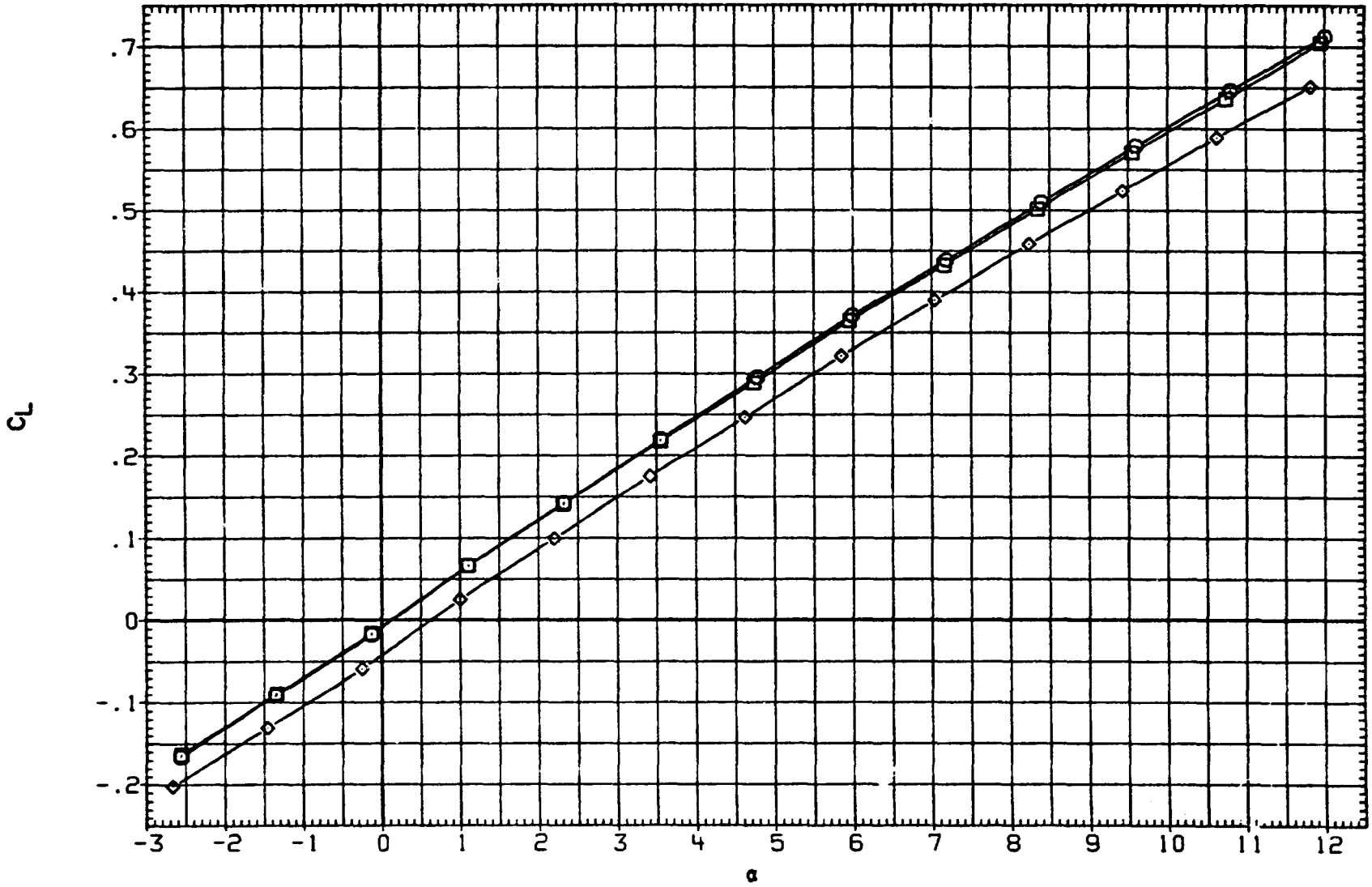

FIG 6. EFFECT OF DIFFERENTIAL OUTBOARD CONFORMAL FLAP DEFLECTIONS.

(A)MACH = 1.50

DATA SET	SYMBOL	CONFIGURATION DESCRIPTION	DTEO-L	DTEO-R	DH	DTEI
(ABD008)	○	BVH3H	.000	.000	.000	.000
(ABD010)	□	BVH3H	5.000	-5.000	.000	.000
(ABD011)	◇	BVH3H	.000	-15.000	.000	.000

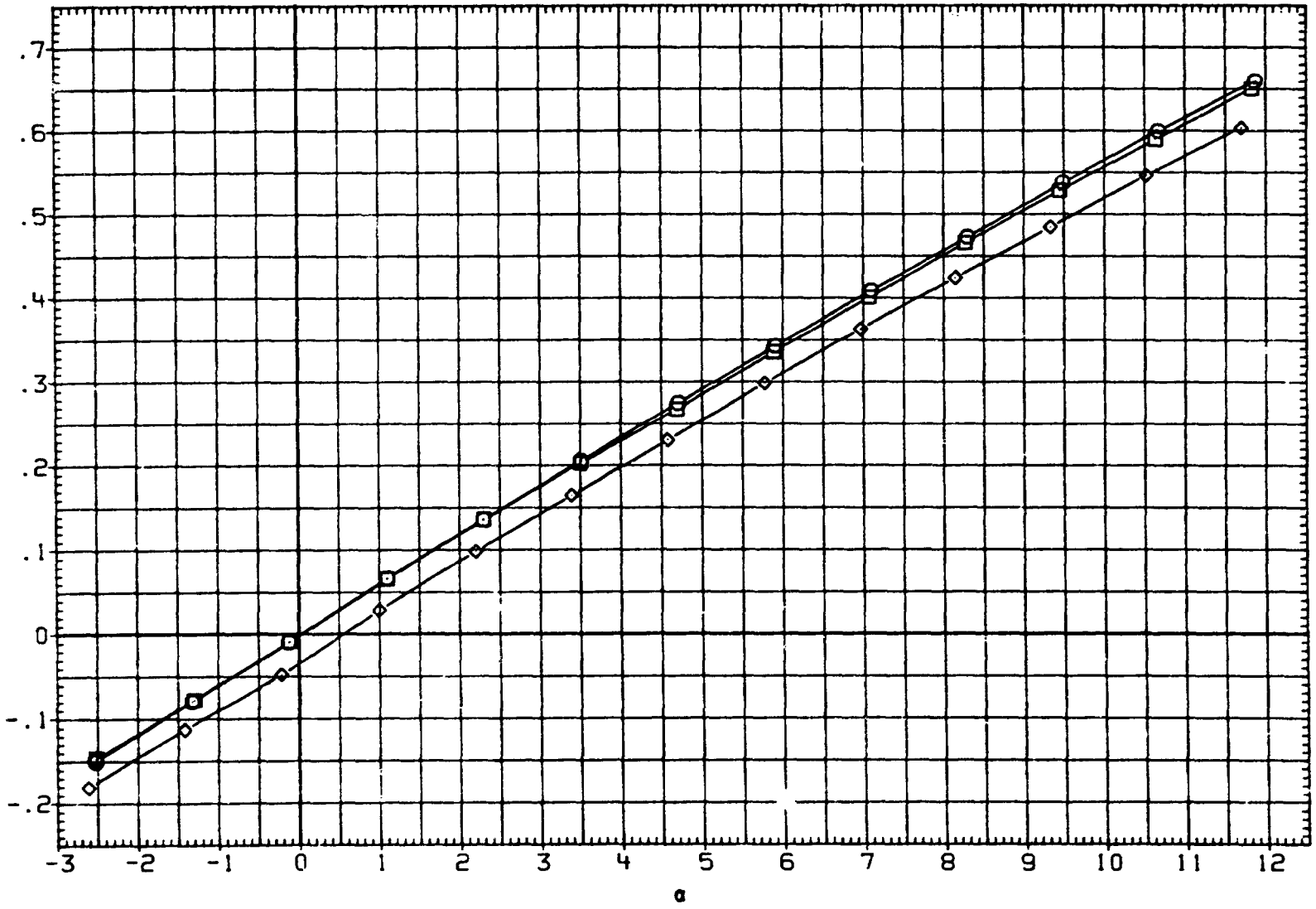

FIG 6. EFFECT OF DIFFERENTIAL OUTBOARD CONFORMAL FLAP DEFLECTIONS.

(B)MACH = 1.60

DATA SET	SYMBOL	CONFIGURATION DESCRIPTION	DTEO-L	DTEO-R	DH	DTEI
(ABD008)	○	BVH3H	.000	.000	.000	.000
(ABD010)	□	BVH3H	5.000	-5.000	.000	.000
(ABD011)	◇	BVH3H	.000	-15.000	.000	.000

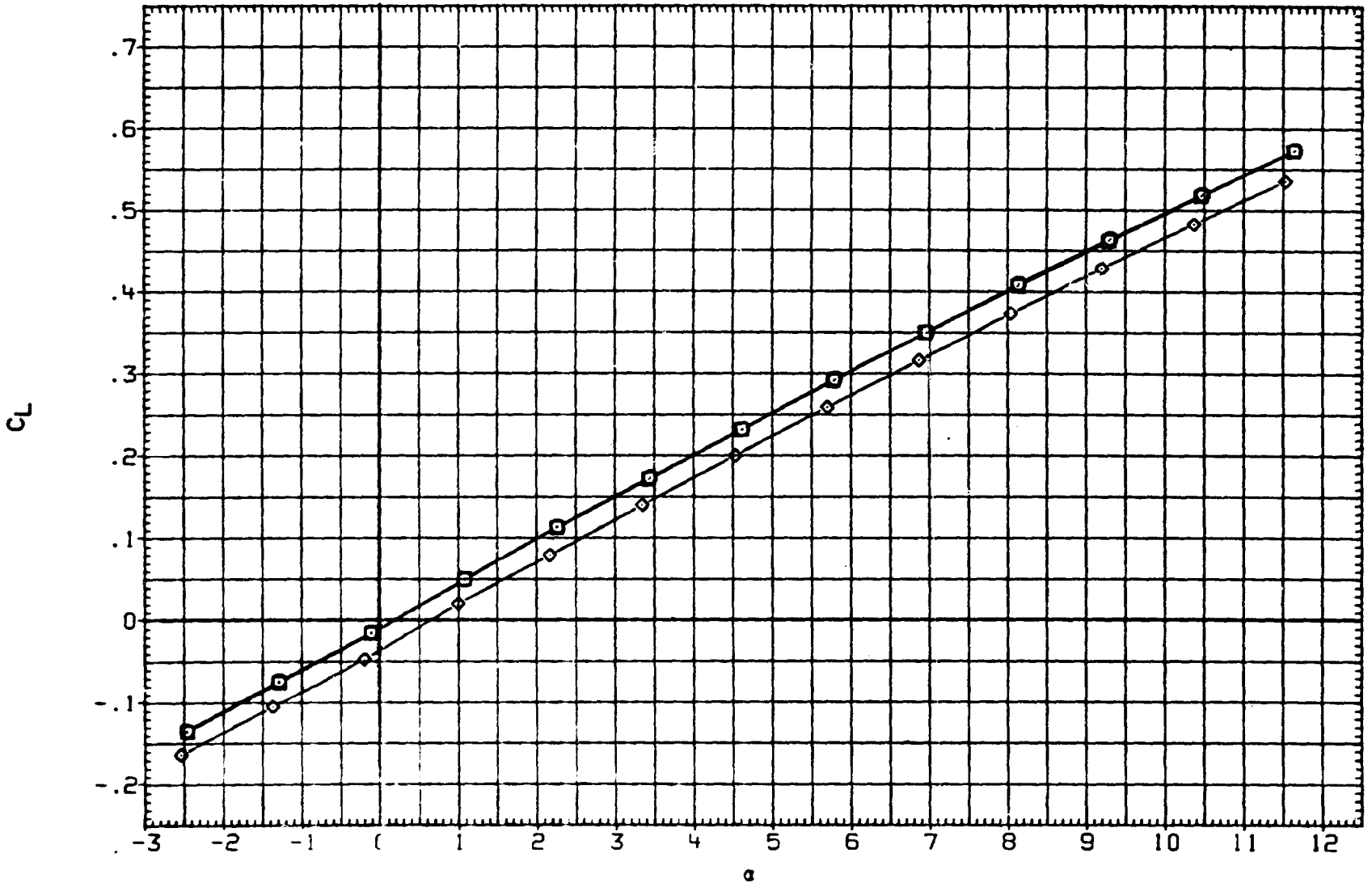

FIG 6. EFFECT OF DIFFERENTIAL OUTBOARD CONFORMAL FLAP DEFLECTIONS.

(C) MACH = 1.80

DATA SET	SYMBOL	CONFIGURATION DESCRIPTION	DTEO-L	DTEO-R	DH	DTEI
(ABD008)	○	BVH3H	.000	.000	.000	.000
(ABD010)	□	BVH3H	5.000	-5.000	.000	.000
(ABD011)	◇	BVH3H	.000	-15.000	.000	.000

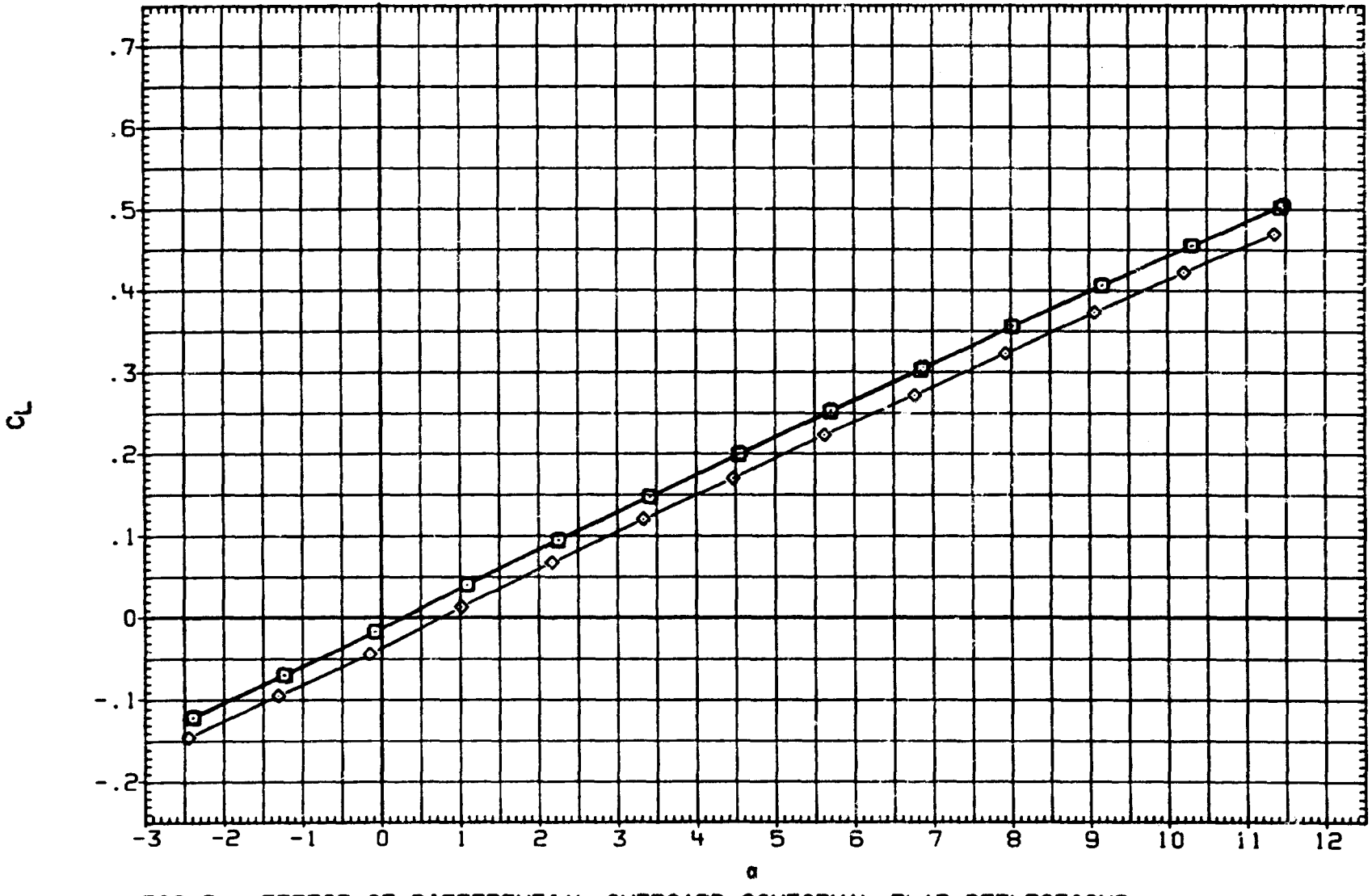

FIG 6. EFFECT OF DIFFERENTIAL OUTBOARD CONFORMAL FLAP DEFLECTIONS.

(D)MACH = 2.00

DATA SET	SYMBOL	CONFIGURATION DESCRIPTION	DTEO-L	DTEO-R	DH	DTEI
(ABD008)	○	BVW3H	.000	.000	.000	.000
(ABD010)	□	BVW3H	5.000	-5.000	.000	.000
(ABD011)	◇	BVW3H	.000	-15.000	.000	.000

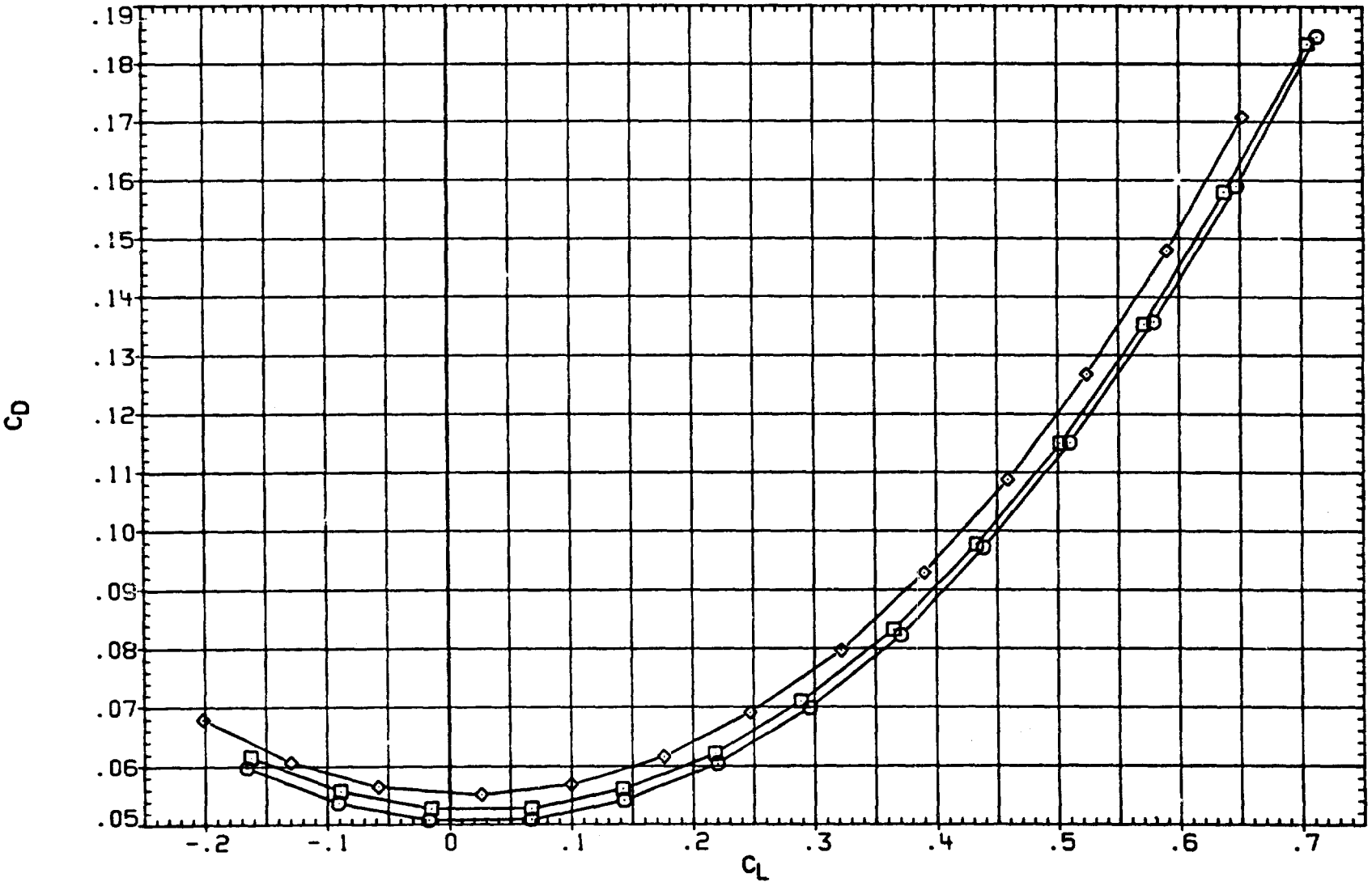

FIG 6. EFFECT OF DIFFERENTIAL OUTBOARD CONFORMAL FLAP DEFLECTIONS.

(A)MACH = 1.50

DATA SET	SYMBOL	CONFIGURATION DESCRIPTION	DTEO-L	DTEO-R	DH	DTEI
(ABD008)	○	BVW3H	.000	.000	.000	.000
(ABD010)	□	BVW3H	5.000	-5.000	.000	.000
(ABD011)	◇	BVW3H	.000	-15.000	.000	.000

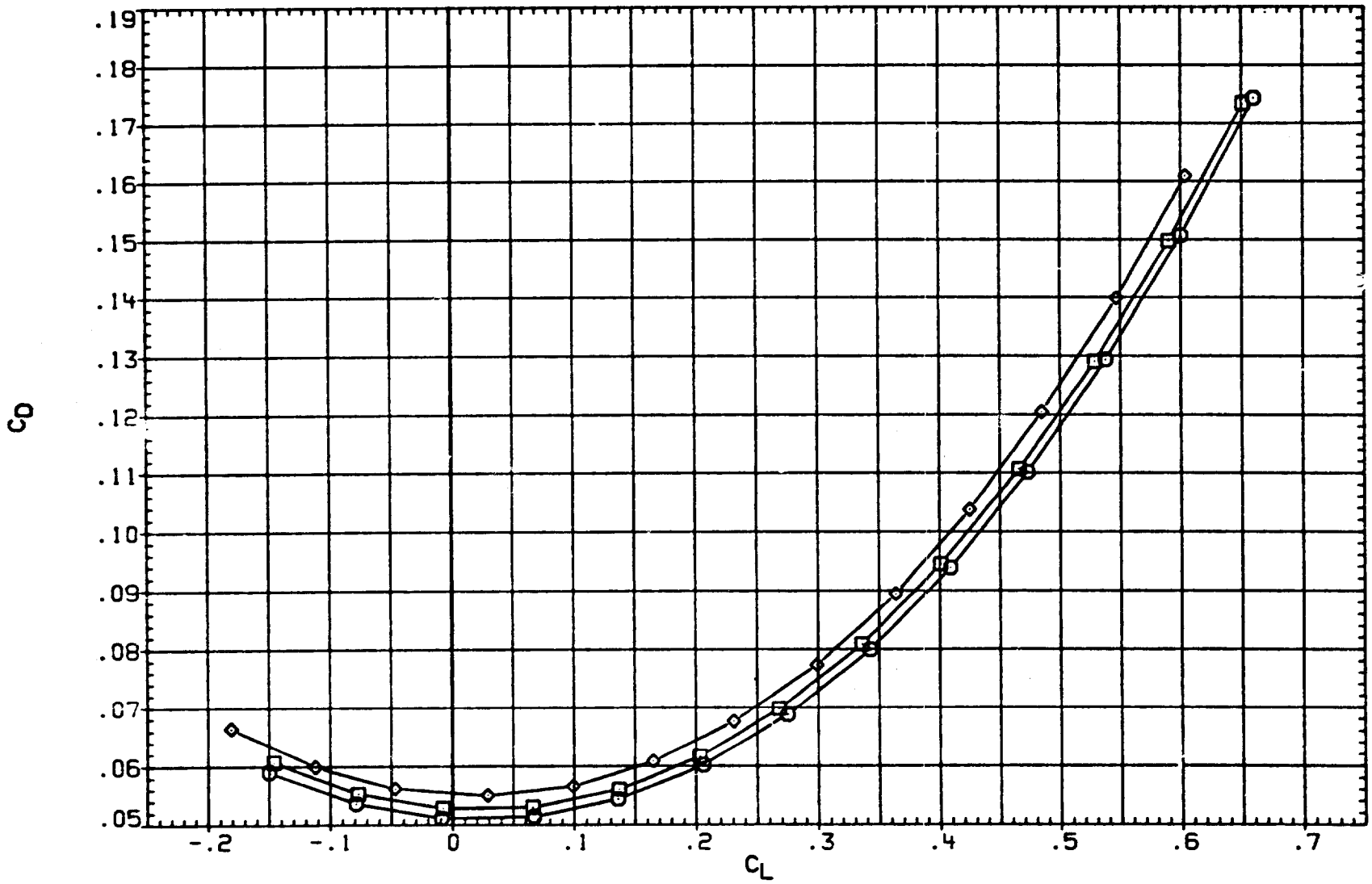

FIG 6. EFFECT OF DIFFERENTIAL OUTBOARD CONFORMAL FLAP DEFLECTIONS.

(B)MACH = 1.60

DATA SET	SYMBOL	CONFIGURATION DESCRIPTION	DTEO-L	DTEO-R	DH	DTEI
(AB0008)	○	BVW3H	.000	.000	.000	.000
(AB0010)	□	BVW3H	5.000	-5.000	.000	.000
(AB0011)	◇	BVW3H	.000	-15.000	.000	.000

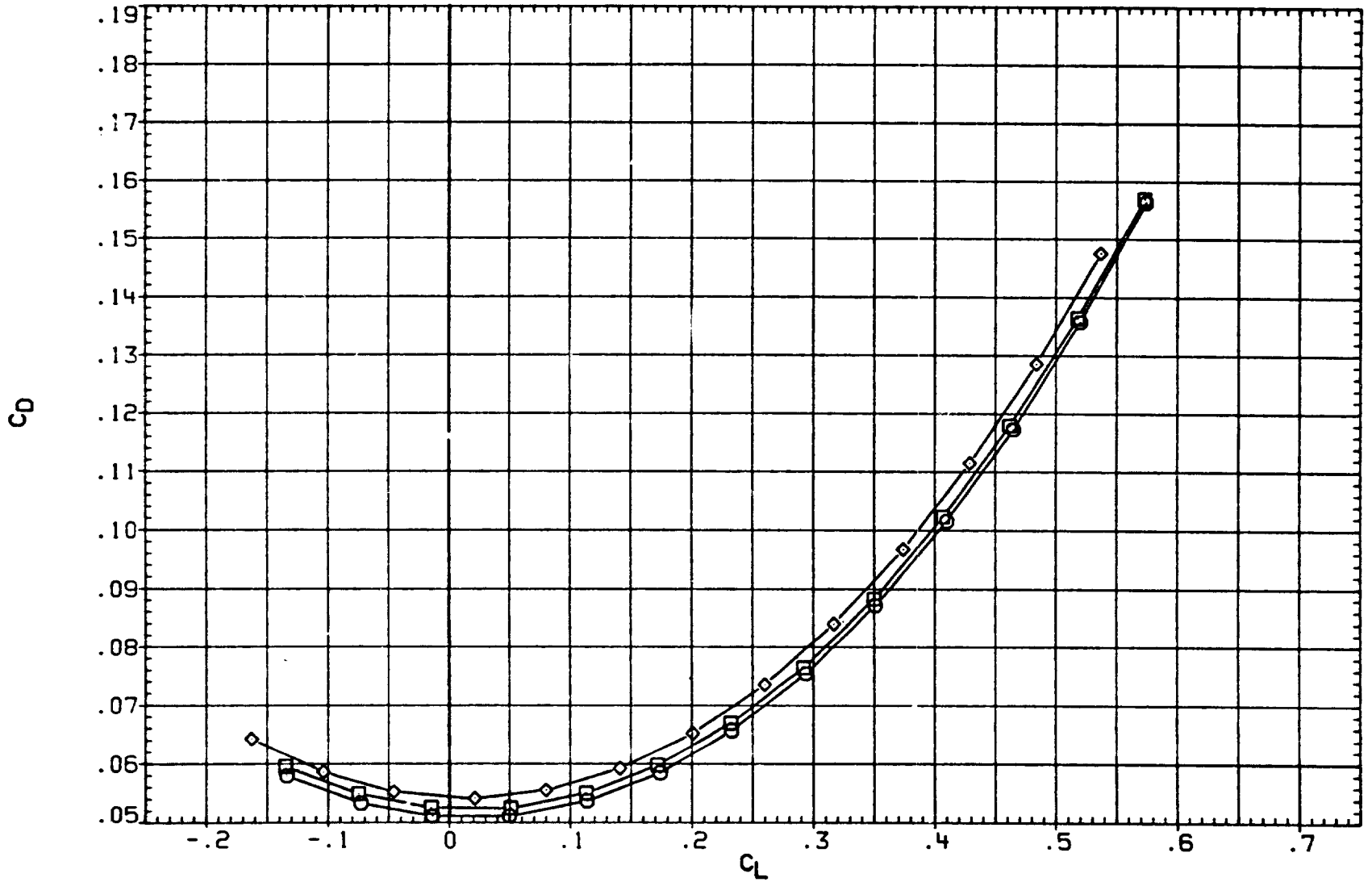

FIG 6. EFFECT OF DIFFERENTIAL OUTBOARD CONFORMAL FLAP DEFLECTIONS.

DATA SET	SYMBOL	CONFIGURATION DESCRIPTION	DTEO-L	DTEO-R	DH	DTEI
(ABD008)	○	BVW3H	.000	.000	.000	.000
(ABD010)	□	BVW3H	5.000	-5.000	.000	.000
(ABD011)	◇	BVW3H	.000	-15.000	.000	.000

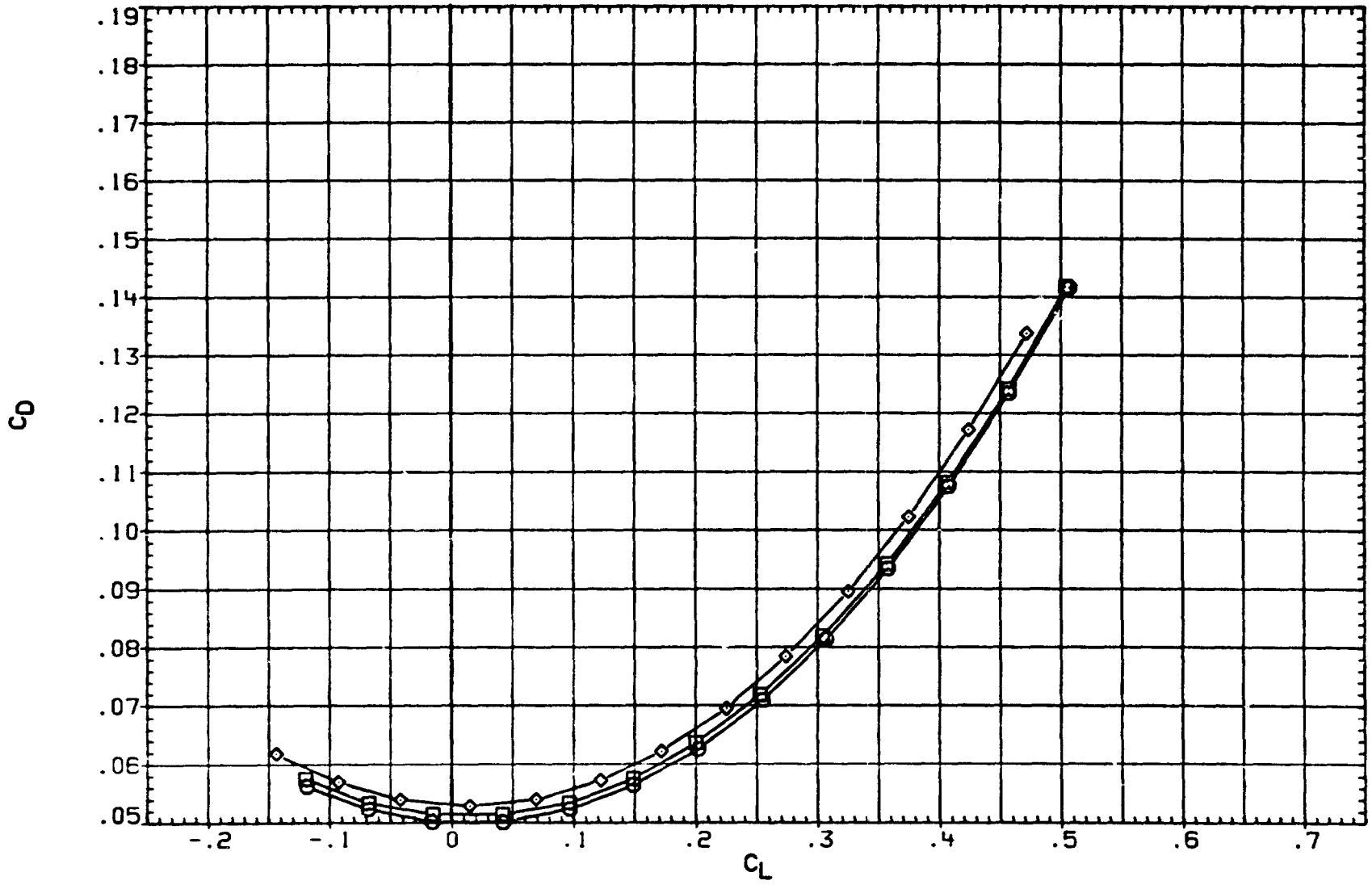

FIG 6. EFFECT OF DIFFERENTIAL OUTBOARD CONFORMAL FLAP DEFLECTIONS.

(D)MACH = 2.00

DATA SET	SYMBOL	CONFIGURATION DESCRIPTION	DTEO-L	DTEO-R	DH	DTEI
(ABD008)	○	BVH3H	.000	.000	.000	.000
(ABD010)	□	BVH3H	5.000	-5.000	.000	.000
(ABD011)	◇	BVH3H	.000	-15.000	.000	.000

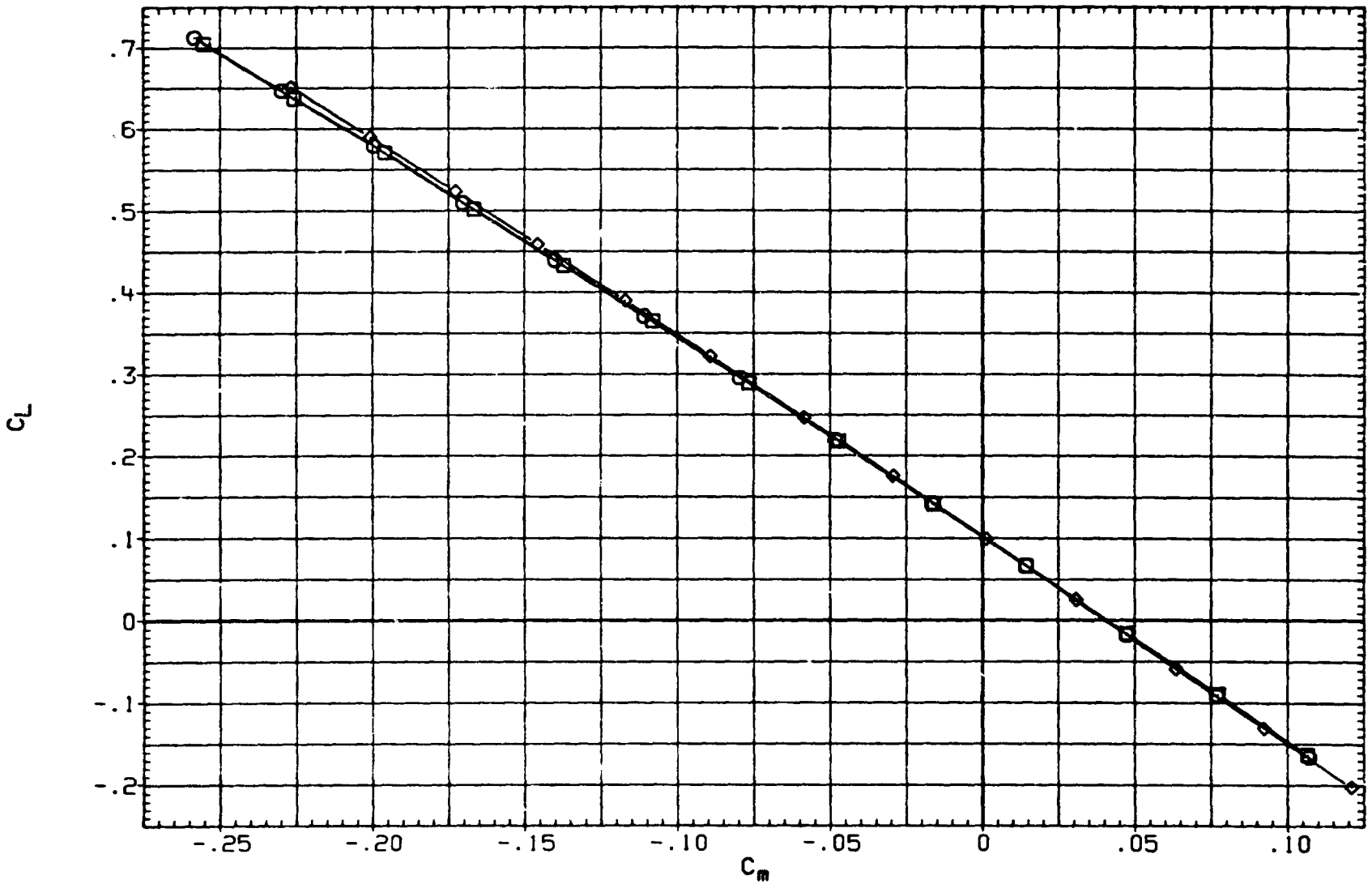

FIG 6. EFFECT OF DIFFERENTIAL OUTBOARD CONFORMAL FLAP DEFLECTIONS.

DATA SET	SYMBOL	CONFIGURATION DESCRIPTION	DTEO-L	DTEO-R	DH	DTEI
(ABD008)	○	BVW3H	.000	.000	.000	.000
(ABD010)	□	BVW3H	5.000	-5.000	.000	.000
(ABD011)	◇	BVW3H	.000	-15.000	.000	.000

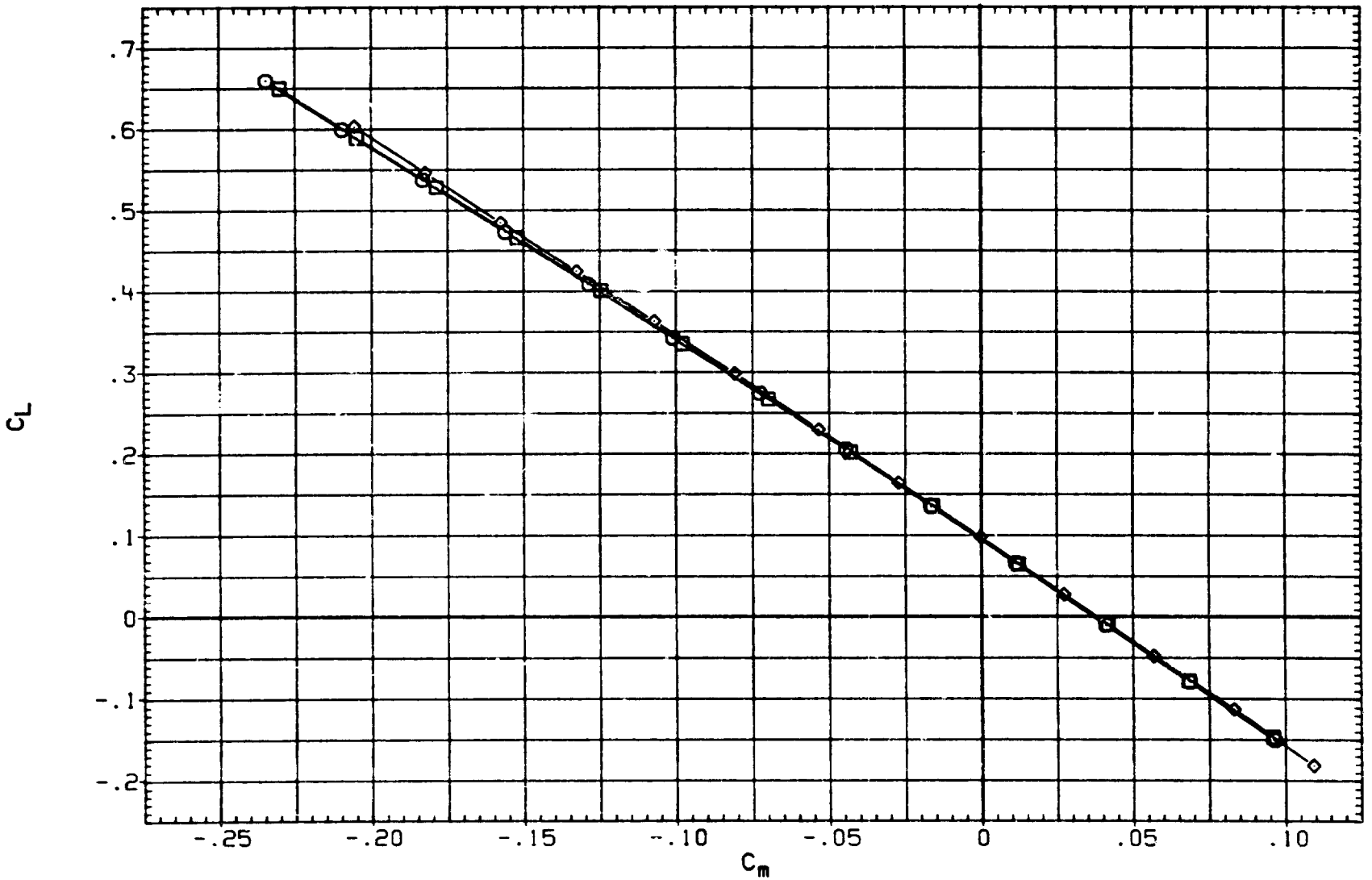

FIG 6. EFFECT OF DIFFERENTIAL OUTBOARD CONFORMAL FLAP DEFLECTIONS.

(B)MACH = 1.60

DATA SET	SYMBOL	CONFIGURATION DESCRIPTION	DTEO-L	DTEO-R	DH	DTEI
(ABD008)	○	BVW3H	.000	.000	.000	.000
(ABD010)	□	BVW3H	5.000	-5.000	.000	.000
(ABD011)	◇	BVW3H	.000	-15.000	.000	.000

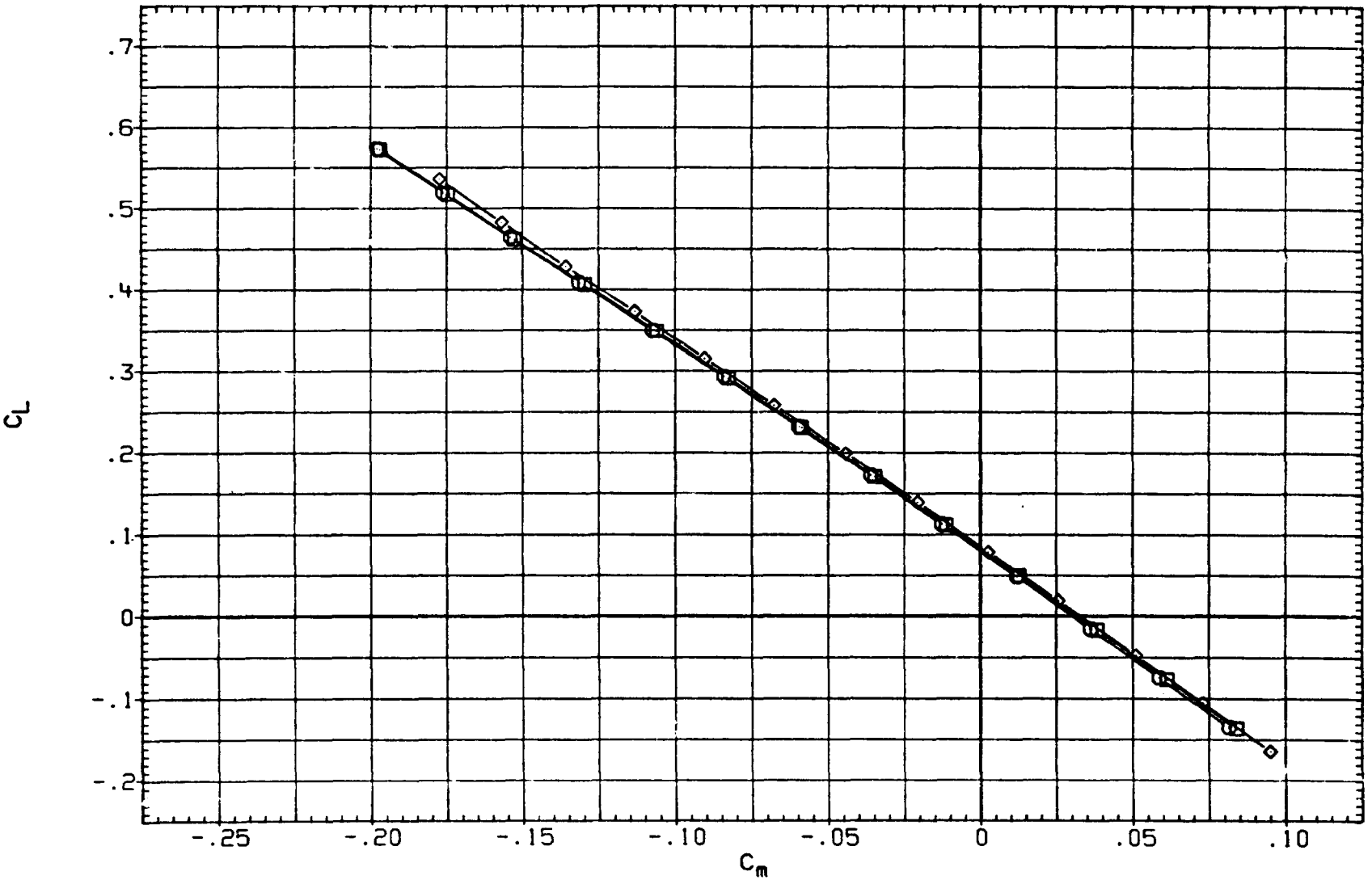

FIG 6. EFFECT OF DIFFERENTIAL OUTBOARD CONFORMAL FLAP DEFLECTIONS.

(C)MACH = 1.80

DATA SET	SYMBOL	CONFIGURATION DESCRIPTION	DTEO-L	DTEO-R	DH	DTEI
(ABD008)	○	BVW3H	.000	.000	.000	.000
(ABD010)	□	BVW3H	5.000	-5.000	.000	.000
(ABD011)	◇	BVW3H	.000	-15.000	.000	.000

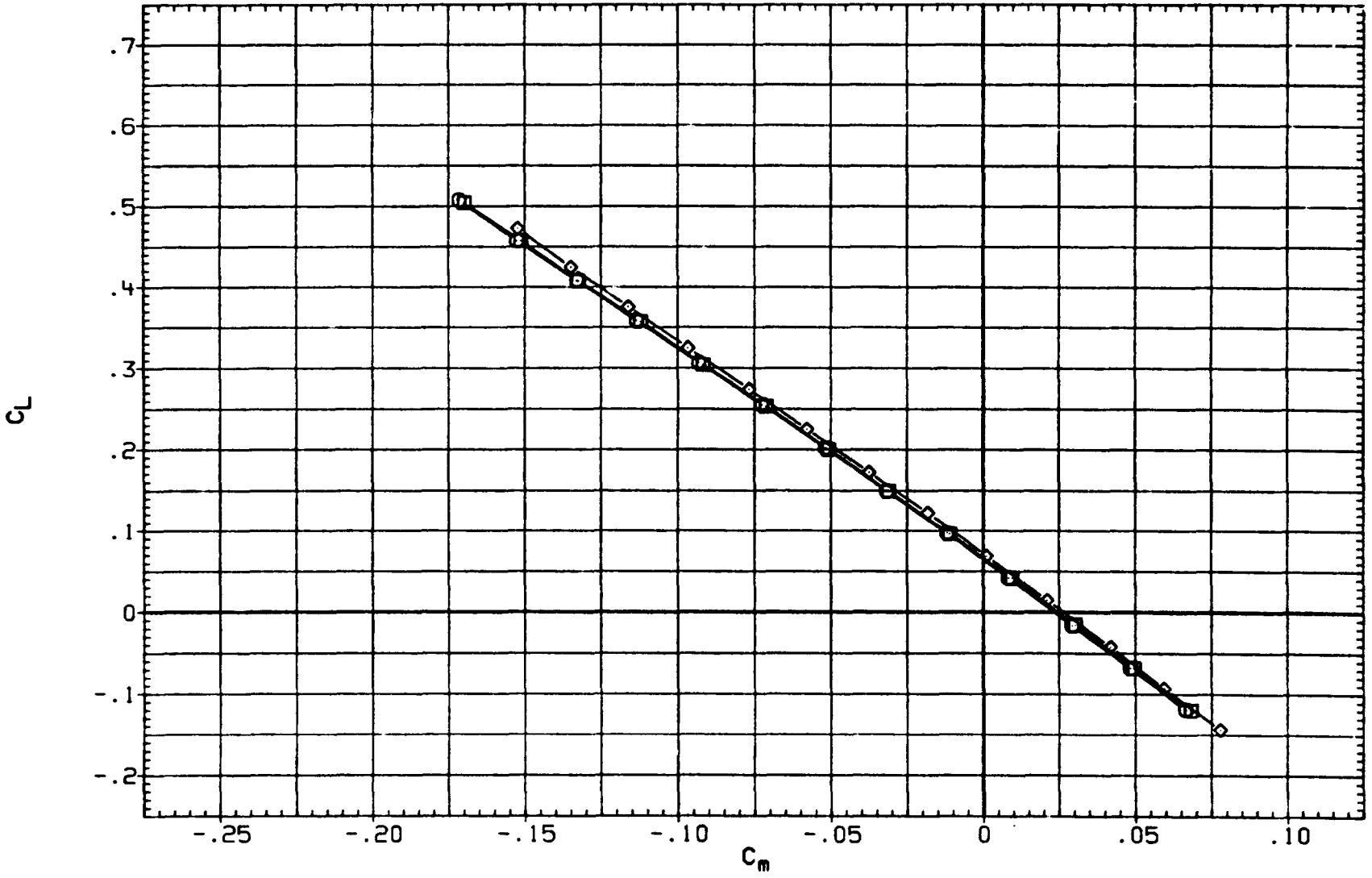

FIG 6. EFFECT OF DIFFERENTIAL OUTBOARD CONFORMAL FLAP DEFLECTIONS.

(D)MACH = 2.00